ERDC/CHL TR-01-27

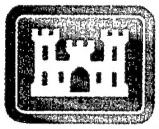

US Army Corps of Engineers®
Engineer Research and Development Center

Monitoring Completed Navigation Projects Program

Monitoring of Boston Harbor Confined Aquatic Disposal Cells

compiled by Lyndell Z. Hales

September 2001

Coastal and Hydraulics Laboratory

Monitoring Completed Navigation Projects Program

ERDC/CHL TR-01-27
September 2001

Monitoring of Boston Harbor Confined Aquatic Disposal Cells

compiled by Lyndell Z. Hales

Coastal and Hydraulics Laboratory
U.S. Army Engineer Research and Development Center
3909 Halls Ferry Road
Vicksburg, MS 39180-6199

Final report

Prepared for U.S. Army Corps of Engineers
Washington, DC 20314-1000

Contents

List of Figures

List of Tables

Preface

The studies reported herein were conducted as part of the Monitoring Completed Navigation Projects (MCNP) program, formerly Monitoring Completed Coastal Projects program. Work was conducted under MCNP Work Unit No. 11M15, "Boston Harbor Confined Aquatic Disposal Cells." Overall program management for the MCNP is provided by the Hydraulic Design Section of Headquarters, U.S. Army Corps of Engineers (HQUSACE). The Coastal and Hydraulics Laboratory (CHL), U.S. Army Engineer Research and Development Center (ERDC), Vicksburg, MS, is responsible for technical and data management, and support for HQUSACE review and technology transfer. Program Monitors for the MCNP program are Messrs. Barry W. Holliday, Charles B. Chesnutt, and David B. Wingerd, HQUSACE. Program Manager is Mr. Robert R. Bottin, Jr., CHL.

The objective of this monitoring by the MCNP program was to supplement other monitoring by the U.S. Army Engineer District, New England; State of Massachusetts; and the dredging contractors. This report is a summary of these pertinent field and laboratory studies that have been performed to evaluate the effectiveness of in-channel confined aquatic disposal (CAD) cells at Boston Harbor. Two studies conducted by Science Applications International Corporation, and by J. Roberts, R. Jepsen, C. Bryan, and M. Chapin, which were both summarized in Chapter 4, were funded by the U.S. Army Engineer District, New England. All other studies summarized herein were funded by the MCNP program. The lessons learned here will assist the New England District and other Corps districts to evaluate the effectiveness of CAD cells as a contaminated dredged material placement option.

The studies reported herein that were funded by MCNP were conducted by Dr. Stephen T. Maynord and Messrs. Timothy L. Welp, Michael W. Tubman, and James E. Clausner, CHL; Drs. John F. Peters and Michael K. Sharp, and Mr. Landris T. Lee, Geotechnical and Structures Laboratory, ERDC; Dr. Tom Fredette, U.S. Army Engineer District, New England; Dr. Donald Hayes, University of Utah; Dr. Carl Albro, Battelle Corporation; and Dr. Scott McDowell, Science Applications International Corp. This work was conducted during the period October 1998 through September 2001 under the general supervision of Dr. James R. Houston, former Director, CHL; Mr. Thomas W. Richardson, Acting Director, CHL; and Ms. Joan Pope, Chief, Coastal Evaluation and Design Branch. Mr. Edward B. Hands, CHL, was the Principal Investigator

for this MCNP work unit. This report was compiled by Dr. Lyndell Z. Hales, CHL.

At the time of publication of this report, Dr. James R. Houston was Director of ERDC, and COL John W. Morris III, EN, was Commander and Executive Director.

Conversion Factors, Non-SI to SI Units of Measurement

Non-SI units of measurement used in this report can be converted to SI units as follows:

Multiply	By	To Obtain
Cubic yards	0.7645549	Cubic meters
Feet	3.785	Meters
Gallons	3.785	Liters
Horsepower	0.746	Kilowatts
Inches	25.4	Millimeters
Pounds (force) per square inch	6894.757	Pascals
Pounds (force) per square foot	47.8803	Pascals
Pound (force) per square foot	47.8803	Newtons per square meter

1 Introduction

Monitoring Completed Navigation Projects Program

The goal of the Monitoring Completed Navigation Projects (MCNP) program (formerly the Monitoring Completed Coastal Projects Program) is the advancement of coastal and hydraulic engineering technology. The program is designed to determine how well projects are accomplishing their purposes and are resisting attacks by their physical environment. These determinations, combined with concepts and understanding already available, will lead to (a) creating more accurate and economical engineering solutions to coastal and hydraulic problems, (b) strengthening and improving design criteria and methodology, (c) improving construction practices and cost-effectiveness, and improving operation and maintenance techniques. Additionally, the monitoring program will identify where current technology is inadequate or where additional research is required.

To develop direction for the program, the U.S. Army Corps of Engineers (USACE) established an ad hoc committee of engineers and scientists. The committee formulated the objectives of the program, developed its operation philosophy, recommended funding levels, and established criteria and procedures for project selection. A significant result of their efforts was a prioritized listing of problem areas to be addressed. This is essentially a listing of the areas of interest of the program.

Corps District and Division offices are invited to nominate projects for inclusion in the monitoring program as funds become available. A selection committee comprised of members of the MCNP Program Field Review Group (representatives from District and Division offices) reviews and prioritizes the projects nominated. The prioritized list is reviewed by the Program Monitors at Headquarters, U.S. Army Corps of Engineers (HQUSACE). Final selection is based on this prioritized list, national priorities, and the availability of funding.

The overall monitoring program is under the management of the Coastal and Hydraulics Laboratory (CHL), U.S. Army Engineer Research and Development Center (ERDC), with guidance from HQUSACE. An individual monitoring project is a cooperative effort between the submitting District and/or Division office and CHL. Development of monitoring plans, and conduct of data collection

and analyses, are dependent upon the combined resources of CHL and the District and/or Division.

Boston Harbor Navigation Improvement Project Background

Navigation channel maintenance is a primary mission of the Corps, sometimes requiring dredging and placement of contaminated dredged material. Sediments in some Corps projects are being found to be contaminated, due primarily to more sensitive testing methods and regulations. Options for placing contaminated sediments are becoming more and more limited. While the use of upland sites is the preferred placement option by many, land for such sites is becoming more expensive to obtain or is not available at all. Existing upland sites are reaching capacity in many locations, and are essentially impossible to locate in urban areas where most contaminated material is found. In-channel confined aquatic disposal (CAD) cells have the potential of providing accessible relatively low cost sites for placement of contaminated sediments.

The Boston Harbor Navigation Improvement Project (BHNIP) involves deepening (maintenance dredging) of the main ship channel and three tributary channels to the Inner Harbor, and associated berthing areas. Lack of an upland disposal site and resource agency denial of permission to place and cap the contaminated sediments at an open water site resulted in the decision to use in-channel CAD cells for placement of contaminated material that would be dredged with an environmentally sensitive clamshell bucket.

The main ship channel includes the Inner Confluence and the mouth of the Reserved Channel, while the tributary channels include Mystic River, Chelsea River, and the Reserved Channel (Figure 1). In addition to the channels, several terminals and berth areas have been dredged.

Phase 1 of the project was conducted in the summer of 1997, when Conley Terminal was dredged. Phase 2 was initiated in the summer of 1998, and CAD cells M2, M4, M5, M8, M12, M18-19, and a very large cell called the Super Cell were filled (Figure 2). During Phase 2, Science Applications International Corporation (SAIC) performed a geotechnical investigation of CAD cell M2 to (a) ascertain changes in sediment characteristics that affect engineering behavior and volume of the material after it is placed in the CAD cell, and (b) determine material properties in the CAD cell to allow analysis of the field behavior (consolidation and erosion) of the CAD cell.

During Phase 1 and the early part of Phase 2, there were important questions raised about both the timing and method of placing the cap material (sand) relative to the goal of creating a stable uniform capping layer at least 3 ft[1] thick.

[1] A table of factors converting non-SI units of measurement to SI units is presented on page viii.

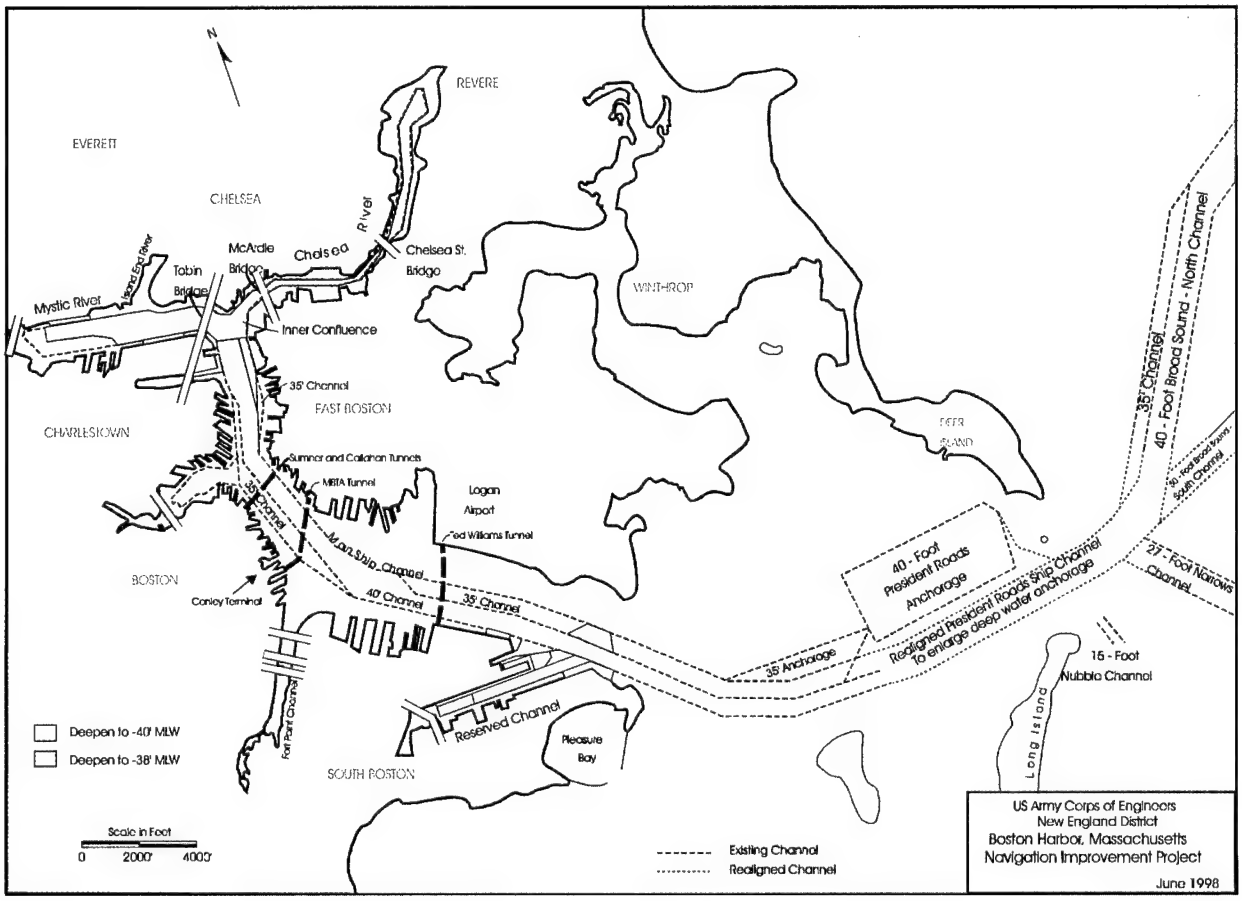

Figure 1. Boston Harbor Navigation Improvement Project (BHNIP) (Science Applications International Corporation (SAIC) 2000a)

Numerous monitoring surveys were conducted to determine whether this goal was being met.

Previous Monitoring

Previous Phase 1 monitoring [1]

During Phase 1 of the BHNIP, an in-channel CAD cell was constructed for containment of unsuitable dredged material from shipping berths at Conley Container Terminal in South Boston. The fine-grained dredged sediments were disposed into the CAD cell and then capped with sufficient sand to cover the deposit with a 3-ft thick layer of sand.

[1] This section is extracted essentially verbatim from Science Applications International Corporation. (2000a).

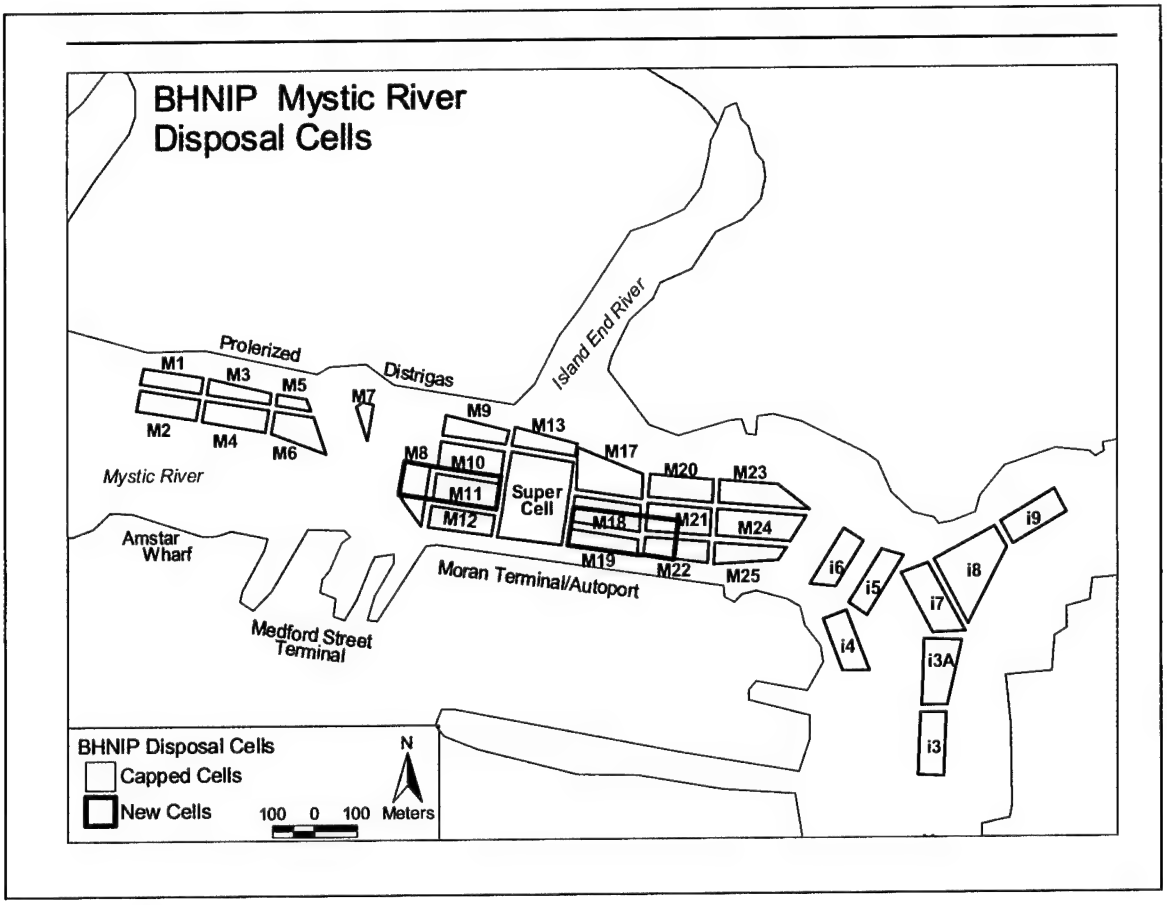

Figure 2. Boston Harbor Navigation Improvement Project CAD cells in the Mystic River (after Science Applications International Corporation 2000a)

Various postcapping monitoring techniques including precision bathymetry, subbottom profiling, and coring were used to evaluate the success of the capping operation. Overall, the survey results indicated that the majority of the CAD cell had been capped with a highly variable thickness of sand, and the southern end of the cell had little or no cap material. Postcapping operations designed to level the sand cap appear to have resulted in highly uneven sand coverage, and potentially served to enhance mixing of the cap and underlying dredged material. Furthermore, the sediment placed in the cell (both dredged material and capping sand) continued to consolidate after capping (SAIC 1999).

Recommendations to modify the requirements for dredging and disposal operations were designed around the primary concerns raised by the Phase 1 results, including lack of spatial coverage of sand, variable thickness of sand, and potential mixing between the sand and the underlying dredged material. The State of Massachusetts Water Quality Certification (WQC) and the dredging project specifications were modified based on the Phase 1 monitoring results. The method of sand placement was viewed as the main factor resulting in both uneven spatial coverage and variable cap thickness. For Phase 2, operations were modified in an attempt to improve placement of the cap material and to increase the ability to diffuse the sand while capping.

As part of the requirements of the WQC during Phase 1, the maintenance materials were dredged using an environmental (closed) clamshell bucket. The bucket is designed to limit sediment suspension in the water column, but it has the added effect of introducing large volumes of water into the dredged sediment and subsequently into the CAD cells during dredged material disposal. For Phase 2, the recommendation was made to increase the time allowed for consolidation of the fine-grained maintenance sediments prior to capping. By increasing the time allowed for the material to consolidate, the strength and bearing capacity of the material were predicted to increase. However, the Phase 1 data provided no clear guidance on the time required for sufficient consolidation prior to capping.

The Phase 1 study also included an evaluation of the monitoring methods used to determine the success of the capping operation. Sediment cores were deemed advantageous in providing good visual evidence of the state of the cap but had the drawback of measuring cap thickness at only a limited number of discrete points within the CAD cell. Assuming the material could be evenly and carefully placed, subbottom profiling was suggested as a promising method to evaluate both the spatial coverage and overall thickness of sand caps under Phase 2.

Previous Phase 2 monitoring of CAD Cells M4, M5, and M12[1]

The dredging contractor for Phase 2 of the BHNIP, Great Lakes Dredge and Dock (GLDD) utilized the operational recommendations stemming from Phase 1 to construct, fill, and cap the first three cells in the Mystic River (Cells M4, M5, M12). As the first cell (M5) was dredged, it became apparent that the original CAD cell specifications (approximately 50 cells averaging 20 ft below the sediment/water interface) could be modified. The stiff Boston blue clay comprising the CAD cell allowed relatively steep side slopes to be maintained, and Cell M5 was dredged to a greater depth than in the project design (approximately 40 ft below the authorized depth of the channel). Similarly, the second (M12) and third (M4) cells were also dredged to deeper depths (70 and 45 ft below channel depth, respectively) than in the original specifications. The steeper side slopes and increased depths resulted in increased capacity and therefore fewer cells were required to contain the maintenance material (approximately 785,000 cu yd) generated under the BHNIP.

The time interval between the last load of maintenance material and the first load of cap material was 30 days for Cell M12, 33 days for Cell M4, and 52 days for Cell M5, in compliance with the WQC and project specifications (30 to 60 days). The time delay between placement of the bulk of the dredged material in Cell M5 and Cell M12 and capping was 83 and 56 days, respectively.

The clean sand was used as the cap material was dredged from the Cape Cod Canal and placed in each CAD cell using a hopper dredge. Cap verification data were collected prior to, during, and following cap placement. Several activities were conducted to support cap verification and assessment. Ocean Surveys, Inc.

[1] This section is extracted essentially verbatim from Science Applications International Corporation. (2000a).

(OSI) collected vibracores, bathymetry, and subbottom profile data in support of the required cap monitoring. SAIC conducted several surveys in support of the U.S. Army Engineer District, New England, studies of cap monitoring techniques including placement of cap measurement tripods, grab sampling, gravity coring, and side-scan sonar (SAIC 1999).

The Phase 2 monitoring showed that each of the three CAD cells had unique characteristics. The most common trend was in a surface fluidized layer of mud and a laterally continuous sand zone, consisting of moderate amounts of sand down to at least the depths of the recovered cores. There were indications of a thick mixed interval of sand and mud across the top of each cell, suggesting that the fine-grained dredged material was unable to support the entire weight of the cap material. Although the mixed sand zone did not precisely meet the project specifications of a discrete, uniform sand layer having a thickness of 3 feet, the three cells were considered successfully capped.

Purpose of Study

The objective of this monitoring effort by the ERDC/CHL MCNP program of the U.S. Army Engineer Research and Development Center, Coastal and Hydraulics Laboratory, was to complement the New England District, State of Massachusetts, and dredging contractor monitoring with supplemental monitoring that would help to evaluate the effectiveness of in-channel CAD cells at Boston Harbor. The MCNP monitoring plan was composed of three primary activities:

a. The first activity conducted water quality monitoring of suspended solids near the operation of two environmentally-sensitive clamshell dredges and a normal clamshell, to document the benefits of the special clamshell buckets. This activity is summarized in Chapter 2, "Clamshell Dredge Bucket Comparison at Boston Harbor." These studies were conducted by Welp et al. (2001).

b. The second activity monitored contaminated dredged material consolidation and strength prior to and after placing the sand cap. Laboratory tests measured consolidation, shear strengths, water content, etc., of both the contaminated sediments and the Boston blue clay to refine predictive techniques for mound and cap performance. These studies are summarized in Chapter 3, "Geotechnical Investigations of Boston Harbor Navigation Improvement Project (BHNIP) Cad Cells." Various tasks of this activity were conducted by Science Applications International Corporation (2000a) ("Geotechnical Investigations of CAD Cell M2"); and Lee (in preparation) ("Boston Harbor CAD Cell Capping Simulation").

c. The third activity calculated cap erosion predictions from both tidal currents and ship propeller wash to characterize the likely amount of cap damage to be expected from either source. These studies are summarized in Chapter 4, "Boston Harbor CAD Cell Cap Erosion from Tidal Currents

and Ship Propeller Wash." Various tasks of this activity were conducted by Science Applications International Corporation (2000b) ("Sediment Resuspension by *MV Matthew*"); Maynord (2001)[1] ("Ship-generated Velocities and Bed Shear Stress"); Roberts et al. (2000) ("Erosion Rates of Boston Harbor Sediments"); and Gailani (2001)[2] ("Modeling of Erosion Due to Propeller Wash").

The lessons learned here will assist the New England District and other Corps districts to evaluate the effectiveness of CAD cells as a contaminated dredged material placement option. Additionally, documentation of sediment resuspension by conventional and closed clamshell buckets, and the amount of water added, will assist districts in optimizing between reducing resuspension during dredging versus added water which could make capping more difficult.

[1] Maynord, S. T. (2001). "Analysis of ship generated velocities and bed shear stress in Boston Harbor," unpublished document, U.S. Army Engineer Research and Development Center, Vicksburg, MS.

[2] Gailani, J. Z. (2001). "Modeling of erosion due to propeller wash," unpublished document, U.S. Army Engineer Research and Development Center, Vicksburg, MS.

2 Clamshell Dredge Bucket Comparison at Boston Harbor[1]

Sediment resuspension and loading characteristics were studied under near-similar operating and environmental conditions in Boston Harbor during August 1999 for three clamshell dredge buckets: (a) GLDD Conventional (open-faced); (b) GLDD Enclosed; and (c) CableArm™. Monitoring was conducted to characterize each bucket's near and far field sediment resuspension characteristics. Bucket loading characteristics were investigated with regard to water-to-solids ratios dredged by the different buckets. Documentation of sediment resuspension in the water column, and loading characteristics with Conventional and Enclosed clamshell buckets (the contractor-built GLDD Enclosed, and the CableArm buckets), will assist Corps districts in making bucket selection decisions, and provide data for the fate of dredged material numerical model verification.

Because a significant fraction of the sediments dredged during the BHNIP Phase 1 had elevated levels of some contaminants, the State of Massachusetts Department of Environmental Protection required that either one of two approved enclosed buckets be used to reduce sediment resuspension and potential for water quality impacts. However, the contractor performed dredging in a normal fashion, attempting to dredge as efficiently as possible to keep production high and costs low. Tests showed no exceedances of the water criteria with either of the approved buckets (GLDD Enclosed bucket or the CableArm navigation bucket). However, the New England District expressed concern that the enclosed buckets were adding additional water to the already soft and weak sediments, possibly causing a further reduction of the bearing capacity of the sediments. This reduction of bearing capacity would, in turn, make the capping operation even more difficult.

[1] This section is extracted essentially verbatim from Welp et al. (2001).

Dredging Equipment

GLDD personnel provided excellent support that facilitated the accomplishment of a successful study. The dredging operations took place under similar physical and environmental conditions with the primary difference being the bucket type used. The dredging operations were conducted in Boston Harbor just below the confluence of the Chelsea and Mystic Rivers, often referred to as the Inner Confluence (Figure 1). The sediment being dredged consisted of a predominantly fine-grained (sandy silt) material. Mean low water (mlw)[1] depth in the area was approximately 11.6 m (38 ft) with a tide range of approximately 3 m (10 ft). Sampling operations were conducted beginning near high tide each day and continued for 4 to 6 hr (time to fill 1 barge). The barges were not allowed to overflow.

The study objectives were accomplished by monitoring continuous dredging operations without significant interruptions and with as little variation in flow velocity and direction as possible. All sampling efforts were conducted on the ebb of the morning high tides.

The buckets used by GLDD are listed in Table 1. Figure 3 shows photographs of each bucket. Leakage occurred from all of the buckets. The CableArm and Enclosed buckets leaked through the joints and ventilation grates in the upper part of the buckets. The Conventional bucket also leaked and loss of some of the exposed sediments appeared to contribute to turbidity.

Table 1
Physical Characteristics and Descriptions of Dredge Buckets Used in Study

Date	Bucket	Size (yd^3)	Description
August 5, 1999	CableArm	29.81 m^3 (39)	CableArm navigational bucket (i.e., not their environmental bucket); with rubber side lip seals and vents (with intake seals) on either side near the top allow water to escape during descent and after the bucket is closed.
August 6, 1999	GLDD Enclosed	29.81 m^3 (39)	Conventional 19.87-m3 (26-yd3) bucket enclosed on the top and sides by welded steel plates; Vents with intake seals approximately 0.45 × 1.82 m (1.5 × 6 ft) on each side of the bucket near the top allow water to escape during descent and after the bucket is closed.
August 7, 1999	GLDD Conventional	19.87 m^3 (26)	Conventional bucket with completely open top.

A video camera was used to record the buckets' digging and dumping cycles to evaluate the difference in operation induced by the buckets. Average cycle times were fastest for the Conventional bucket (51.1 sec), compared to the Enclosed bucket (55.5 sec) and CableArm bucket (62.3 sec); however, the variation was not excessive as the CableArm bucket was only 22 percent (11.2 sec) slower than the Conventional bucket and 12 percent (6.8 sec) slower than the Enclosed bucket.

[1] All elevations cited are referenced to the National Geodetic Vertical Datum (NGVD).

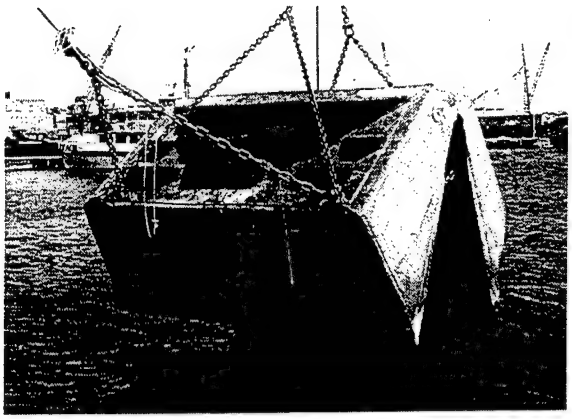

a. CableArm bucket

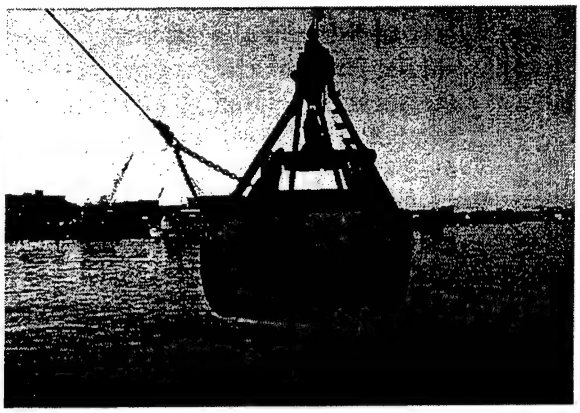

b. GLDD Enclosed bucket

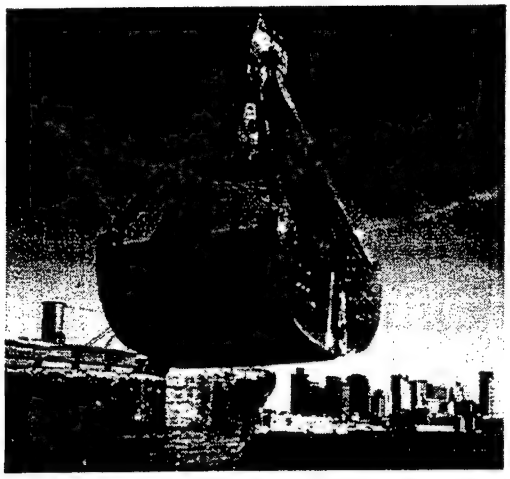

c. GLDD Conventional bucket

Figure 3. Clamshell dredge buckets used during comparison (after Welp et al. 2001)

Sediment Resuspension Data Collection Methods

Sediment resuspension data consisted of suspended solids samples and turbidity measurements collected within 8 m (in the horizontal plane) of the bucket position (near field) and 25 to 400 m from the dredge (far field). Near field data included continuous turbidity measurements taken at four depths (1.5 m, 5.5 m, 8.0 m, and 10.5 m in a water depth of about 11.6 m) and discrete water samples analyzed for total suspended solids (TSS). Far field data included indirect turbidity observations using a Broad Band Acoustic Doppler Current Profiler (BBADCP), and direct turbidity observations, conductivity, and temperature measurements, and discrete water samples for TSS calibration collected by the Battelle Ocean Survey System (BOSS).

Near field sediment resuspension data collection

Near field data collection consisted of continuous readings from D&A Instrument Co. OBS-3 Turbidity Sensors (Figure 4) calibrated for a range of 0 to 2,000 FTU (formazin turbidity units), discrete water column samples analyzed for total suspended solids, and a video recording of the dredging operation. Five turbidity sensors labeled A, B, C, D, and E were initially deployed, but Sensor A was not used because of erratic readings and calibration problems. The remaining four turbidity sensors (B, C, D, and E) were placed at depths of 1.5 m, 5.5 m, 8 m, and 10.5 m, respectively, in a vertical array deployed at the front center of the dredge barge (water depth was approximately 12 m). The sensors were calibrated and checked before being deployed each morning using a 440 FTU formazin suspension. The turbidity sensors were within 8 m (in the horizontal plane) of the bucket's digging location at all times.

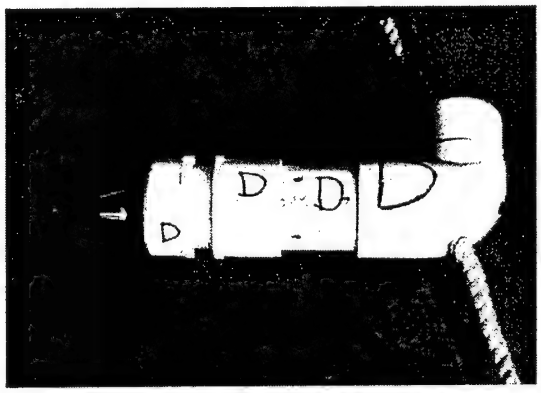

Figure 4. OBS-3 turbidity sensor (after Welp et al. 2001)

The four turbidity sensors were connected to a Campbell Scientific CR10X datalogger for data collection and storage. The datalogger received readings from each sensor at the maximum sampling rate of once per second. A laptop PC software monitored the sensor readings continuously and logged them to an ASCII data file. The software allowed the readings to be monitored real-time to identify problems and associate turbidity conditions with dredge operations.

Discrete water samples were collected and analyzed for total suspended solids (TSS) along with other TSS samples collected in the far field water column each day. Sample times and depths were recorded so the results could be correlated with simultaneous turbidity readings.

A time-stamp video camera synchronized with the datalogger clock was used to record dredge operation during most of the monitoring operations. The camera was located on the disposal barge deck where power was available and a wide view of the operation was available. The video recordings were used to recreate the dredge operation, calculate cycle times, and identify times when the dredge was down and eliminate erroneous data.

Far field sediment resuspension data collection

The Broad Band Acoustic Doppler Current Profiler (BBADCP) and Battelle Ocean Survey System (BOSS) were installed aboard the 14-m (45-ft) Battelle survey vessel *Aquamonitor* to monitor far field resuspension characteristics.

Broad Band Acoustic Doppler Current Profiler (BBADCP). The BBADCP transmits 1,200 kHz acoustic signals through the water and measures the acoustic signals that are returned to the instrument. Four of the five beams point down at a 20-deg angle from the vertical. These four beams measure the water velocity and the velocity of the boat across the bottom. Current speed and direction are determined by adjusting absolute velocity measurements for boat speed. The fifth beam points straight down, and its measurements of backscattered acoustic energy are used solely for detecting the presence of suspended sediment in the water column. Sediment particles in suspension will scatter some of the transmitted acoustic signal, returning a portion of the scattered signal back to the instrument (called backscatter). The strength of this backscatter is a function of the sediment particles' characteristics and the amount of sediment in suspension. Acoustic measurements of suspended sediment plumes uniquely provide the capability to produce three-dimensional images of plumes during a relatively short time interval. These images can be used to locate the positions of other measurements relative to a plume's boundaries and the spatial distribution of suspended-sediment concentrations. The acoustic instrument used to monitor the plume during these dredging operations was an RDI 5-beam Broad Band Acoustic Doppler Current Profile (BBADCP) (Figure 5).

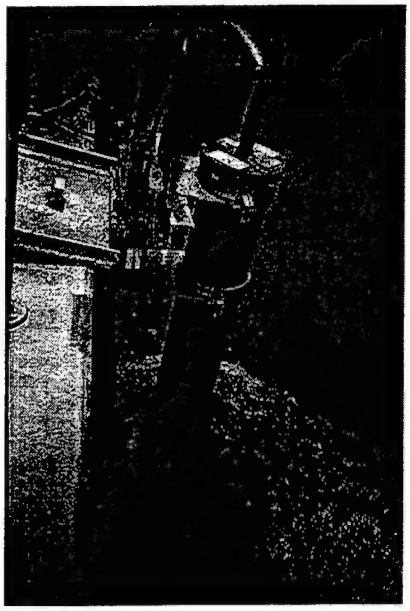

Figure 5. Broad Band Acoustic Doppler Current Profiler (BBADCP) (after Welp et al. 2001)

Battelle Ocean Survey System (BOSS). The BOSS was also installed aboard the survey vessel *Aquamonitor* for in situ water property monitoring and collection of water samples. The BOSS is comprised of an underwater towed sensor package (conductivity, temperature, depth, and in situ turbidity sensors) (Figure 6), a stainless steel seawater pump for continuous delivery of water samples to the shipboard laboratory, a winch and handling system for on-deck installation, and a PC-based software system interfaced with Differential Geographic Positioning System (DGPS) navigation for data acquisition, storage, and real-time

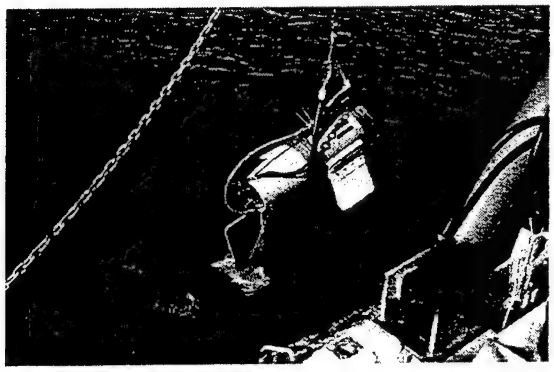

Figure 6. Battelle Ocean Survey System (BOSS) towfish (after Welp et al. 2001)

display. Water depth data from a vessel-mounted echosounder within the vessel's laboratory is provided continuously to the BOSS data acquisition system.

During the monitoring operations, the BOSS served three major functions: (a) to acquire continuous, real-time data on the BOSS towfish position; (b) to acquire real-time, in situ measurements of temperature, salinity, sensor depth, and turbidity while the sensor package was either profiling vertically or being towed horizontally; and (c) to deliver a continuous flow of seawater at a rate of approximately 12 L/min from the depth of the towed instrument package to the onboard laboratory for collection of discrete water samples. A total of 305 discrete water samples were collected using the BOSS during the background phase of the monitoring program. Collection of these discrete samples was accomplished by the onboard technician placing an empty sample bottle under the continuous flow of seawater. These water samples were filtered onboard.

Real-time data on the BOSS towfish position was computed from the known vessel position (via DGPS) and from the computed lay-back of the towfish (the horizontal distance from the DGPS antenna to the towfish). Specialized software routines developed by Battelle were used to display the salinity, temperature, turbidity, and depth data in real-time on a color monitor. Sensor data were merged with the DGPS position data and automatically stored in a BOSS data file.

Bucket Loading Characteristic Data

The average densities of dredged material placed in the barges were calculated to investigate bucket-loading characteristics with regard to the material's water to solids volume ratio. The dredged material weight was determined by recording the barges' drafts and using the displacement tables to calculate hopper material weight, and its volume was determined by measuring the height of material in the hopper and using the ullage tables (tables that relate level of dredged material in barge to material volume) to calculate hopper material volume. Other data required to calculate the water to solids ratio included the dredged material mineral and water densities. Sediment samples were collected from the hopper and analyzed to determine the mineral density, while the water density was calculated with the conductivity and temperature data collected from the towed-body previously described. No chemical analyses were conducted on any water or sediment samples collected during the study.

Laboratory tests of the average dry solids (mineral) densities of sediment samples collected from the three barges were 2.69 g/cc, 2.70 g/cc, and 2.69 g/cc, respectively, for August 5 (CableArm bucket), August 6 (Enclosed bucket), and August 7 (Conventional bucket). An average value of 1.014 g/cc for water density above the water-sediment interface was measured by the BOSS. The water-to-solids volume (loading) ratios of the buckets were calculated to be 3.75 for the CableArm, 3.97 for the Enclosed bucket, and 3.76 for the Conventional bucket, respectively. Parameters that may have influenced these ratios include the following factors. Predredge and postdredge surveys indicated that the dredged material face thickness (vertical thickness of dredged material be dredged) was

similar for the Enclosed and CableArm, but the Conventional bucket excavated approximately one-fourth full barge in a thinner face before it was relocated to an area with a similar face thickness, thereby increasing its water to solids loading ratio. More than 50 percent of the CableArm bucket's side lip seals were also missing throughout the duration of the demonstration. This condition would have allowed more water to leave the bucket as it was lifted from the water, thereby decreasing its water to solids loading ratio. Due to these varying parameters, a definitive statement cannot be made regarding the question of additional water entrainment of enclosed buckets, but the Conventional bucket still had the second lowest loading ratio overall, even after dredging in a thinner face for a significant portion of time.

Near Field Monitoring Results

Turbidity observations were the primary near field data collected during the study. However, a limited number of discrete water samples were taken coincident with turbidity readings. Thirty-three samples were collected and analyzed for total suspended solids to corroborate the turbidity data during the bucket operations. Turbidity can be used as a surrogate for TSS, but it must be recognized that factors other than sediment concentration influence turbidity. These factors, which include particle size, shape, and organic content, complicate conversion of turbidity measurements to TSS concentration. Although the data correlating turbidity and TSS values in this study were scattered, they show a definite relationship; $r^2 = 0.65$. More than 226,000 turbidity observations were collected during the three partial days used to study the three buckets. The primary advantage of using turbidity is the rapid number of measurements that can be obtained at very little additional cost per sample measurement. Additionally, the observations can be monitored on a real-time basis to gather direct knowledge about the dredging operation itself. Turbidity data collected during extended downtimes were assumed to represent background conditions and used to adjust turbidity data. Measured ambient turbidity conditions are summarized in Table 2. The results show turbidity conditions with relatively small ranges and standard deviations. These data seem to reasonably represent ambient turbidity conditions. Thus, average values were subtracted from all other turbidity observations to adjust them for ambient conditions.

Table 2
Summary of Near Field Background Turbidity Statistics; All Turbidity Values In FTU

Depth (m)	Average	Standard Deviation	Minimum	Maximum
1.5	3.9	0.34	3.0	7.4
5.5	3.3	0.56	2.2	11.7
8.0	4.0	1.0	2.7	9.0
10.5	21.4	3.8	13.3	31.0

The turbidity measurements (adjusted for ambient turbidity conditions) of the CableArm, Enclosed, and Conventional buckets are presented in Figures 7, 8, and 9. The vertical line inside the box represents the median turbidity while the shaded box represents upper and lower quartiles on either side of the mean. The whiskers extend over the range of observed data.

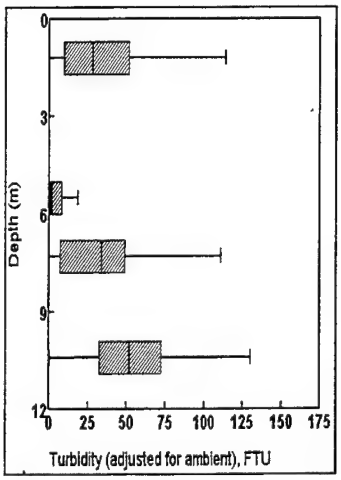

Figure 7. CableArm bucket turbidity (after Welp et al. 2001)

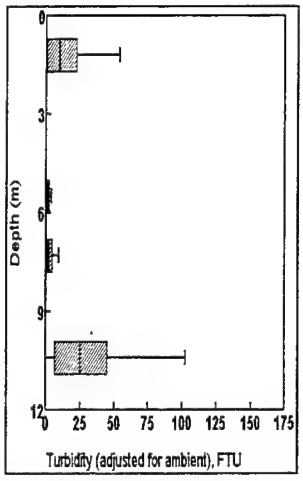

Figure 8. Enclosed bucket turbidity (after Welp et al. 2001)

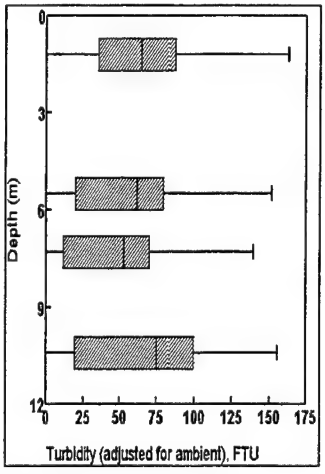

Figure 9. Conventional bucket turbidity (after Welp et al. 2001)

The Conventional bucket (Figure 9) generated the highest turbidity and suspended sediment, probably because of loss of sediments from the open top. The depth-averaged turbidity for the Conventional bucket was 57.2 FTU and suspended solids concentration was 210 mg/L (not adjusted for ambient TSS). Consistent with a prior study (McLellan et al. 1989), the Conventional bucket distributed turbidity throughout the water column. The TSS ranged from 105 mg/L in the middle of the water column to 445 mg/L near the bottom. Average turbidity varied a bit less and ranged from 46 to 64 FTU.

Although both the CableArm (Figure 7) and Enclosed bucket (Figure 8) leaked substantially through the seals and grated vents in the upper part of the buckets, neither resulted in as much turbidity or TSS as the Conventional bucket. The depth-averaged turbidities were 31 FTU and 12 FTU, respectively, for the CableArm and Enclosed buckets. The depth-averaged TSS values for the CableArm and Enclosed buckets were 31 mg/L and 50 mg/L, respectively (compared to 210 mg/L for the Conventional bucket). Six water samples were collected for TSS analysis for the CableArm bucket. Of these six samples, two were taken at a time when excessive debris were being encountered that kept the bucket from closing properly which lead to unrepresentively high TSS values (200+ mg/L) so only four samples were used to calculate the TSS depth-averaged value.

The most significant difference was in the middle water column where turbidity values were substantially less than at the bottom and near the surface. Turbidity for the CableArm bucket ranged from 6 to 55 FTU, and TSS from

14 mg/L to 66 mg/L. The Enclosed bucket resulted in turbidity from 1 to 31 FTU and TSS from 14 to 112 mg/L.

Far Field Monitoring Results

The BBADCP records data for both current and fifth-beam backscatter in bins that represent 25-cm-thick slices across each beam, continuously along the beam. The bins start 50 cm from each beam's transducer and produce valid data to near bottom. The data from all five transducers and all bins for each transducer are recorded every 2 sec.

In the monitoring reported here, the naturally occurring variations in ambient acoustic backscatter were determined from measurements made by the BBADCP along transects across the study area during times when there was no dredging. In each of the fifth–beam's 25-cm bins, the standard deviation of the acoustic backscatter was calculated for all measurements made along these transects. Since the fifth beam points straight down, these values for each bin represent the standard deviation of acoustic backscatter as a function of depth. Just prior to the start of the dredging operations, a transect was made in the area where the plume from the dredging operation was expected to be located. Acoustic backscatter values from this transect were subtracted from the values obtained during monitoring of the plume, and the results were divided by the standard deviations of the background variations. This resulted in numbers that represent the observed acoustic backscatter above background (ABAB). Horizontal positions of the BBADCP and dredge (determined by DGPS systems) were logged and, after postprocessing of the BBADCP data, plots of the ABAB relative to the dredge position and depth were produced as shown in Figures 10, 11, and 12.

Figure 10 shows the results from a transect run on 5 August, down the axis of the plume, starting near the dredge and running downstream (north to south). The distances along the horizontal axis are distances from the end of the crane that was used to conduct the dredging. An interesting feature of this transect is that near the dredge, the maximum ABAB values (and therefore the highest concentrations of suspended sediments) are not on the bottom, but approximately 3 m above the bottom. On this day, dredging was conducted with the CableArm bucket. Examination of the bucket revealed that less than half the seals on the bucket were intact, and it is possible that the higher ABAB values 3 m above the bottom are from sediment being washed from the bucket. Figure 11 shows a transect down the axis of the plume on 6 August, when dredging was being conducted with the GLDD Enclosed bucket. This figure shows maximum suspended sediment concentrations near the bottom. The relatively high ABAB values at the surface are believed to be from spillage over the side of the scow that resulted from the placement of some sample dredged material on the side deck of the scow for geotechnical sampling purposes. Figure 12 shows the dredge monitoring results for the Conventional bucket. Maximum concentrations cover more than half the water column and extend all the way to the bottom. In a general qualitative way, the conclusion drawn from these three figures is that for this operation, the

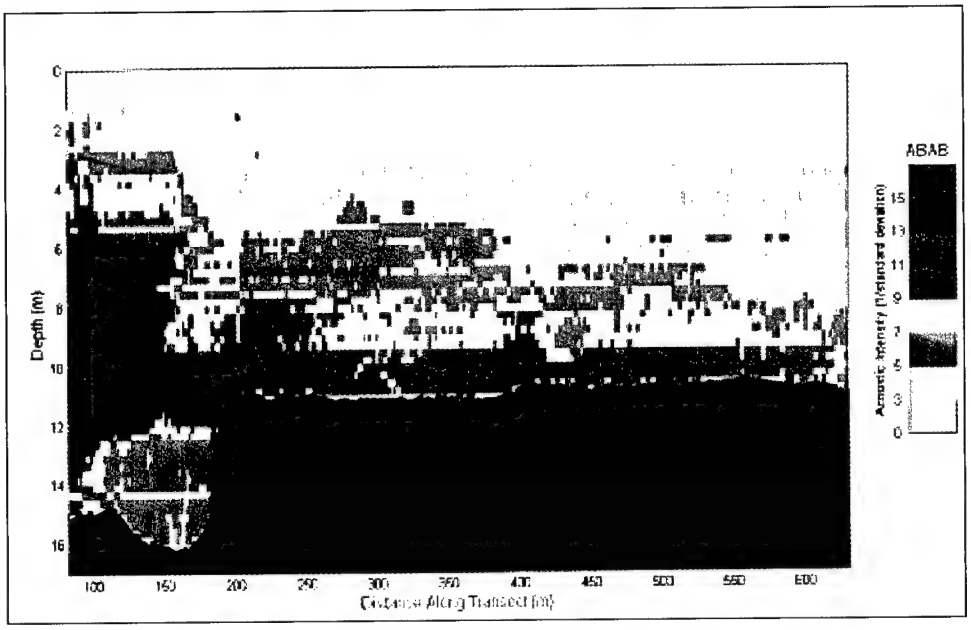

Figure 10. CableArm bucket observed acoustic backscatter above background (ABAB) (after Welp et al. 2001)

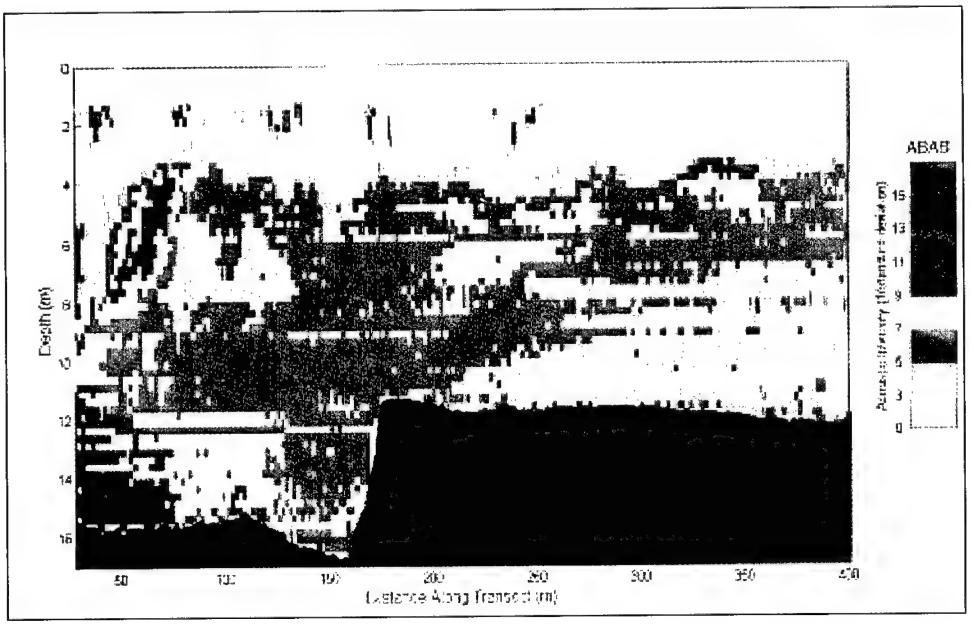

Figure 11. Enclosed bucket observed acoustic backscatter above background (ABAB) (after Welp et al. 2001)

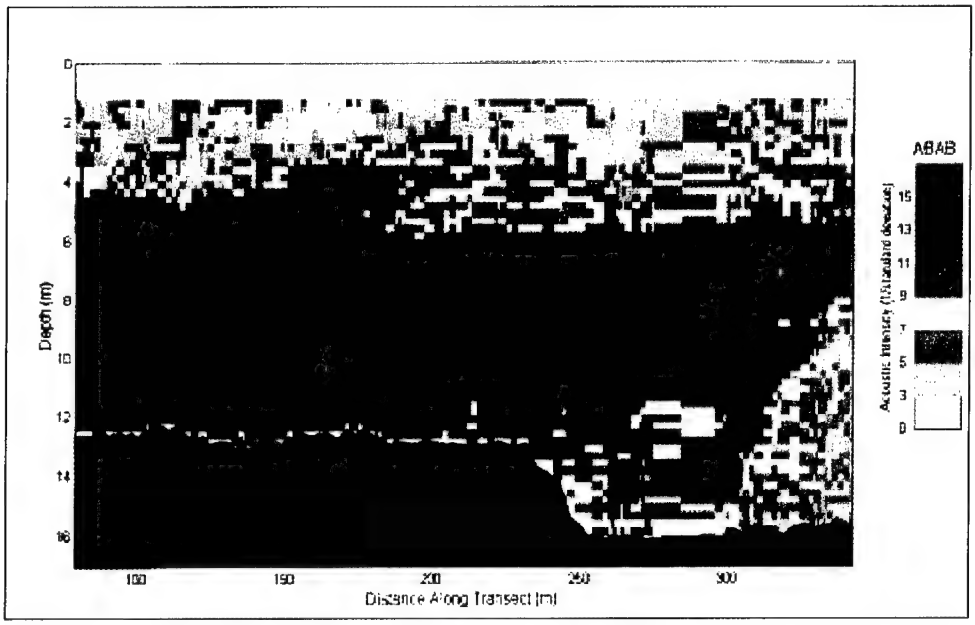

Figure 12. Conventional bucket observed acoustic backscatter above background (ABAB) (after Welp et al. 2001)

Enclosed bucket created less suspended sediment than the CableArm, and that they both produced less suspended sediment than the Conventional bucket.

The BOSS was used to acquire in situ water property data and discrete water samples at vertical profiling stations and along horizontal profiles (tows). The objective of the vertical profiling (conducted while the survey vessel was stopped/drifting) was to acquire data on temperature, salinity, seawater density, and relative turbidity throughout the water column, but an error in the BOSS data acquisition software resulted in profile measurements achieving a maximum depth of only 69 percent of that intended (and displayed in real-time aboard the survey vessel). Consequently, no data were acquired in the lower 30 to 40 percent of the water column during either the vertical profiling or horizontal towing on any of the three days of monitoring operations.

The calibration relationship between TSS concentration (mg/L) of 305 discrete water samples versus simultaneous turbidity measurements of the BOSS in situ transmissometer (in beam attenuation units of 1/m) exhibited a good correlation between the optical turbidity measurements and laboratory analysis of water samples ($r^2 = 0.93$). Consequently, all BOSS turbidity data have been converted and presented herein in units of mg/L. Figure 13 illustrates an example of one of the vertical profiles of total suspended solids (TSS), in units of mg/L (not adjusted for ambient TSS), that were obtained at four vertical profiling stations along a line extending southward from the dredge when it was using the CableArm bucket. Stations 61 and 58 were approximately 90 and 210 m south of the dredge, respectively. These profiles illustrate considerable TSS variability, presumably as a result of distance from the dredge, as well as patchiness in the suspended sediment plume that was being advected southward at a speed of roughly 17 cm/secec during the ebb tide. Closest to the dredge (at sta 61), maximum TSS values of roughly 185 mg/L were observed at 7-m (23-ft) depth,

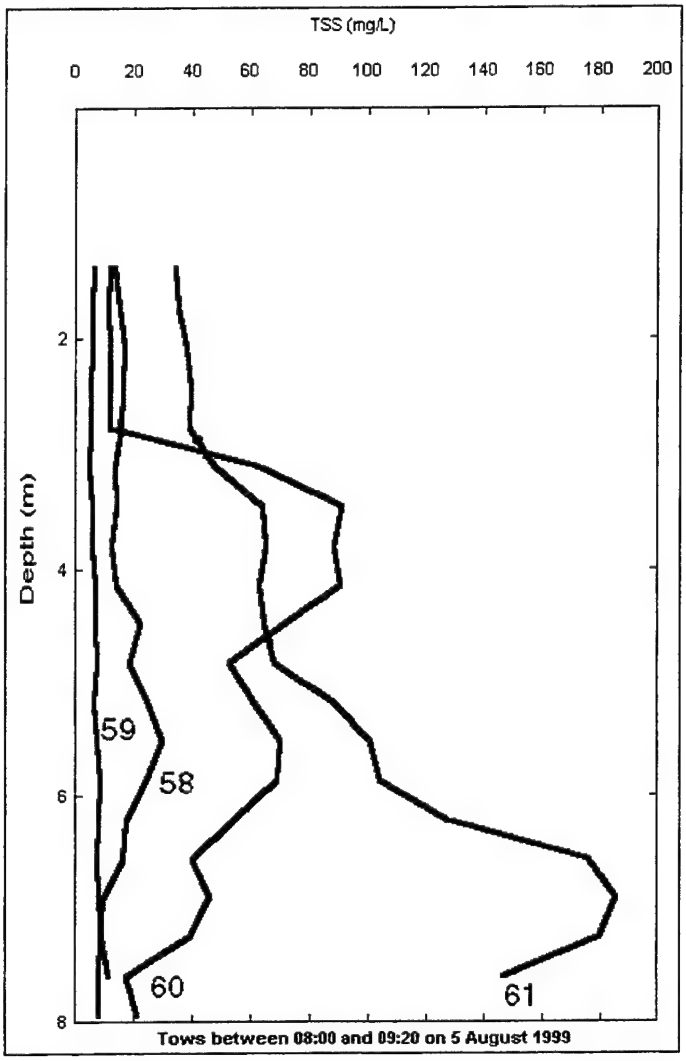

Figure 13. BOSS plots of TSS (not adjusted for ambient TSS) versus depth (numbers next to the plot lines indicate station numbers) (after Welp et al. 2001)

but note that no data were acquired in the depth range from 7 m to 10.5 m (bottom depth). Hence, if a plume of concentrated suspended sediments did exist in the lower portion of the water column, it would not have been detected by the BOSS sensors that were always situated at shallower depth.

The following is a summary of the maximum TSS concentrations encountered during the BOSS monitoring operations in the upper two-thirds of the water column:

Buckets	Maximum TSS (mg/L)	Depth (m)
CableArm bucket	200	3.5
Enclosed bucket	75	8
Conventional bucket	80	3.5 – 6.0

From these observations of maximum TSS concentrations, during each of the three days of sampling operations, it would appear that the CableArm bucket released more suspended solids in the upper two-thirds of the water column than either of the other two buckets, which is contrary to expectations. Inspection of the near field results does, however, show that maximum TSS concentrations encountered during the CableArm dredging were high and comparable to those during the conventional bucket dredging at the 1.4-m (4.5-ft) and 8-m (26.5-ft) sampling depths. These results point out that comparisons between maximum TSS observations for each day of sampling can be misleading because they do not account for variations in hydrodynamic conditions that dilute the far field suspended matter.

It is very unfortunate that the BOSS software problem precluded data collection in the lower third of the water column during this measurement program. The plumes of suspended solids in the lower 3 m of the water column most likely contained the greatest mass of suspended sediment (as indicated by the near field and BBADCP data).

Summary of Clamshell Dredge Bucket Comparison

Near field

Based on turbidity measurements, the Conventional bucket produced the highest amount of sediment resuspension spread throughout the water column. Use of the CableArm bucket appeared to reduce sediment resuspension in the water column as the observed depth-averaged turbidity was 46 percent less than observed for the Conventional bucket; insufficient TSS data were collected during the CableArm bucket operation to completely confirm this reduction, although the few data collected show an even higher reduction. The Enclosed bucket had the lowest overall turbidity and substantially less in the middle of the water column. Observed depth-averaged turbidity for the Enclosed bucket was 79 percent less than observed for the Conventional bucket. This compared well with observed TSS which showed depth-averaged TSS concentrations for the Enclosed bucket 76 percent less than for the Conventional bucket. Functional seals on the CableArm bucket would have probably further reduced water quality impacts; however, according to the contractor, these seals were difficult to maintain on this navigation job.

Far field

The BBADCP provided good qualitative data to indicate relative amounts of sediment resuspension in the plume and delineate its boundaries. BBADCP data results correspond to results from those data collected in the near field. BBADCP coverage provided insight on where to sample with the more quantitative sampling equipment of the BOSS. Regrettably, the depth error in the BOSS-collected

data limited its coverage. Collectively, the three systems yielded data that provided good insight on the different buckets' sediment resuspension characteristics, but plumes are difficult to track and measure. This difficulty stresses the need to continue developing methods to standardize plume data collection and analysis methodologies for future projects. Also, to account for variations in sediment characteristics, thickness of the dredge cut, etc., multiple days of sampling with each bucket are recommended to provide a more valid statistical basis for comparison.

3 Geotechnical Investigations of Boston Harbor Navigation Improvement Project CAD Cells

Geotechnical Investigation of CAD Cell M2[1]

The sediments placed in CAD Cell M2 were sampled and evaluated by Science Applications International Corporation (SAIC 2000a) for engineering properties during several stages: (a) prior to dredging (in situ survey); (b) during transport (barge sampling); (c) immediately after placement in the CAD cell (T_0 survey); (d) immediately prior to capping (T_1 precap survey); and (e) after capping (postcap survey).

Chronology of the geotechnical investigation

Dredging of the Mystic River began in May 1999. From May to June, material was placed in CAD Cell M2. On June 25-26, SAIC conducted both the in situ and T_0 surveys, which included surface grab sampling and gravity coring. From June until November 1999, the dredged material was left undisturbed to allow time for self-weight consolidation. In October, SAIC conducted the T_1 grab and core surveys, immediately prior to capping. In November, Cells M2 and the Super Cell were capped with clean sand from the Cape Cod Canal. Two weeks after capping was completed, Ocean Surveys, Inc. (OSI) collected sediment vibracores from Cell M2, completing the postcap geotechnical investigation survey.

[1] This section is extracted essentially verbatim from Science Applications International Corporation (2000a).

Predredging sampling (in situ survey)

The geotechnical investigation was initiated near the end of dredging of the Mystic River; therefore the in situ survey involved collecting in situ material in the Mystic River channel representative of the dredged sediments. Samples were collected in areas of the Mystic River that were not previously dredged as part of the BHNIP. The in situ survey took place simultaneously with the T_0 survey in June of 1999.

Grab sampling. Grab sampling for the in situ survey was conducted on June 22. Surface sediments were collected using the grab sampler at eight locations in the Mystic River, including three in CAD Cell M2, and two in the Super Cell. Three stations were located in the Mystic River, outside the CAD cells, to obtain samples representing the in situ material prior to dredging. At each station, five to seven grabs were obtained within a 50-ft radius of the target station location. Grabs were collected in order to collect enough surficial sediment to fill one 5-gal bucket per station.

Core sampling. Coring for the in situ survey was conducted on June 24-25. Using a 10-ft barrel, a total of 10 gravity cores were collected at eight stations in the Mystic River. Stations MR-E and MR-H were sampled a second time due to low recovery in the initial cores. The second core samples obtained at these stations were labeled MR-EB and MR-HB (see SAIC (2000a), Figure 2-2).

Sampling in the transport barge (barge sampling)

Dredging operations in the Mystic River had been completed by the time of the barge sampling; therefore, material originating from the Inner Confluence (an area similar to the Mystic River) was sampled. Dredging of the Inner Confluence began July 28, 1999. Five-gallon bucket samples were collected from a barge on July 30. Although the Inner Confluence material is influenced by input from the Chelsea River (which is sandier), this was considered to be the optimum material match for this sampling.

Grab sampling. On July 30, 1999, three 5-gal bucket samples were collected from a full barge of material dredged from the Inner Confluence. One 5-gal bucket sample was collected from the surface of the barge, representing the most fluid material resident in the scow. This was conducted by tying a rope to the bucket handle and pulling the bucket across the top of the material in the barge. In addition, GLDD assisted by using a clamshell bucket to subsample the barge and placing the material on the deck at the edge of the scow. Two 5-gal bucket samples were collected from this material: one from a soft, siltier area, and one from a sandier unit. It is possible that this material had de-watered prior to bucket sampling. The three 5-gal bucket samples were deemed to represent end-member units of material in the barge.

Core sampling. No core samples could be taken in the transport barge.

CAD sampling immediately after placement of material (T_0 survey)

The last disposal of Mystic River silt into the CAD cells was June 1 for Cell M2 and June 7 for the Super Cell. On June 20, after conferring with the BHNIP Technical Advisory Committee (TAC), Cell M2 was selected for the geotechnical investigation program. This cell was chosen because it is more representative of the majority of other CAD cells and located farther away from the center of the channel, yielding less ship traffic. For the T_0 survey, grab and core samples were collected from Cell M2 in June 1999. Grab samples were also collected from two stations in the Super Cell and shipped to ERDC for analysis.

Grab sampling. Grab sampling for the T_0 survey was conducted on June 22, immediately after the completion of all disposal of dredged material in Cell M2. Grab samples of the dredged material were obtained at three stations randomly located within the cell. At each of these stations, six grabs were required to fill the 5-gal bucket. Grab sampling also took place in the Super Cell during the T_0 survey. Within the Super Cell, six grabs at Station SC-A and seven grabs at Station SC-B (see SAIC (2000a), Figure 2-1) were used to fill the 5-gal buckets.

Core sampling. Core sampling in Cell M2 as part of the T_0 survey took place on June 24-25. Nine core samples were obtained at seven stations located randomly within the cell. One additional gravity core sample was collected at sta M12-A in Cell M12 (see SAIC (2000a), Figure 2-2), which had been capped in 1998. This core was collected to provide comparison with gravity cores collected in M12 prior to capping.

CAD sampling immediately prior to capping (T_1 survey)

CAD Cell M2 was left undisturbed for a period of 5 months, allowing time for self-weight consolidation. SAIC collected grab and core samples from Cell M2 (T_1 survey), in late October, prior to the commencement of capping on November 3, 1999.

Grab sampling. Grab sampling for the T_1 survey (immediately prior to the capping of the dredged material) took place on October 20, 1999. A total of six individual grabs were collected in Cell M2: two grabs from Station M2-Aa; two grabs from Station M2-Bb; and two grabs from Station M2-Cc (see SAIC (2000a), Figure 2-3). Target locations used for grab samples in the T_1 survey were also used in the T_0 survey.

Core sampling. Core sampling for the T_1 survey took place on October 22, 1999. Using a 10-ft steel core barrel, gravity cores were taken at eight stations in Cell M2, immediately prior to capping. A total of 12 gravity cores were collected, 11 cores from the eight stations in Cell M2 and one from sta M12-CTR within the capped Cell M12. Duplicate cores were collected using additional drive weight for stations M2-Dd, M2-Ee, and M2-Ff (see SAIC (2000a), Figure 2-4), due to poor yield on the first attempt.

CAD sampling after capping (postcap)

The capping of Cells M2 and the Super Cell began on November 3 and was completed on November 18. Under contract to Great Lakes Dredge and Docks (GLDD), OSI conducted a vibracore survey of Cell M2 from November 31 to December 2. Postcap cores were provided to SAIC by GLDD on December 3, 1999, for analysis under the geotechnical investigation.

Grab sampling. There were no grab samples collected in the postcap survey.

Core sampling. The postcap coring survey was conducted by Ocean Surveys, Inc. (OSI) under contract to GLDD from November 30 to December 2, 1999. Six 20-ft vibracores were obtained at six stations in Cell M2. SAIC obtained the M2 cores from GLDD on 3 December along with the geodetic location of each core. These cores had been cut to 6-ft sections; each section was clearly marked with top and bottom indicators as well as station names.

Water content analysis

The geotechnical data collected during the various stages of the geotechnical investigation challenge the typical process of evaluating capping effectiveness. The only clear diagnostic change of properties between the T_0 and T_1 surveys was in the water content of the sediments collected in the grab samples. The average water content of the surface sediment as collected by the grabs decreased between the two surveys, from 209 percent to 165 percent. The surface conditions detected were expected, due to past survey operations and the dewatering of dredged material over time. The T_0 survey contained a slightly greater amount of water (209 percent) than the in situ survey (181 percent). This increase in water between in situ and T_0 surveys was expected, due to the introduction of water to the material through dredging. The average water content in the upper 50 cm of the cores collected during the two surveys showed little change over time and remained approximately 100 percent. Cap readiness is most dependent on the upper sediment column and comparing the upper core and grab sample data may be the most important factor in determining cap-readiness. The water content data support the field observations conducted by GLDD during the consolidation period. Grab samples were collected from the surface of the pit and placed on a target board with concentric circles documenting the relative spread of the material. The series of photographs, showing decreasing spread of the material with time, provided evidence of the decrease of water content in the surface sediments through the consolidation period.

Other than the water content of the surface grabs, no clear, statistically different changes in the physical parameters measured would suggest the CAD sediments were ready to be capped, yet most of the sediments in Cell M2 were successfully covered with relatively clean cap material. In addition, the presence of the single postcap core with no sand suggests that the mechanisms of settlement and stability of the dredged material/cap deposit may be more complex than what was revealed through the evaluation of sediment properties.

Grain size analysis

Statistically the changes in grain size were insignificant. However, in evaluating capping success, the sand content of the material is important. The initial grab grain size results indicate the in situ Mystic River samples were almost identical to those found in Cell M2. A higher sand component and less clay were found in the T_0 survey compared to the T_1 survey results. The primary difference between precap surveys was in the relative lack of coarse sand in the earlier surveys and a decrease in the amount of medium and fine sands while self-weight consolidation was taking place in the CAD cell. The results suggest that coarser sediment grains settled within the sediment to deeper depths in the CAD cell. The amount of clay present at the surface interface increased by 3.2 percent between the two surveys, potentially from fines settling from the water or from the channel above the cell.

The variation in grain size between surveys is an indication of the high variability of the material in the cell. The percent sands detected in the cores between surveys ranged from 2.56 (in situ) to 8.75 (T_0). Postcap grain size samples were collected from in the sand cap as well as below the sand cap in an effort to obtain data on potential mixing of the sand cap with the dredged material. The samples collected from the sand cap contained 0.63 percent silt and clay. While the percent of fine sand detected below the sand cap was the highest of all the surveys (16.4 percent), it was only 6 percent higher than the average of the T_0 survey (10.6 percent). The decrease in sand from the precap surveys suggests that mixing of the cap material was minimal to nonexistent. The silt and clay content was fairly consistent between surveys indicating little change in material composition below the cap. The lack of sand in the material below the cap indicates that the cell material had a bearing strength capable of supporting the higher density of the sand cap.

Atterberg limit analysis

One of the goals of the geotechnical investigations was to evaluate how the process of dredging changes the engineering characteristics of sediments. Hydraulic dredging completely remolds the sediment, thereby changing the geotechnical properties from the original in situ values (Poindexter-Rollings 1990). Although the BHNIP dredged material was removed using mechanical methods (closed clamshell), the dredging process appeared to have altered the sediment's inherent strength characteristics. Atterberg limits data from the in situ sediments, along with data from the other phases, were compiled into Casagrande's plasticity chart that shows the relationship between the liquid limit and plasticity index relative to standard soil classifications (Figure 14). The plasticity chart provides an indication of the physical state of sediment, ranging (for saturated sediments) from plastic to liquid states as a function of the natural water content.

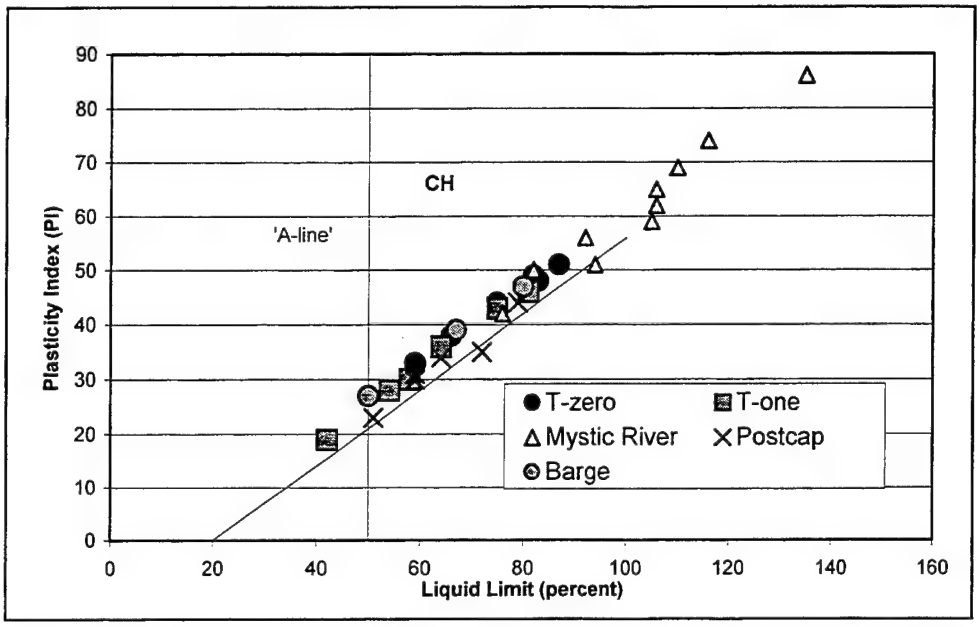

Figure 14. Plasticity chart for five survey phases showing Atterberg limit data relative to the "A-line" soil classifications (CH is the standard classification for inorganic clays of high plasticity) (after Science Applications International Corporation 2000a)

All of the samples collected from this project fell into the CH classification relative to the plasticity chart, representing inorganic clays of high plasticity. The samples collected from the in situ cores, however, had liquid limits (LL) values of >100 percent and plasticity index (PI) values of >50, while almost all of the samples collected from both the barge and Cell M2 were less than 100 percent LL and 50 percent PI (Figure 14). The three barge samples fell into the range of the cell M2 survey data and outside of the range of the in situ Atterberg limit data. The decrease in the liquid limits of the in situ sediments after dredging indicates that dredging disturbed the fabric of the sediments, reducing the cohesion of the fine-grained sediments and thereby reducing the strength. Shear strength data were consistent with this observation. The shear strength of the upper 50 cm of cores from the in situ and T_0 surveys decreased from an average of 1.8 kPa to 0.4 kPa (excluding all data from Boston blue clay).

Shear strength analysis

One of the major elements that controls the construction of a successful cap is that the shear stress along the interface between the cap and underlying sediments must not exceed the strength of the dredged material (Bokuniewicz and Liu 1981). Shear strength is the greatest stress that a material can withstand before failure. Shear strength increases in consolidated sediment, and generally increases with depth. Lengthening the time allowed for consolidation of the dredged material prior to capping should theoretically increase the shear strength of the sediment. The strength of the deposit will further increase under the weight of an over-burden, that is, the sand cap. Because of the importance of the strength element in

the assessment of the engineering properties of the dredged material, shear strength of the cored sediments recovered in different phases of the geotechnical investigations was evaluated more closely.

Shear strength measurements were plotted as a function of depth in the sediment cores for the three Cell M2 phases (Figure 15). A best-fit curve (first order polynomial) was selected to show the general trends of increasing shear strength with depth. Shear strength values from Boston blue clay and the sand cap were excluded from this analysis. The data showed that there was a rapid increase of shear strength down core, specifically in the upper 1 m of the cores for the T_0 and T_1 surveys. Part of this increase may be an artifact of coring, as the sediment consolidates more rapidly in the core liner and an increase in strength of the sediments at the bottom of the core is expected. Shear strength sample graphs for the BHNIP geotechnical investigations are shown in Figure 16.

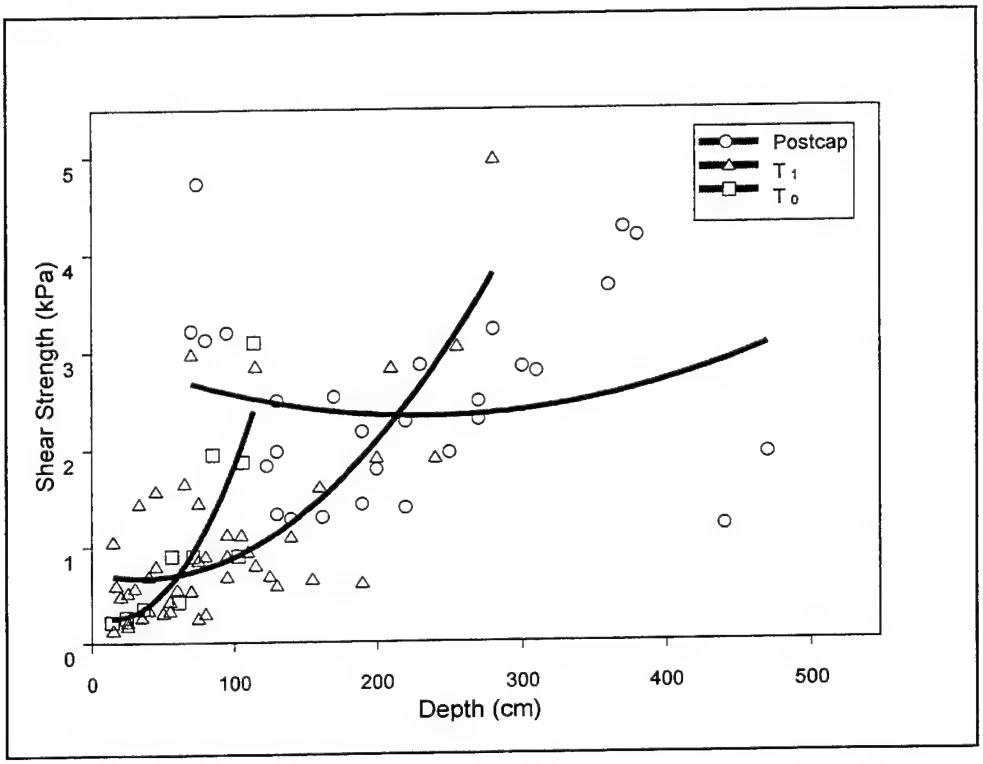

Figure 15. Water content for upper sediments for three project phases (after Science Applications International Corporation 2000a)

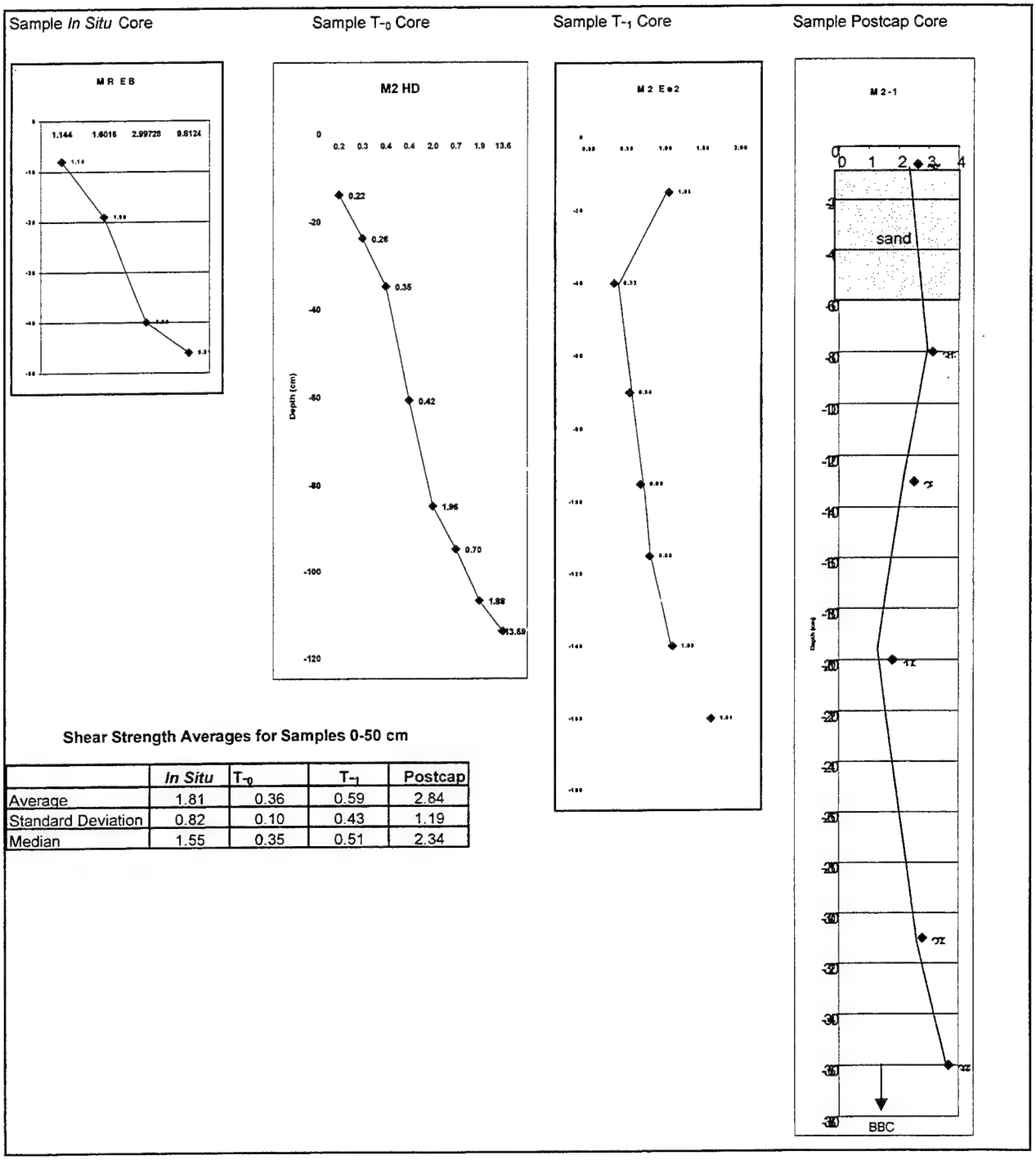

Shear Strength Averages for Samples 0-50 cm

	In Situ	T_0	T_1	Postcap
Average	1.81	0.36	0.59	2.84
Standard Deviation	0.82	0.10	0.43	1.19
Median	1.55	0.35	0.51	2.34

Figure 16. Shear strength sample graphs for the Boston Harbor Navigation Improvement Project (BHNIP) geotechnical investigation (after Science Applications International Corporation 2000a)

Most notable was the increase of shear strength in the sediments immediately below the cap. In fact, the shear strengths were higher in the top meter as compared to the sediments below, suggesting that the placement of the cap caused the surface sediments to consolidate, but the deposit had not reached equilibrium relative to a standard strength profile.

The data from only the upper 100 cm of cores collected during each phase of the investigation were evaluated for significant change. Samples from the upper meter of fine-grained sediment below the cap were evaluated for the postcap data. The average shear strength decreased from the in situ sediments (Mystic River, 1.7 kPa) to being placed in Cell M2. Both the T_0 and T_1 sediments had very similar shear strength properties (average of 0.7 kPa), and then increased again with placement of the cap to values that were higher than the in situ sediments (average of 2.1 kPa). These data would suggest that the capping process itself was much more effective in increasing the bearing strength of the sediments as compared to self-weight consolidation. Capping-induced consolidation resulted in sediments of strength similar to in situ material, suggesting that precapping might be useful for future projects.

The very low shear strength of the sediments in the CAD cell during both of the precap surveys increases the uncertainty of the actual bearing strength of these sediments. Although the viscometer used for the soft material had a very high sensitivity (0.03 kPa), some caution is warranted to try and evaluate the strength characteristics of this material between these two surveys. The coring process, as well, can serve to alter the in situ shear strength.

Diagnostic measurements to determine cap readiness

One of the goals of this study was to determine the material properties that would allow predictive modeling of consolidation and sediment strength to be used in future projects. The cap at Cell M2 was the most successful to date of the BHNIP, with up to 1 m of tan to gray/black sand overlying the dredged material in five of six cores collected. The homogeneity of the sand was apparent in the bulk density log data, showing the higher bulk density of the sand cap (approximately 2.0 g/cc) overlying the dredged material (approximately 1.5 g/cc). The log data also showed an increase of bulk density with depth in the sediments below the cap, suggestive of a normal pattern of consolidation. The one exception was Core M2-4, which had no evidence of sand throughout the whole core. The physical parameters of this core were extremely uniform all the way down the core, including no apparent increase of bulk density to the bottom of the core (Figure 17).

After sand cap deposition at Cell M2, the sediments consolidated more rapidly than under self-weight conditions, as shown by the lack of topographic change after the cap material was added to the top of the deposit. The process of consolidation requires an expulsion of pore water that may cause layers to deform. In the case of the BHNIP, because of the impermeability of the Boston blue clay which formed the sides and bottom of the cell, the expelled pore water was restricted to movement up through the cap. The recovery of Core M2-4 indicates

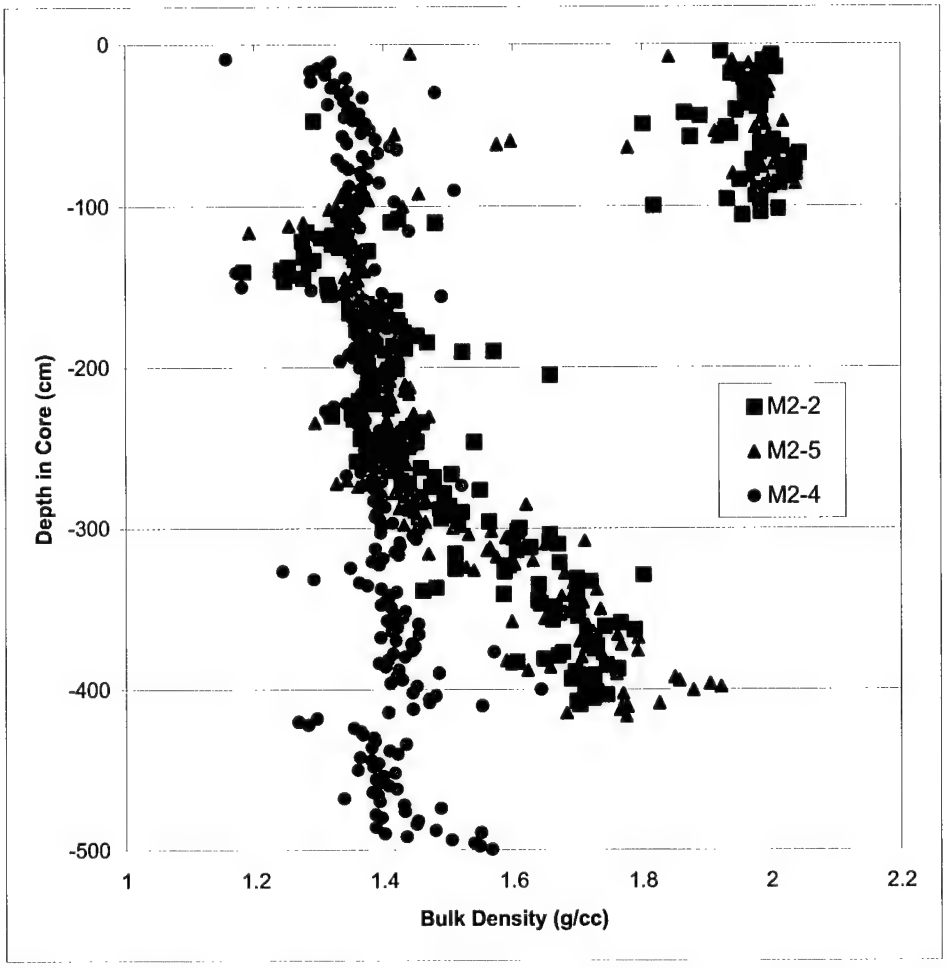

Figure 17. Logged bulk density data from selected postcap cores (after Science Applications International Corporation 2000a)

it is also possible that pore water expulsion, and the resulting release of excess pore pressure, was focused in destabilized areas of the cap. This diapiric process has been suggested as a mechanism for the presence of fine-grained sediments that were above the caps in the earlier cells. Subbottom data collected from Cell M2 showed potential diapir-like structures (mud flows) through the cap. The subbottom data collected in the Super Cell along with cores collected and analyzed by OSI also support the theory of diapirs. The presence of these diapirs is consistent with the physical properties of Cell M2 Core M2-4, which showed that the sediments were relatively constant with depth. In the case of the BHNIP, the fact that the cells were dredged in essentially impermeable Boston blue clay was potentially the most important variable for capping success, in that expulsion of pore water was restricted to upward movement.

The ability to predict and evaluate the efficacy of capping in a confined environment depends not only on accurate geotechnical measurements of the dredged and capping material, but also on a thorough understanding of the geotechnical framework of the disposal site. During Phase 1, the cell had two weeks to consolidate before being capped. The consolidation time allotted for the

first three cells in Phase 2 varied, as did the final capping results. Cell M5 had approximately 2.75 months between the bulk of disposal and capping, which seem sufficient for that cell. Cell M4 had approximately 1 month to consolidate before the capping began and Cell M12 had the majority of the material deposited 2 months prior to capping. In each cell, sand and silt mixing occurred and was unique.

The additional time given to Cell M2 (5 months) during the second round of Phase 2 capping was adequate to support the sand cap with little to no mixing. Subbottom data and core results indicate that additional time might have been needed for the Super Cell to self-weight consolidate. This is assumed to be primarily due to the size of the cell, the impermeability of Boston blue clay, and the additional water added to the dredged material through dredging. Based on the results of all the cap surveys conducted under the BHNIP protect, it is evident that the size of the cell, as well as the geotechnical properties of the material, need to be evaluated to determine the appropriate self-weight time. During the 5-month consolidation time of Cell M2, the change in water content of the surface sediments (as collected in the grab samples) was the single measured geotechnical parameter that clearly provided an indicator of "cap-readiness."

In looking at the diapir type anomalies within the capped cells, it is noted that diapirs most frequently formed near the edges and corners of the cell. This suggests that the more fluidized material was collecting near the edges or being forced to the edges during the capping process. The material may have also required the strength of the cell wall to aid in upward movement. Diapir formation may be dependent on numerous factors involving the material's water content, shear strength, the capping process by which the sand is placed in the cell, the potential relationship with the cell wall, and the wall's permeability.

In the broader view, evaluation of the relative success of a capping project needs to be measured against the overall environmental goals of the project. In the case of the BNHIP, the sand cap in Cell M2 was determined to be providing a practical barrier between the majority of the underlying dredged sediments. If additional protection were required for a project, a phased capping approach might be considered, as the process of capping appears to serve as the best mechanism to stabilize the underlying sediments.

Conclusions

The natural cohesion and strength of the Mystic River sediments were altered by the dredging process, resulting in sediments in the CAD cell that were unstable due to high water content and low shear strength.

During the 5-month consolidation time, the change in water content of the surface sediments (as collected in the grab samples) was the single measured geotechnical parameter that clearly provided an indicator of cap-readiness.

Capping-induced consolidation resulted in sediments of strength similar to in situ material, suggesting that precapping might be a useful operational approach for future projects.

The results from Core M2-4 and subbottom profiling records suggested that excess pore water was released not only through the cap but also was vented through diapir structures that served to breach the caps in discrete areas.

Future projects should include an evaluation of the geological environment that is under consideration for a CAD project, such as an evaluation of the in situ strength of the material to be capped and the porosity and permeability of the CAD cell sediments. Consideration of innovative capping approaches, including a phased capping approach, should also be considered.

Future project sampling plans should be designed to focus on the top meter of material within the CAD cell and at set intervals.

Boston Harbor CAD Cell Capping Simulation[1]

Geotechnical analysis of some capped cells indicated that the dredged material placed in those cells most likely had insufficient upper surface bearing capacity to adequately sustain the induced sand cap weight. One cell in particular (Cell M2), which performed adequately, was chosen for a more detailed performance analysis prior to, during, and after the cap was placed. Cell M2 observations showed that extending the dredged material sediment consolidation period prior to capping allowed the sediment shear strength to increase sufficiently to adequately resist the superimposed cap weight. Changes in sediment characteristics and material properties most critical to predicting cap performance were observed during field sampling efforts. As an example, changes in sediment consistency were monitored by dropping grab sample contents onto a flat surface and observing the concentric spread diameter and changing sample height. The Cell M2 dredged material sediment was undergoing in situ self-weight consolidation while achieving higher shear strengths and lower water contents during the 5-month period prior to sand capping. Just prior to sand capping, sediment samples were taken, and it was determined that the upper 3-ft (1-m) layer of precapped sediment had achieved very low shear strengths of about 20 psf (1 kPa), with water content (weight of water per weight of solid) averaging 100 percent in the upper 20 in. (50 cm). The Cell M2 was then capped with a 3-ft (1-m) layer of fine sand, and postcap samples indicated that the underlying dredged material sediment adequately resisted the overlying sand cap weight.

Simulations were performed using analytical modeling with geotechnical software, physical modeling with a centrifuge, and laboratory testing to obtain material properties. The goals of the simulations were to (a) apply modeling techniques to obtain geotechnical performance parameters and characteristics enabling better understanding of the sediment capping process, (b) enable better

[1] This section is extracted essentially verbatim from Lee (in preparation).

predictions of required minimum geotechnical parameters necessary for capping, and (c) expand upon a potential field monitoring method to enable faster characterization of sediment properties.

Sediment material characteristics testing

A surrogate dredged material having similar geotechnical properties was chosen to represent the actual contaminated sediment material. Homogeneous soil types of lean clay (CL), fat clay (CH), white kaolinite clay (CL), and silt (MH) were mixed with varying amounts of water to achieve a water content ranging from 31 percent to 102 percent. Each soil's remolded undrained shear strength was taken at the corresponding water content using the laboratory miniature vane shear device (American Society for Testing Materials (ASTM) 2000). The kaolinite soil was chosen as the surrogate dredged material for physical modeling in the centrifuge based on the laboratory test results most closely resembling those from the Cell M2 sediment.

An expanded method for obtaining in situ sampled sediment properties consisted of modifying the flat board method used at Boston Harbor Cell M2. A device similar in function to the concrete slump test method (ASTM 1999) was utilized for the dual purpose of correlating undrained shear strength to water content as well as providing a method to monitor those properties for the physical model. The remolded soil was placed in the slump cylinder, filled to the top, and leveled. The cylinder was then slowly lifted in an upward motion similar to the concrete slump test method, and the height difference (slump) was measured after the soil flowed out and reached its equilibrium height (Figure 18). The dredged material slump cylinder may be utilized as an indication of soil slurry consistency, which is related to the soil water content and shear strength. Figure 19 illustrates the relationships between soil consistency (slump), water content, and undrained shear strength for the kaolinite soil.

Analytical modeling of the CAD cell

A two-dimensional finite element program developed at ERDC, STUBBS, was available to model the geotechnical parameters assigned to simulate dredged material sediment underlying sand cap layers. The software simulated the complete cap placement process by sequentially placing layered elements until the final confined aquatic disposal cell geometry mesh was created (Figure 20). The dredged material was modeled as a homogeneous frictionless material with a cohesion parameter equal to the undrained shear strength. This representation was based on the assumption that in the initial nonconsolidated state, the material

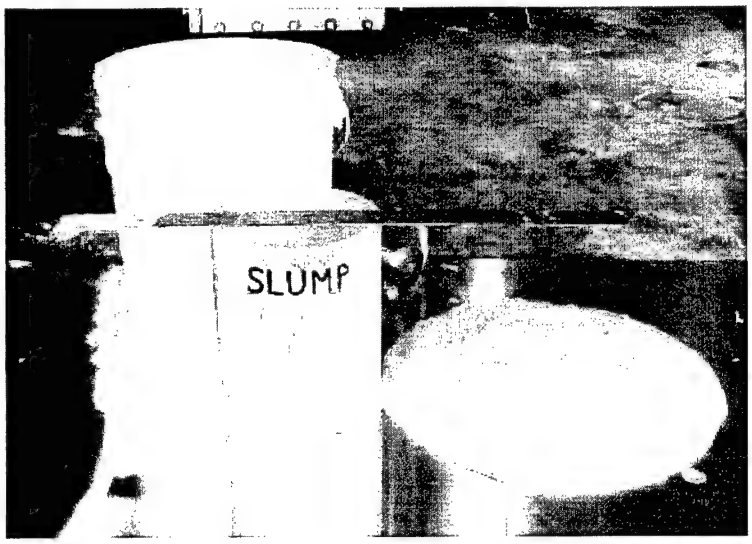

Figure 18. Slump test of kaolinite soil with approximate shear strength of 25 psf (1.2 kPa) (after Lee, in preparation)

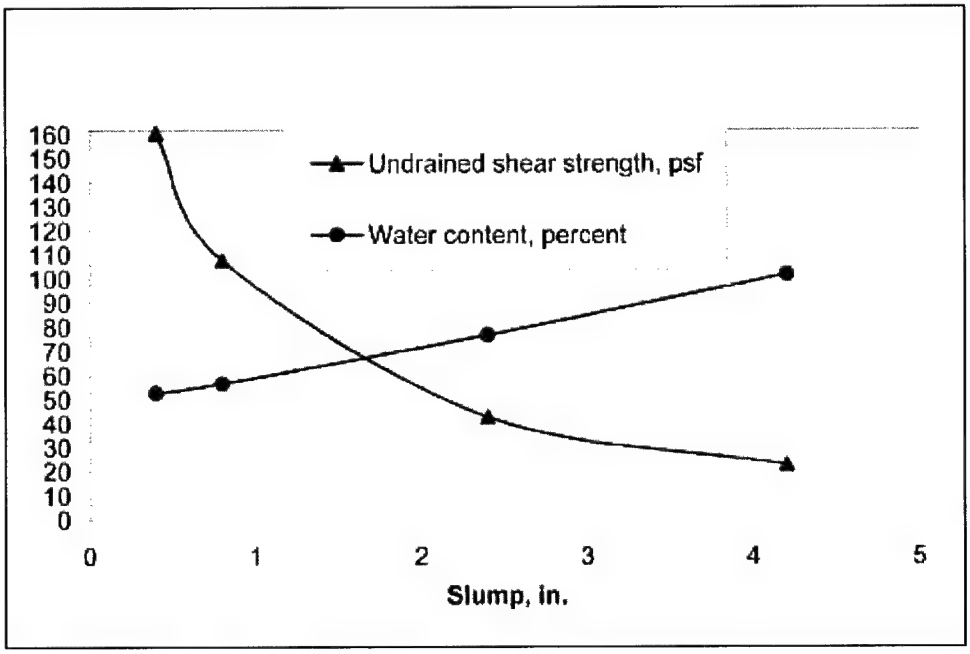

Figure 19. Kaolinite soil slump, water content, and shear strength relationships (after Lee, in preparation)

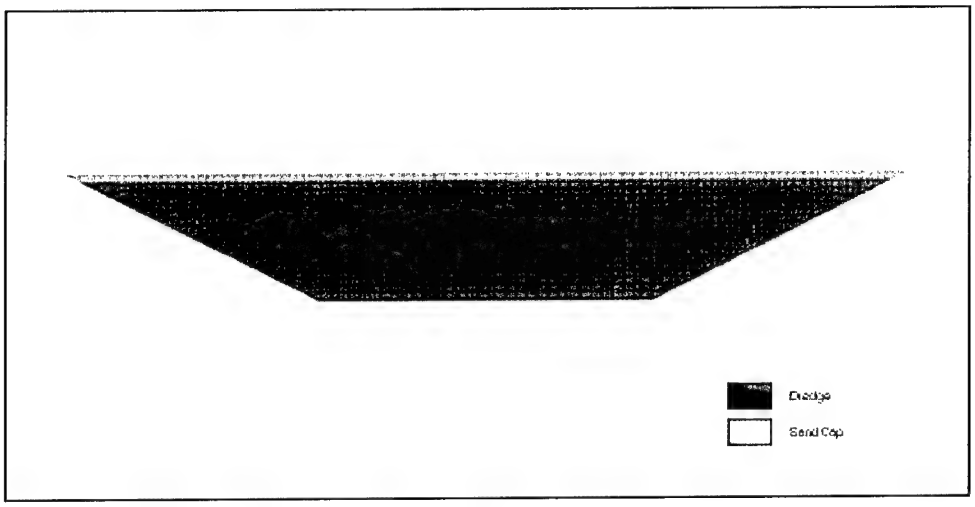

Figure 20. STUBBS finite element mesh for sand cap stability analysis (purple indicates dredged material sediment; orange indicates overlying sand cap) (after Lee, in preparation)

would be similar to the as-disposed uniform state. The physical modeling with the centrifuge served to confirm this conservative assumption. The stresses and displacements were computed for the partially filled cell after each layer was placed. The geotechnical stability of the capped cell was characterized by the extent of plastic yielding within the dredged material. Initial upper strength boundary conditions were assigned, and a series of computations were performed. As the shear strength of the dredged material was reduced toward a lower bound, the yielding deformation pattern grew into a state of failure. As the lower bound strength was approached, the model became unstable, and eventually the stress computations did not converge.

The surface geometry of the overlying sand layer was modeled after in situ depth soundings at Cell M2, which indicated that the surface slope of the sand typically varied by a few percent. The mesh elements in the sand layer were thickened to create a small 100-ft- (33-m-) wide mound on the sand surface. The mound reached a maximum height of 0.5 ft (0.15 m) above nominal elevation of the sand surface to create a 1 percent slope (Figure 21).

Significant yielding under this slight mound was observed when the assumed strength of the clay sediment was decreased to 17 psf (0.8 kPa) (Figure 22).

At 5 psf (0.2 kPa) the modeled deformation yielding indicated an essentially complete failure mechanism, although an equilibrium solution was maintained (Figure 23).

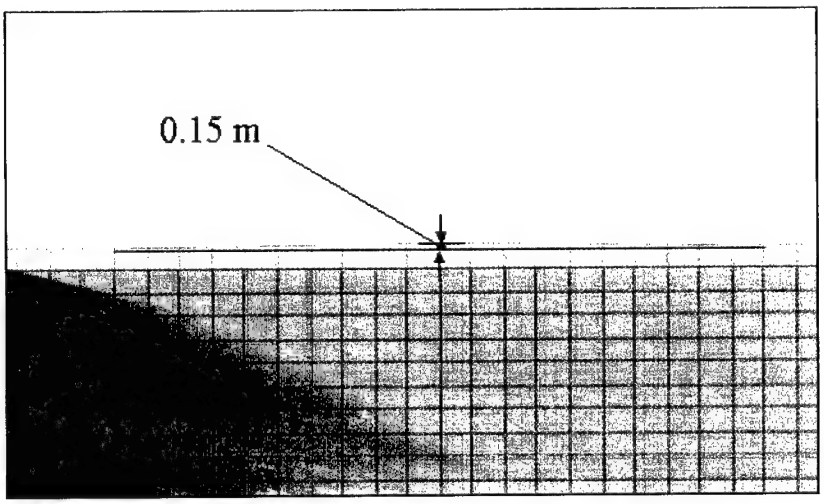

Figure 21. STUBBS finite element mesh showing maximum height variation of overlying sand cap and details of sand "hump" (after Lee, in preparation)

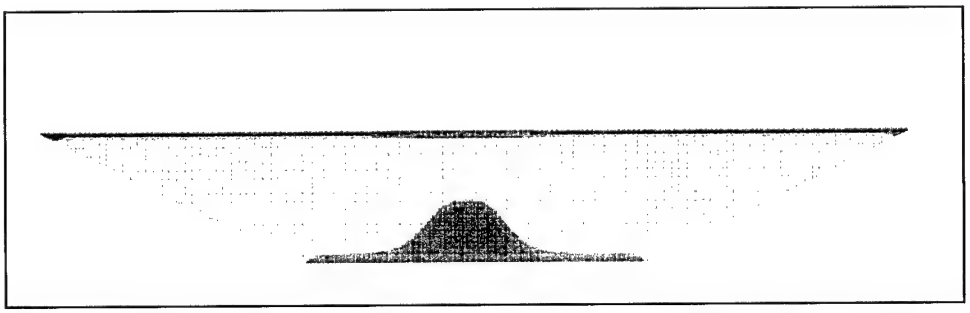

Figure 22. STUBBS finite element mesh indicating onset of failure for undrained shear strength at S_u = 17 psf (0.8 kPa) (after Lee, in preparation)

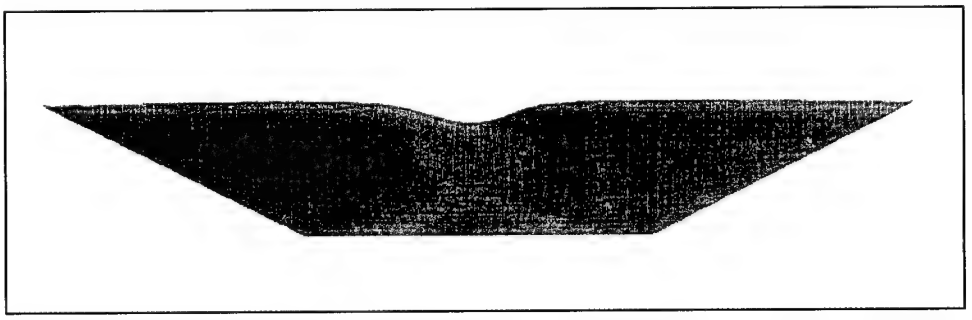

Figure 23. STUBBS finite element mesh indicating deformation failure for undrained shear strength at S_u = 5 psf (0.2 kPa) (after Lee, in preparation)

At 2.5 psf (0.1 kPa) convergence in the solution could not be obtained. The deformation pattern in all modeled cases indicated that the principal plane of shear developed along the base of the confined aquatic disposal cell rather than within the fill material, suggesting that the size and shape of the cell bottom controlled the critical shear surface. From these modeling results it appeared that an undrained shear strength of about 20 psf (1 kPa) was a reasonable criteria for dredged material strength prior to capping provided the cap thickness can be maintained to the tolerance of the Cell M2.

Physical modeling of the CAD cell capping process

The numerical modeling results provided insight into the lower range of required undrained shear strength in the dredged material and the results appeared to be consistent with Cell M2 field performance. However, the numerical model was based on numerous assumptions, and did not account for possible pore pressure effects related to pore water upwelling as the consolidation process took place. The present scope of numerical modeling did not address such transient effects, although STUBBS has the capability to deal with such effects including coupled flow and deformation (consolidation). In addition, field observations did not include pore-pressure effects. To observe cell cap performance due to these effects, and to help validate the analytical modeling effort, it was necessary to perform physical modeling.

Physical modeling on the geotechnical centrifuge provided a link between the numerical computations and field observations. The centrifuge intensifies the gravity-induced body forces to allow dimensionally correct scale models that more accurately reflect the physical processes. Physical modeling was accomplished using the U.S. Army Centrifuge Facility at the U.S. Army Engineer Research and Development Center, Vicksburg, MS (Figure 24).

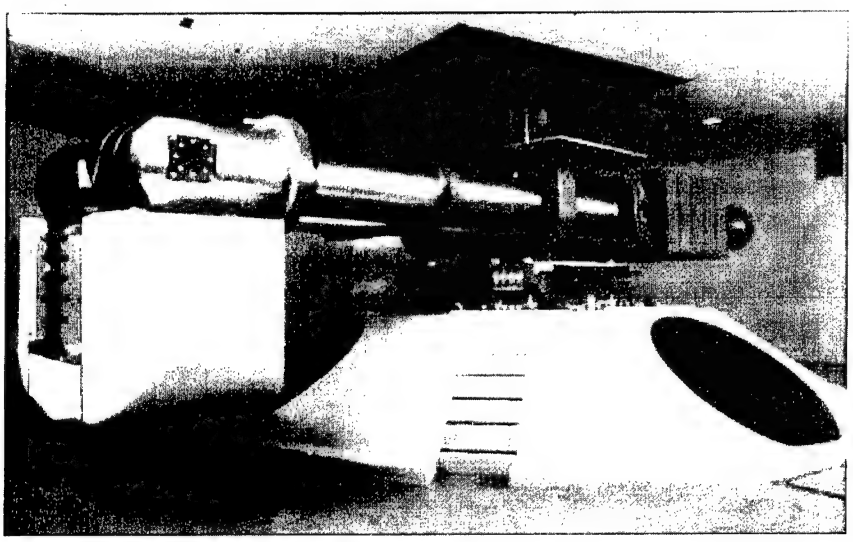

Figure 24. U.S. Army Centrifuge Research Facility, U.S. Army Engineer Research and Development Center, Vicksburg, MS (after Lee, in preparation)

A rectangular box was constructed to contain the surrogate contaminated dredged material and sand cap (Figure 25). The clay-water mixture representing the dredged material fill was placed at a water content which allowed an undrained shear strength of between 20 to 30 psf (1 to 1.4 kPa), based on previous laboratory testing results. At this lower strength range, based on the analytical modeling results, the sand cap would be assumed to be minimally stable. To simulate the physical layout of Cell M2, the model was built to scale proportions for which a unit model length equaled 10 length units in the full-scale prototype Cell M2. During centrifuge flight, a specially designed sand dispenser was operated in a fashion imitating the two-dimensional dump scow placement process for the prototype Cell M2 sand cap.

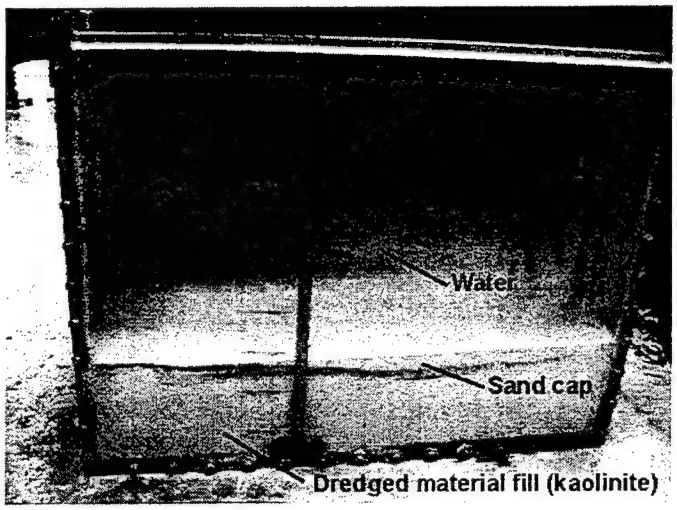

Figure 25. Physical test model flown on the centrifuge (after Lee, in preparation)

After flight, the soil model was analyzed and the layer geometry was noted (Figure 26). As expected, the sand cap remained stable although significant settlement was observed in the sand surface. This settlement likely occurred due to the time-dependent consolidation process in the kaolinite clay. No significant disturbance in the sand cap was noted due to pore fluid moving upward from the consolidating clay.

Summary

The analytical and physical model simulations indicated the sand cap was unstable when placed on top of clay material having undrained shear strengths greater than 17 psf (0.8 kPa) was water contents below 100 percent. Actual cap performance in Boston harbor Cell M2 appeared to substantiate the model results. The laboratory testing of the clay material indicated that measuring the soil's consistency (slump) correlated to its physical properties such as water content and shear strength may be a promising method adaptable to field monitoring usage.

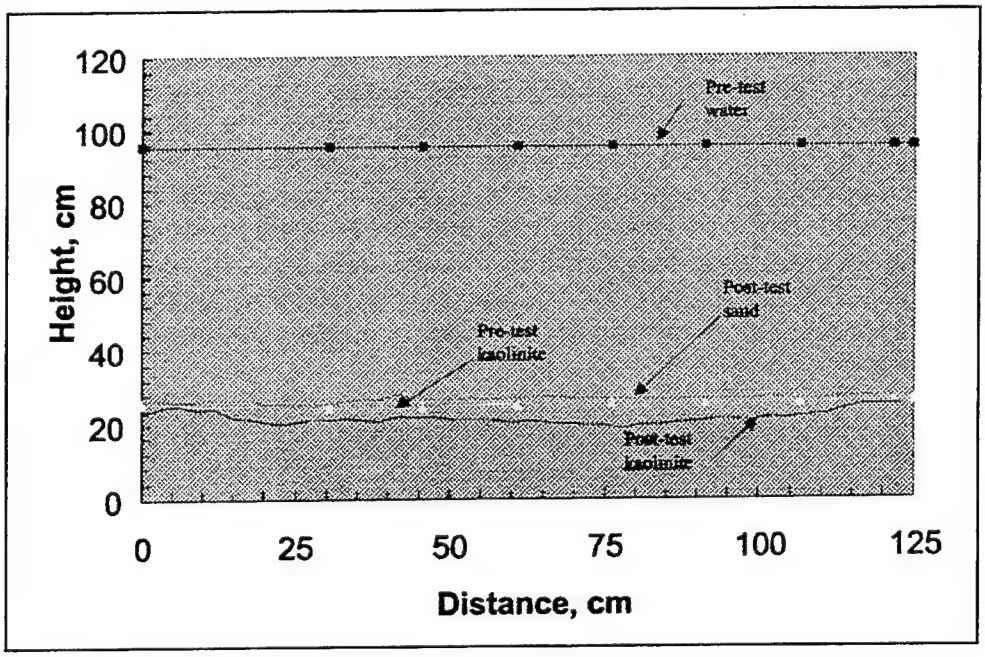

Figure 26. Pretest and posttest sand cap locations in the test model

4 Boston Harbor CAD Cell Cap Erosion from Tidal Currents and Ship Propeller Wash

Boston Harbor Navigation Improvement Project (BHNIP) CAD cell cap erosion predictions from both tidal currents and ship propeller wash were calculated to characterize the likely amount of cap damage to be expected from either source.

Effect of Sediment Resuspension by *MV Matthew* on Water Quality[1]

During channel deepening associated with the BHNIP, about 785,000 cu yd of unacceptably contaminated sediments were dredged. The method selected for containing these contaminated sediments was confined aquatic disposal (CAD) cells located in the navigation channel. One topic of concern associated with the CAD cells in Boston Harbor was whether the passage of large vessels would induce resuspension of contaminated dredged material that had been placed within the cells prior to capping, and whether this process resulted in more sediment transport than would occur under ambient, predredging conditions. The primary question was whether fine-grained, hydrated dredged material would be transported out of the cells prior to being capped by larger-grained material (e.g., sand).

To complement the BHNIP field monitoring program, the New England District funded several activities, including the measurement of currents and resuspended sediments during passage of large vessels over the CAD cells. Science Applications International Corporation (2000b) and Battelle conducted underway measurements of temperature, salinity, and turbidity within the water column using the Battelle Ocean Sampling System (BOSS). Concurrent measurements of water column currents and acoustic backscatter intensity were

[1] This section is extracted essentially verbatim from Science Applications International Corporation (2000b).

made by the ERDC, using a BBADCP mounted on the survey vessel. Data were acquired while the survey vessel followed close behind the 900-ft-long liquid natural gas (LNG) carrier (*MV Matthew*) as it departed from the Mystic River at the head of Boston Harbor. The track of the LNG carrier passed over uncapped CAD Cell M8/M11 and capped Supercell, then along the navigable channel exiting the Inner Harbor. The 35-ft draft of this vessel was approximately 88 percent of the water depth in the navigable channel.

The primary objective of this brief monitoring project by Science Applications International Corporation (2000b) in March 2000 was to determine whether large vessels transiting the Mystic River induce resuspension of unconsolidated dredged material that resided within uncapped CAD cells, by analyzing discrete water samples. Background water property measurements made prior to departure of the *MV Matthew* showed that total suspended solids (TSS) concentrations were low (generally less than 10 mg/L) and spatially homogeneous throughout the Mystic River and Inner Harbor. As the *MV Matthew* departed the Mystic River, four transects made perpendicular to the vessel's wake revealed elevated TSS concentrations (up to 40 mg/L) within a few meters of the bottom beneath the wake. Although these results indicate that bottom sediments are temporarily resuspended during departure of large vessels, the volume of sediments resuspended from capped and uncapped CAD cells is very small (well less than 1 cu m) for each vessel passage. Subsequent monitoring indicated that the resuspended sediments settle to the seafloor within 1 hr of resuspension.

Laboratory analysis of water samples

Following the field survey, the 21 discrete water samples that were collected by the BOSS were analyzed for total suspended solids concentration (TSS) at Battelle's laboratory facility in Duxbury, MA. Analyses were performed according to Battelle's Standard Operating Procedure (SOP) for Laboratory Analysis of Total Suspended Solids. These data confirm the low background TSS characteristics throughout the study area, but they also are useful for calibration of the in situ measurements of relative turbidity acquired by the transmissometer within the BOSS towfish.

Because the TSS concentrations of the 21 background water samples all were relatively low (less than 13 mg/L), this data set alone is insufficient for development of an empirical calibration equation for the transmissometer's response at higher TSS concentrations (i.e., 40 mg/L), such as those observed within the near-bottom sediment plumes during vessel passage. Consequently, Science Applications International Corporation (2000b) chose to supplement the TSS data from these 21 samples with additional TSS calibration data acquired during a 3-day BOSS survey that was conducted in August 1999 during dredging in the Inner Confluence. This latter data set consists of TSS calibration data from 299 discrete water samples and concurrent in situ transmissometer measurements. And because these samples were collected in close proximity to dredging operations, these calibration data span a range of TSS concentrations from roughly 3 to 88 mg/L.

Figure 27 presents a composite of TSS transmissometer calibration data from the two BOSS surveys (March 31, 2000 and August 5-7, 1999) with 21 and 299 samples, respectively. This combined data set was used to empirically determine the relationship between the actual TSS concentration of the discrete water samples and the corresponding optically derived in situ measurement of turbidity from the SeaTech transmissometer in the BOSS towfish. As indicated in Figure 26, the majority of the data fall close to a linear fit having the following equation: TSS (mg/L) = (3.405 x BA) - 7.242 mg/L, where BA is the Beam Attenuation reading in units of 1/m. The regression coefficient of this linear fit to the data was 0.924, indicating a good correlation between the in situ transmissometer measurements and the laboratory TSS analysis of the discrete water samples collected simultaneously. Consequently, it was believed that when the in situ transmissometer encountered elevated beam attenuation readings (i.e., 10-15 1/m) within the near-bottom plumes of resuspended sediment during vessel passage on March 31, 2000, these observations represent moderate TSS concentrations, in the range of 30-45 mg/L. There is no doubt that there is lack of sufficient project-specific data for accurate calibration of the transmissometer, but the calibration results indicate that the BOSS transmissometer is a reasonable instrument of distinguishing background water properties from those within sediment plumes that have TSS concentrations well above 15 mg/L (the approximate upper limit of the background concentrations).

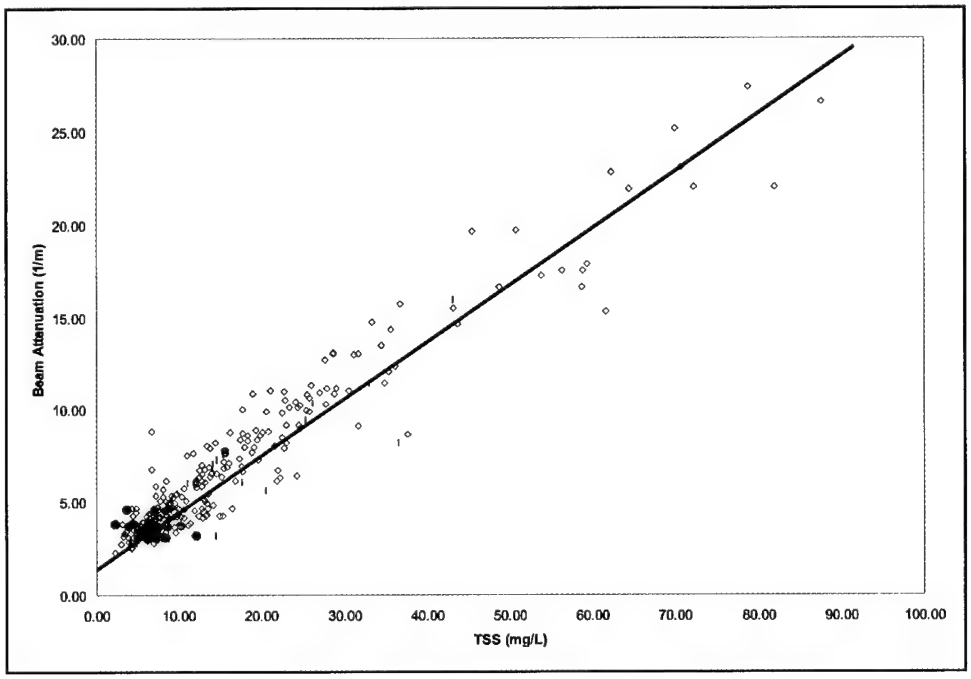

Figure 27. Laboratory results from analysis of total suspended solids (TSS) concentration in discrete water samples (TSS mg/L = (3.405 x BA) – 7.242 mg/L. Red circles are from water samples acquired March 2000; blue diamonds are from water samples acquired during BOSS survey August 1999) (after Science Applications International Corporation 2000b)

Upon closer inspection of the TSS data from March 2000, it was determined that the beam attenuation (BA) data from the background water samples fall into two groups, which differ significantly in terms of their range and variability in beam attenuation readings.

Group A. This group of samples acquired along Transect T1B had BA values ranging from approximately 3.6 to 4.6 1/m and TSS concentrations ranging from approximately 2 to 10 mg/L. Although these samples were acquired along the entire along-channel transect, no spatial trend was evident in the BA data along the transect. Furthermore, the correlation between BA and TSS at these relatively low background levels was poor, which could have been due to a variety of factors including (a) uncertainties in the transmissometer calibration due to variability in the physical characteristics of the suspended particulate matter, (b) procedures for laboratory analysis of TSS samples, and (c) uncertainties in the plumbing lag-time of the BOSS water sample delivery system.

Group B. The second group of samples was acquired at the background transects in the Mystic River, more than 1 hr after completion of Transect T1B. For these samples, BA values ranged from approximately 3.0 to 3.2 1/m and TSS concentrations ranged from approximately 5 to 12 mg/L. As had been observed for Group A, the correlation between BA and TSS was poor for these background samples from the Mystic River. Curiously, all BA values in Group B were considerably lower than those of Group A, although the TSS concentrations were slightly higher for Group B than for Group A. The lower BA values of Group B may have been a result of (a) a change in the calibration of the transmissometer between Transect T1B and subsequent measurements in the Mystic River; and/or (b) a change in the physical characteristics of the suspended particulate matter.

Summary. The correlation between in situ transmissometer-based turbidity data and laboratory analyses of TSS concentrations from the discrete water samples was poor for the background sampling events. It is believed that a good correlation exists between the in situ BA values and the TSS concentrations of water samples collected currently with the BA data, but only at higher TSS concentrations (i.e., TSS greater than 10 mg/L) as illustrated in Figure 27. For the present study, the transmissometer was useful for identifying relative changes in turbidity, such as distinguishing between background water properties and plumes associated with resuspension of bottom sediments. In the absence of discrete water samples from these plumes, and hence, data for calibration of the transmissometer, accurate, quantitative estimates of the TSS characteristics within the sediment plumes cannot be provided; rather, the TSS data provided herein are ultimately based upon transmissometer calibration results from the August 2000 survey in Boston Harbor.

WES Broad Band Acoustic Doppler Current Profile (BBADCP) survey

An RDI 5-beam Broad Band Acoustic Doppler Current Profiler (BBADCP) also was installed on the survey vessel to acquire data for determination of whether the *MV Matthew* induced resuspension of bottom sediments during its

departure from the Mystic River. The BBADCP transmits 1,200 kHz acoustic signals vertically through the water column and measures the acoustic signals that are returned to the instrument. The returned signals are a result of backscattered acoustic energy from both the water column and the bottom. Four of the acoustic transducers on the BBADCP are used for determination of horizontal currents beneath the vessel, whereas the fifth acoustic transducer points downward, projecting an acoustic beam from the survey vessel to the bottom. The measurements of backscattered acoustic energy from this transducer are used solely for detecting the presence of suspended sediment in the water column. Each backscatter measurement represents characteristics within a 50-cm-thick layer of the water column that extends horizontally over the distance the survey vessel travels in 2 sec (a distance of approximately 3 m at 4-knot vessel speed). The measurements begin approximately 1.5 m below the surface and extend to near the bottom.

The BBADCP backscatter data acquired during the monitoring survey are presented in units of acoustic backscatter above background (ABAB) that is proportional to suspended sediment concentration. The background acoustic backscatter level was determined by making BBADCP measurements just prior to the departure of the liquid natural gas carrier *MV Matthew* from its berth in the Mystic River. This background value was then subtracted from all of the ABAB measurements made simultaneously with the BOSS data. The monitoring plan did not include making multiple transects to gather statistics on the variability of the background, so the differences between the monitoring measurements and the background measurements were divided by a standard deviation of 1.5 to give the nondimensional ABAB values. The standard deviation of 1.5 for the background variability is typical of that measured during acoustic monitoring operations with the same BBADCP system in Boston Harbor during August 1999.

When viewing the BBADCP backscatter results, it is important to remember that air bubbles trapped in the wake of a vessel from propeller cavitation can produce stronger ABAB signals than does suspended sediment. When the ABAB values are associated with suspended sediment, larger values mean higher concentrations of suspended sediment if the grain-size distribution remains constant. For the same concentration of suspended sediment, larger particles produce higher ABAB values than smaller particles. Because of the wake effect on the acoustic measurements it is, however, difficult to draw conclusions about suspended sediments directly within or under the wake of the liquid natural gas carrier *MV Matthew*.

Conclusions

The primary objective of this brief monitoring project by Science Applications International Corporation (2000b) was to determine whether large vessels transiting in the Mystic River induce resuspension of unconsolidated dredged material that resided within uncapped CAD cells. Answers to five specific questions were desired.

a. To what extent is unconsolidated dredged material that resides within a filled cell (prior to capping) resuspended during passage of large vessels?

Near-bottom observations of suspended particulates within uncapped cell M8/M11 showed that bottom sediments were resuspended during the passage of the liquid natural gas carrier *MV Matthew* on the morning of March 31, 2000. A plume of suspended sediments with maximum concentration of 40 mg/L was observed within 1-2 m of the bottom approximately 3 min after passage of the *MV Matthew*. This plume was approximately 10 m wide at a height of 2 m above the bottom. The maximum height that the plume extended above the bottom could not be determined from the profile measurements acquired along the single near-bottom transect of Cell M8/M11 that was made shortly after vessel passage. Results from concurrent BBADCP measurements of acoustic backscatter may, however, be useful for delineating the three-dimensional structure of the plume.

b. To what extent are bottom sediments that reside in fully capped cells and in other portions of the navigable channel (away from CAD cells) resuspended during passage of large vessels?

Within the capped Supercell in the Mystic River (adjacent to cell M8/M11) a near-bottom plume of resuspended sediments was observed during measurements acquired at a height of 3 m above the bottom approximately 5 min after the vessel had passed through the cell. This plume was considerably wider than that observed within Cell M8/M11 (38 m vs. 10 m) but its maximum (25 mg/L) and average (12 mg/L) suspended sediment concentrations were less than those observed in Cell M8/M11. These differences between observations in the two cells could be due to the following factors: First, the bottom of the Supercell was approximately 5 ft shallower than that of Cell M8/M11, which could mean that vessel-induced currents were stronger in the Supercell than within its deeper neighbor, and thus a reason for the wider plume in the Supercell if the vessel-induced currents were relatively stronger there; second, the Supercell had received a large quantity of sand during capping such that the average grain size of its surface sediments would be significantly larger than those found within uncapped cell M8/M11. Consequently, the material within the Supercell may be less susceptible to erosion by vessel-induced currents, and thus the lower suspended sediment concentrations. Additional monitoring and sediment analyses would, however, be needed to test these hypotheses.

Near-bottom plumes of resuspended sediments also were observed at two additional locations within the navigational channel south of the Inner Confluence. Both of these sites had water depths comparable to those within the Mystic River. The near-bottom plumes at both of these locations had widths of 45-50 m, which were greater than those observed at the Mystic River measurement locations. It is believed the observed increase in plume width with increased distance from the point of vessel departure in the Mystic River is associated with vessel speed which was observed to increase from a few knots at Cell M8/M11, to speed of 7-9 knots near the Reserved Channel.

Maximum suspended sediment concentrations in plumes observed at the two channel transects (18 and 24 mg/L) were comparable to those observed in the

Supercell (25 mg/L) and substantially less than those observed in the uncapped Cell M8/M11 (40 mg/L). The sediment plume created during vessel passage near the Reserved Channel extended to the sea surface (confirmed by visual observations) which may be further evidence that the relatively high speed of the *MV Matthew,* as it approached the entrance to Boston Harbor, may be a major factor in the resuspension of bottom sediments in the harbor.

c. Were the background concentrations of suspended particulate matter in the Mystic River and navigable channels of Boston Harbor sufficiently low and spatially homogeneous to be distinguished from near-bottom sediment plumes that may be caused by resuspension of bottom sediments during passage of large vessels?

During the morning ebb tide on March 31, 2000, background concentrations of suspended particulate matter were low (generally 3-8 mg/L) and spatially invariant throughout the study area within the Mystic River and navigable channel, as far south as the Reserved Channel. Vertical profile measurements indicated that particulate concentrations had minimal vertical variability. Consequently, the background conditions were ideal for recognition of any vessel-induced resuspension of bottom sediments.

d. Was a significant volume of dredged material resuspended during passage of the *MV Matthew* over uncapped Cell M8/M11?

The monitoring activities were not designed to resolve the three-dimensional structure of the vessel-induced sediment plume at Cell M8/M11, nor quantify its sediment load during the first few minutes of vessel passage. Rather, the monitoring effort focused on obtaining a quick look at near-bottom sediment resuspension immediately after vessel passage at four cross-channel transects as the *MV Matthew* steamed down channel.

The BOSS data acquired along the single transect of the plume in uncapped Cell M8/M11 revealed suspended particulate concentrations at one depth level across the plume, but the vertical extent of the plume could not be resolved without additional measurements, which were sacrificed to acquire data from other locations in the channel and Supercell. When the final results become available from the underway acoustic backscatter measurements of the ERDC-operated BBADCP, it may be possible to estimate the vertical extent of the resuspension plume in uncapped Cell M8/M11, but only if the vessel wake did not contain large quantities of air bubbles that would confound interpretations of suspended particulates. Preliminary results from the BBADCP measurements suggest the following; (a) bubbles in the wake of the *MV Matthew* persisted from the surface down to about 8-10 m (half of the water depth), (b) acoustic backscatter values near the bottom were significantly higher than background, suggesting that the backscatter was associated with resuspension of bottom sediments, and (c) backscatter values at middepth (in the wake of the *MV Matthew*) were less than those near the surface and near the bottom. This may be evidence that a near-bottom plume of resuspended sediments could be distinguished from the near-surface bubble-infested wake of the *MV Matthew*.

There is lack of field observations of the true three-dimensional structure and suspended particulate load of the sediment plume observed within Cell M8/M11. There is uncertainty about whether the observed plume contained a large volume of suspended sediment and hence, there should be concern about the volume of dredged material that could be lost with each passage of a large vessel (assuming the worst-case scenario that the material would be transported out of the cell prior to resettling to the seafloor). If the near-bottom BOSS observations and preliminary BBADCP results are used to estimate the dimensions of the plume, a plume width of 10 m and a height of 6 m is obtained. And if Cell M8/M11 has a length of 240 m (along which the *MV Matthew* traveled), then the volume of the plume would have been 14,400 m^3. If it is assumed that the average suspended sediment concentration in the plume was 20 mg/L (half of the observed maximum value from the BOSS measurements), then the plume would contain 288 kg of suspended dredged material. If the density of the material was 1,340 kg/m^3, this would equate to a volume of 0.21 m^3 (~$1/5^{th}$ m^3 or 243 liters or 64 gal) of suspended dredged material in the near-bottom plume. Even if this preliminary calculation was underestimated by a factor of 5, it could still be expected that less than 1 m^3 of dredged material would be resuspended during each passage of the *MV Matthew*.

If the plume's entire load of suspended dredged material were transported out of the cell before resettling, it would translate to a very small volume (i.e., 1 m^3) of material lost. But since the near-bottom currents in the vicinity of Cell M8/M11 were observed to be very weak (generally less than 5 cm/sec), a parcel of resuspended dredged material would travel less than 180 m in 1 hr, which is less than the length of the cell. Consequently, if the material were to resettle to the bottom in less than 1 hr after vessel passage, the majority of the resuspended sediments would be redeposited within the cell from which they originated.

e. Did the resuspended dredged material remain in the water column for an hour or longer?

No. There was no evidence that plumes of resuspended bottom sediments remained in the water column up to 1 hr after passage of the *MV Matthew*. Near-bottom measurements in Cell M8/M11 1 hr after vessel passage revealed suspended sediment concentrations that were equivalent to background values. And near-bottom measurements at the location of the current-following drogue that had been deployed in the water mass containing the plume that was initially within Cell M8/M11 also showed background concentrations of suspended sediments. The plumes that were observed farther downstream during vessel passage were also absent within 1 hr of their initial detection.

These results support the hypothesis that any dredged material that was resuspended from uncapped Cell M8/M11 during passage of the *MV Matthew* on the ebb tide would resettle to the bottom before it had traveled a significant distance (e.g., 200 m) downstream.

Sediment Resuspension by Tidal Currents and *MV Matthew*[1]

When capping of a cell was complete, geotechnical and geophysical surveys were conducted within the cell to determine cap coverage and thickness. These studies indicated that because of the relatively high water content of the dredged material placed within the cells, it is critical that sufficient time (i.e., 6 months) be given to allow the material to gradually increase its load-bearing capacity via the process of self-weight consolidation. When a 3-ft thick sand cap was applied within 1-2 months after the dredged material had been placed in a CAD cell, monitoring results revealed that vertical diapers of dredged material penetrated upward through the cap with the result that a layer of dredged material was formed on top of the newly placed cap at some locations within the cell. As a result of these findings, the time period between completion of dredged material placement within the cells and placement of the sand cap was maximized to achieve the design goal of a contiguous cap across the cell, with no geotechnical processes that could allow the dredged material to escape.

Concurrent with the study to determine the effect of sediment resuspension by the *MV Matthew* on water quality (Science Applications International Corporation 2000b), Science Applications International Corporation (2001) also conducted monitoring to determine whether tidal currents and deep-draft vessels could erode the sand cap and expose dredged material in the cells. This monitoring was conducted during passage of the deep-draft LNG carrier *MV Matthew* during its departure from the Mystic River approximately 2 hr after high water on the morning of 31 March 2000. The vessel transited through the uncapped CAD Cell M8/M11 and the capped Supercell. General concerns over the effectiveness of in-channel capping and the potential for later release of contaminated dredged material into the harbor's ecosystem translated into two additional questions.

a. Could tidal currents or other natural estuarine processes provide sufficient energy to erode the sand cap and thereby expose the dredged material contained within the CAD cells?

During a 14-day measurement period in March and April 2000, currents in the Mystic River were very weak, with near-bottom current speeds generally below 10 cm/sec within the two CAD cells monitored. The semidiurnal tide did not drive a strong east-west flow along the channel axis within the Mystic River. Near-bottom turbidity was relatively low (less than 15 mg/L) and apparently unaffected by the tides. Observations during the spring tidal phase demonstrated that the amplitude of the local tide had no significant effect on currents or turbidity within the Cad cells. From those results Science Applications International Corporation (2001) concluded that the typical currents within the Mystic River are insufficient to induce major erosion of bottom sediments in the navigable channel or within the CAD cells which are 1- to 4-m deeper than the channel. It is possible that currents are intensified during major storm surge events and during

[1] This section is extracted essentially verbatim from Science Applications International Corporation (2001).

periods of intense river discharge, but field observations during these relatively brief event processes are not available.

b. Could the cap be catastrophically eroded when deep-draft vessels pass over the CAD cells?

The LNG carrier *MV Matthew*, having a length of 290 m and draft of nearly 11 m, is one of the largest vessels that pass through the Mystic River which has a navigable channel depth of approximately 11-12 m at mllw. Although its transits are carefully scheduled near the time of high water to maximize vessel safety, there is only about 3 m of clearance between the hull and the seafloor within the navigable channel. Consequently, the vessel causes intensified currents at the seabed during the few minutes the vessel passes over a fixed point in the channel. Currents decrease substantially after the vessel passes, but speeds remain above their low background levels for a period of 5 to 15 additional minutes as the aft-directed momentum of the vessel's wake pushes water past a fixed point on the seafloor. Near-bottom current speeds can achieve maximum values on the order of 65 cm/sec (averaged over 10 sec) and possibly higher for instantaneous speeds as the propeller(s) of the vessel pass over a fixed location. These speeds are sufficient for erosion of sediments in the navigable channel as well as within the CAD cells. The in situ measurements of currents and near-bottom turbidity from within two cells demonstrated the correspondence between intensified, vessel-induced currents and local resuspension of bottom sediment, both within the uncapped Cell M8/M11 and the capped Supercell (e.g., regardless of the grain size). The near-bottom suspended sediment concentrations within the cells did, however, return to their relatively low background levels within a few minutes of vessel passage, supporting the hypothesis that only a small volume of sediment was actually resuspended along the trackline of the vessel through the cell.

The representativeness of these in situ observations during passage of the *MV Matthew* is supported by similar events that were evident in the moored current and turbidity records from within the two CAD cells. In the early morning of 31 March, a tug was towing a loaded cement barge westward through the Mystic River. Although neither the exact trackline of this tow nor its position relative to the moored arrays are known, its effects on the near-bottom currents were certainly noticeable above the background conditions. Bottom sediment resuspension was detected during a brief period by the moored array in the Supercell, suggesting that the tow passed closer to this array than to the array in Cell M8/M11. Similar short-duration events of intensified bottom currents and elevated turbidity levels were apparent within the 14-day record that began on 31 March 2000. Four separate events having elevated near-bottom current speeds were detected, each occurring near the time of local high water when large vessels are most likely to pass through the Mystic River. Although the turbidity record during these events did not show elevated levels corresponding with the elevated current speeds, the 10-min data averaging period of this 14-day record probably filtered out both the high speeds and possibly high turbidities that could have occurred for a short (1- to 4-min) duration during vessel passage. Additionally, high-frequency measurements would be necessary for development of a statistically significant quantitative estimate of bottom current intensification and

sediment resuspension during passage of the various types of vessels operating in the Mystic River.

Ship-generated Velocities and Bed Shear Stress[1]

Two vessels were used in this analysis by Maynord (2001). First, the liquid natural gas carrier *MV Matthew* is a 10.7-m draft, 41.2-m beam, and 290-m-long ship having an installed power of 36,000 hp. Second, the tug *MV Matthew Tibbetts* is a 3.4-m forward draft, 4.3-m aft draft, 7.9-m beam, and 30-m-long tug having an installed power of 2,000 hp. Details of both ships are provided in Table 3. This evaluation investigated the displacement effects of the ship and the propeller jets from the ship and tug.

Table 3
Characteristics of *MV Matthew* and *MV Matthew Tibbetts*

Parameter	*MV Matthew*	*MV Matthew Tibbetts*
Length, m	290	30
Beam, m	41.2	7.9
Draft forward, m	10.7	3.4
Draft aft, m	10.5	4.3
Vertical distance from center of propeller to keel, m	3.81	3
If 2 props, horizontal distance from center of propeller to vessel center line, m	-	3.7
Rudder arrangement	1 rudder on CL of shaft	2 rudders on CL of shafts
Propeller diameter (pitch), m	7.62	2.44(2.18)
Number of blades	5	4
Installed power, hp	36,000	2,000
Propeller RPM at installed power	92-95	240
Propeller RPM at time vessel passed current meter	30	130

Displacement effects of ships

Return velocity and shear stress. As a ship moves through water, the water displaced by the ship has to constantly move from in front of the ship to behind the ship. The movement of water from bow to stern results in a conversion of potential to kinetic energy that results in a lowering of the water level near the ship. This lowering of the water level results in lowering of the ship that is referred to as squat. In open water where widths and depths are large, the velocity

[1] This section is extracted essentially verbatim from Maynord, S. T. (2001). "Analysis of ship generated velocities and bed shear stress in Boston Harbor," unpublished document, U.S. Army Engineer Research and Development Center, Vicksburg, MS.

of the water along side and beneath the ship is low as is the lowering of the water level. In channels where limited depths and widths confine the movement of water from bow to stern to a much smaller area, the velocity and lowering of the water level can be significant. The movement of water from bow to stern is often called return velocity (V_r), and the lowering of the water level is called drawdown (d_r). Techniques for estimating return velocity and drawdown are given in Maynord (1996) as a function of ship speed, ship size, and channel size and shape, and are based on one-dimensional equations of energy and mass conservation with some empiricism.

This location along the channel for these tests was selected because it was the most confined section of channel (i.e., it had the lowest channel area). The pilots stated that the *MV Matthew* is operated when the tide is no lower than halfway between low and high tide. Water levels of el 0[1] and el +3.4 were used as representative of low and high tide based on observed water-surface elevations. On September 9, 1999, field experiments were conducted during transit of another ship not used in this analysis (*MV Adriatic*). Calculations of return velocity and drawdown were conducted for el +1.7 and el +3.4. The area used in the return velocity and drawdown calculations includes the CAD cell, and equals 3,813 sq m for el +1.7 and 4,315 sq m for the el +3.4. Based on the size of the *MV Matthew*, the ship is taking up 12 percent of the channel area at el +1.7 and 10 percent at the el + 3.4. While this is not as severe as in some channels where the ship can take up as much as 25 percent of the channel, 10-12 percent will result in large drawdown and return velocity if ship speeds are large enough. The speed of the *MV Matthew* varies from 1.5 to 3 m/sec. Calculations were made for both speeds and both water levels, and peak values of return velocity, drawdown, V_{bow}, and τ_{bow} are shown in Table 4.

Table 4
Peak Values of Return Velocity, Drawdown, Bow Displacement Velocity, and Bow Displacement Shear

Speed m/sec, knots	Tide mllw	V_r North, m/sec	V_r South, m/sec	d_r North, m	d_r South, m	V_{bow}, m/sec	τ_{bow}, Pa
1.5 (2.9)	+1.7 m	0.28	0.41	0.05	0.07	0.63	15
3 (5.8)	+1.7 m	0.51	0.74	0.17	0.25	1.27	59
1.5 (2.9)	+3.4 m	0.25	0.36	0.04	0.06	0.56	12
3 (5.8)	+3.4 m	0.46	0.65	0.15	0.22	1.12	47

The relatively large drawdown shown for ship speeds of 3 m/sec suggests that this speed is not used in this reach of the Boston Harbor. In addition, subsequent calculations show that the 30-rpm propeller speed reported by the pilots results in speeds close to 1.5 m/sec. The time-history of return velocity and shear due to return velocity is shown in Figures 27 and 28 for the south side of the ship which has the largest shear. The distribution is based on the distribution of return

[1] All elevations in this chapter are in meters referenced to the National Geodetic Vertical Datum (NGVD).

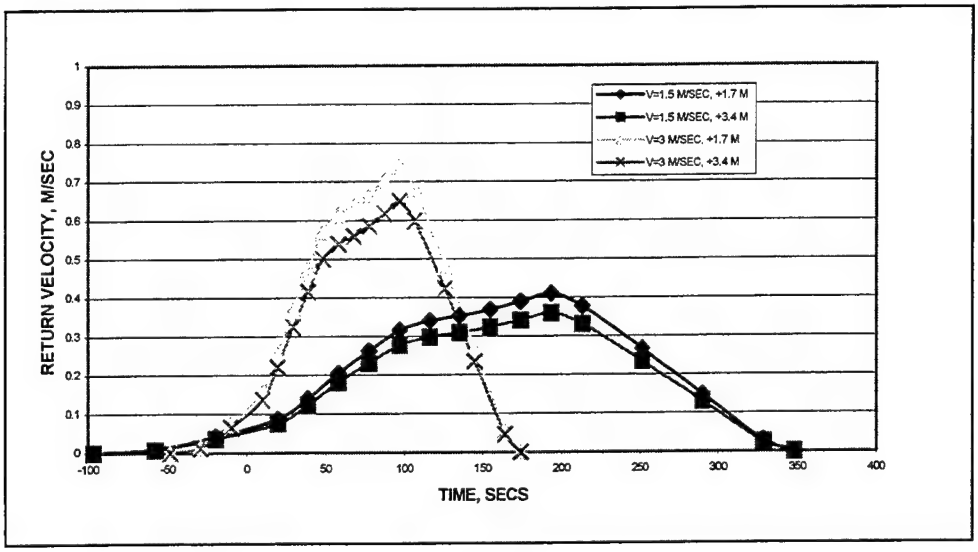

Figure 28. Return velocity time-history, *MV Matthew* (return velocity computed for south side of ship) (after Maynord 2001)

velocity from a shallow draft tow. The conversion from return velocity to shear stress uses the equation applicable to the absence of ambient current given by

$$\tau_{vr} = 1/2 \; C_{fr} \rho \; V_r^2 \tag{1}$$

where C_{fr} is given by the equation

$$C_{fr} = \left(2.87 \; + \; 1.58 \; \log \; \frac{xbl}{K_s} \right)^{-2.5} \tag{2}$$

where xbl is the distance to boundary layer development and equal to 1 m, and K_s = sand grain roughness = $3d_{50}$, where d_{50} is the average bed particle size. For the Boston Harbor sand cap of 0.2 mm, $C_{fr} = 0.0045$.

Bow displacement velocity and shear stress. In addition to return velocity, the displacement of the ship causes a rapid acceleration of flow underneath the bow of the vessel in a direction opposite to the travel direction. This rapid acceleration results in a large, but short lived, spike in velocity (V_{bow}) and bed shear stress (τ_{bow}). Techniques for estimating the velocity and bed shear stress have been developed for shallow draft barge navigation based on measurements in a large physical model. The equation for peak bow shear is equal to the average of the upbound and downbound equations used in Maynord (2000) and is given by

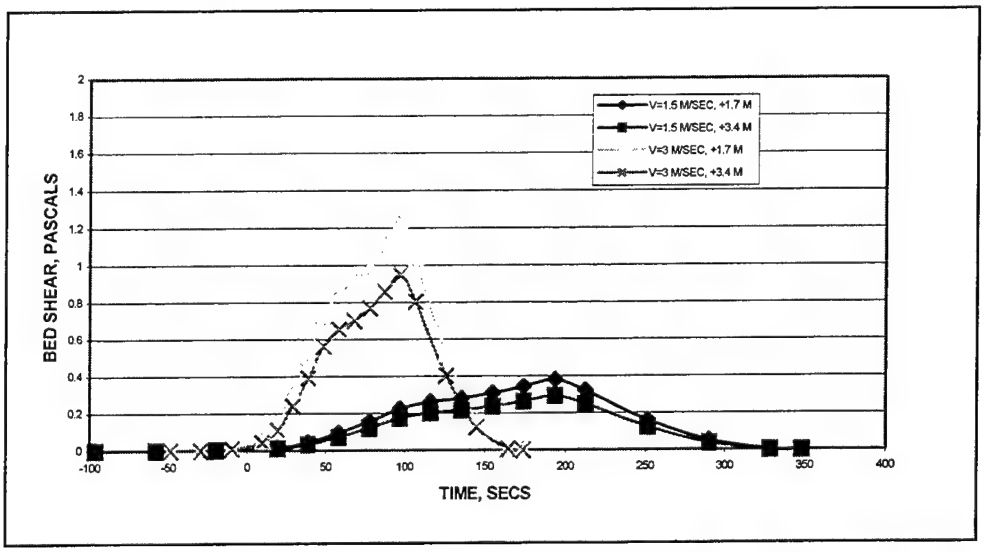

Figure 29. Bed shear from return velocity time-history, *MV Matthew* (based on return velocity computed from south side of ship) (after Maynord 2001)

$$\tau_{bow}(peak) = 0.013\ \rho\ C_{rough} \left(\frac{depth}{draft}\right)^{-2.85} V^2 \qquad (3)$$

where ρ = water density, C_{rough} = conversion of smooth bed lab measurements to rough bed = 1.6 for 0.2 mm sand used in CAD cells, and V = ship speed. The minimum depth to draft ratio in those experiments was 1.5 whereas the depth to draft ratio over the Boston Harbor CAD cells is 1.5 based on a 10.7-m draft, 13.0-m channel depth, and 3 m between the channel bed and the top of the CAD cell. One concern is the difference in the relatively blunt bow of a shallow-draft tow versus the streamlined shape of most ship bows. The techniques for tows will likely produce larger values of velocity and shear stress than actually occur beneath a ship. The barge tow techniques will be used with this caution noted. The time-history of the bow shear is shown in Figure 30. The shallow-draft tow model measurements showed the bow shear to be constant across the width of the vessel. Lacking data on ships, this same assumption is used herein.

Propeller jet velocities and bed shear stress

Propeller jet velocities are determined by first determining the velocity exiting the propeller and then decaying this velocity based on the distance of the propeller above the bed and the propeller diameter. The velocity exiting the propeller can be determined based on either (a) propeller speed, size, and other characteristics that define the thrust coefficient of the propeller, or (b) the applied power and the propeller diameter. The first technique is the most reliable but the thrust coefficient of the propeller is difficult to determine. The second technique is less reliable but estimates of applied power and propeller size can usually be determined. The most critical question in the applied power approach is "what is

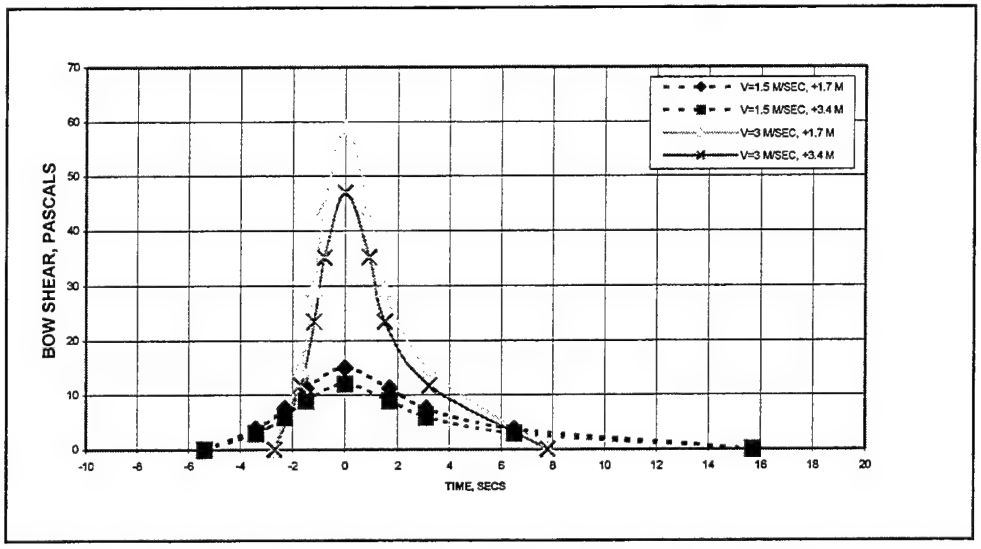

Figure 30. Bow shear time-history, *MV Matthew* (after Maynord 2001)

the applied power that will be used in design?" In many cases, the assumption of the maximum power will result in excessive estimates of scour or protection requirements. The equation for velocity exiting the propeller V_p is

$$V_p = C_2 \left(\frac{P}{\rho \, D^2} \right)^{1/3} \tag{4}$$

where $C_2 = 1.33$ for open wheel propellers, P = power/propeller in watts for metric and ft-lbs/sec in English units (1 hp = 550 ft-lbs/sec = 0.746 kW), and D = propeller diameter.

The equation for decaying the velocity exiting the propeller to the maximum near bed velocity $V_{b,\max}$ (0.3 m above bed) is

$$V_{b,\max} = E \left(\frac{D}{H_p} \right) V_p \tag{5}$$

where E is a coefficient that varies with propeller type (ducted or open), stern shape, and the rudder arrangement, H_p is the distance from the propeller center to the channel bed. A value of $E = 0.43$ will be used for the *MV Matthew Tibbetts* and is based on studies in Maynord (2000) of a twin screw towboat, tunnel stern, and rudders centered on each propeller. The appropriate value to use for the *MV Matthew* will have to be taken from the literature for the single screw ship with a central rudder. A value of $E = 0.65$ is used from Bergh and Magnusson(1987) for a fine stern shape with a central rudder and is in agreement with the $E = 0.71$ reported by Fuehrer, Romisch, and Engelke (1981). Data supporting the values of E are generally based on D/H_p of greater than 0.3.

Equation 5 is used to determine the maximum near bed velocity without regard to its location. Other techniques attempt to define the distribution of bottom velocity. Most distribution equations are based on the equation for a submerged jet. These equations perform poorly, primarily because of the influence of the bottom and water surface on spreading of the jet and the influence of a central rudder on the distribution.

MV Matthew Tibbetts. Based on conversations with pilots of the *MV Matthew Tibbetts,* the tug is often used to maneuver ships during which full power of the tug is used with the tug being nearly stationary. At full power, the power per propeller is 1,000 hp = 746 kW. Using Equation 4, the velocity exiting the propeller is 6.7 m/sec. At the 14.3-m depth over the CAD cell at mllw, the vertical position of the propellers results in an H_p = 13.1 m. For the 2.44-m diameter propellers, D/H_p = 0.186 which is well below the value for which data has been collected. Based on Equation 5 and E = 0.43, the maximum bottom velocity is 0.53 m/sec.

The distribution of near bed velocity is based on empirical techniques in Maynord (2000). The region behind the tug is broken into two zones: zone 1 is the region where the two propeller jets act as individual jets, and zone 2 is the region further from the propellers where the jets have combined into a single jet. Near bed velocities in zone 1 for the large H_p = 13.1 m for the *MV Matthew Tibbetts* are negligible. Velocities in zone 2 are based on the equation for the maximum jet velocity (at the surface in zone 2) along the center line of the ship (Y = 0) defined for open wheel propellers as

$$\frac{V(xp)_{\max}}{V_p} = 0.66 \ \exp(-0.0178 \ \frac{xp}{D}) \tag{6}$$

where $V(xp)_{\max}$ = maximum jet velocity at $Y = 0$ at the water surface, Y = lateral distance from axis of ship, and xp = distance from propeller. The lateral decay of this surface velocity is given by a modification of the jet diffusion equation

$$V_{xp,y}(surface) = V(xp)_{\max} \exp(\frac{- Y^2}{2C_{z2}{}^2 \ xp^2}) \tag{7}$$

where $V_{xp,y}$ (surface) = surface velocity at (xp, Y) and $C_{z2} = 0.84(xp/D)^{-0.62}$. The final equation decays the surface velocity at (xp, Y) to a near bed velocity according to

$$\frac{V_{xp,y}(bottom)}{V_{xp,y}(surface)} = 0.34 \left(\frac{D}{H_p}\right)^{0.93} \left(\frac{xp}{D}\right)^{0.24} \tag{8}$$

The near bed velocity distribution based on Equations 6 through 8 for full power at mllw is shown in Figure 31. The bed shear stress is shown in Figure 32, and was determined using Equation 1 with $V_{xp,y}$ (bottom) for V_r and $C_{fr} = 0.016$ based on Maynord (1998) for a bed particle size of 0.2 mm. Results show small bed shear when compared to the propeller jet from the *MV Matthew.*

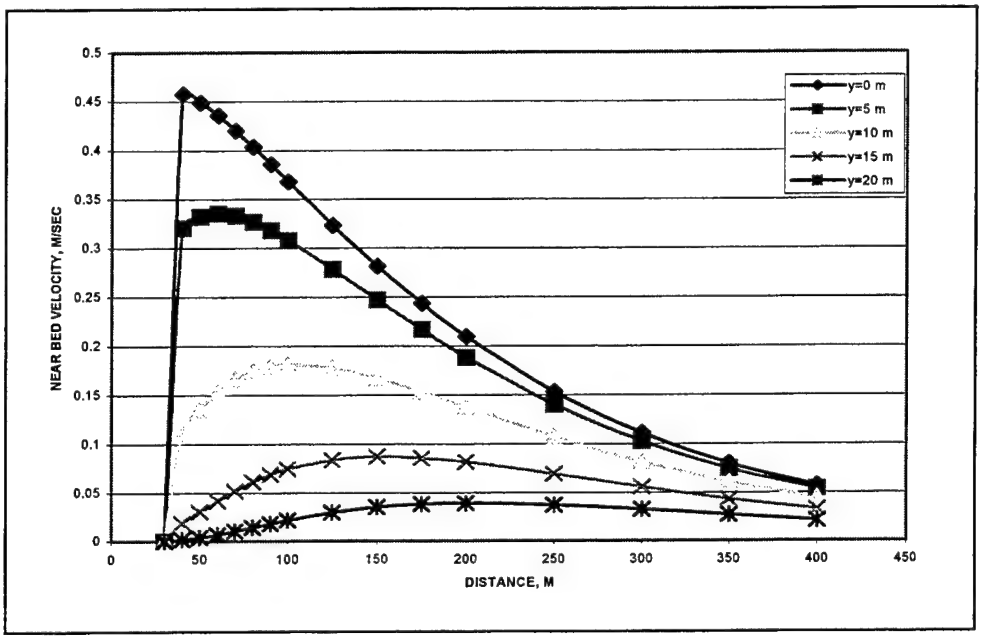

Figure 31. Near-bed velocity versus distance from propeller, *MV Matthew Tibbetts*, stationary tug, mllw (after Maynord 2001)

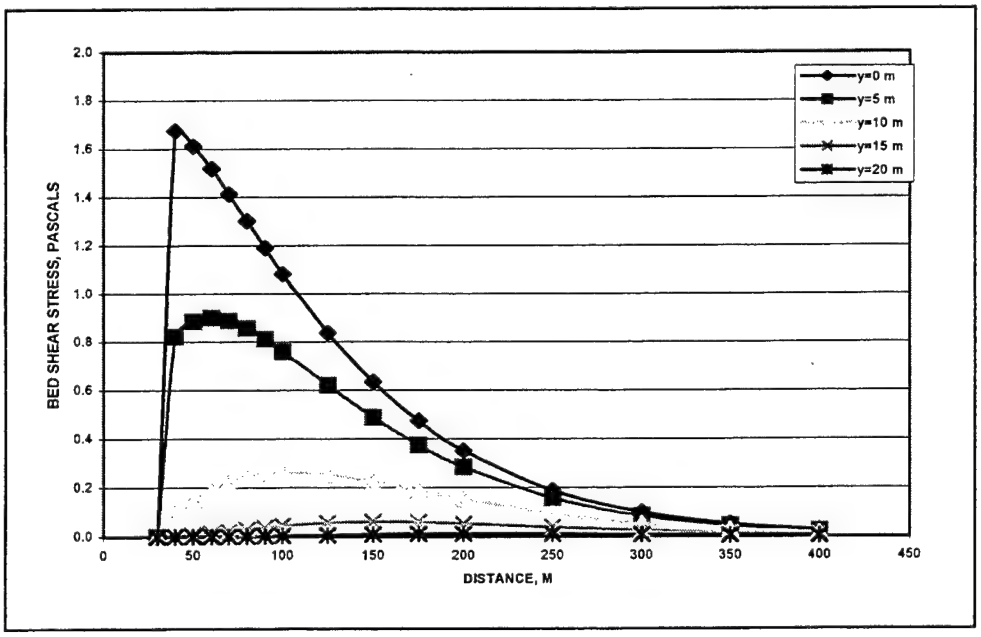

Figure 32. Bed shear stress versus distance from propeller, *MV Matthew Tibbetts*, stationary tug, mllw (after Maynord 2001)

MV Matthew. Determining propeller jet velocities and bed shear stress for the *MV Matthew* requires careful consideration of the power used during passage over the CAD cells. Ship speeds of 1.5-3 m/sec were used earlier in the displacement calculations. The propeller rpm during passage was 30 rpm out of a maximum propeller speed at full power of 92-95 rpm (about 1.55 rev/sec). The following computations provide an estimate of the vessel speed at 30 rpm.

a. Based on thrust coefficients ($K_t = 0.23$) for 5 bladed propellers at the design vessel speed in open water of 18.5 knots, the propeller thrust was computed to be 420,000 lbs based on 1.55 rps and propeller diameter of 7.62 m. The coefficients for pressure (form) loss were adjusted so that the resistance equaled 420,000 lbs at 18.5 knots.

b. Estimate vessel speed, determine thrust coefficient, and compute thrust based on 0.5 rps. Using the estimated speed, compute the resistance using the pressure coefficients in step 1. Repeat vessel speed estimates until the thrust based on K_t is equal to the resistance. At about 1.4 m/sec the $K_t = 0.32$ and $n = 0.5$ rps resulted in a thrust of 60,000 lbs. The resistance equations gave a resistance of 60,000 lbs at $V = 1.3$ m/sec for +1.7 mllw and 1.5 m/sec for +3.4 mllw.

Velocity exiting an open wheel propeller can be estimated from

$$V_p = \frac{1.6}{D}\sqrt{\frac{T}{\rho}} \tag{9}$$

Powers and ship speeds for the different operating conditions are shown in Table 5.

Table 5
Applied Power and Ship Speed for Different Operating Conditions of the *MV Matthew*

Water Level	Ship Speed, m/sec	Applied Power, hp[1]	V_p, m/sec (Eq. 9)	H_p, m	$V_{b,max}$, m/sec (Eq. 5)	Peak Shear at Y = 0, Pa
+1.7 m	1.3	1,350	3.44	9.1	1.9	29
+3.4 m	1.5	1,350	3.44	10.8	1.6	21

[1] based on V_p from Equation 9 as input to Equation 4.

Velocities exiting the propeller based on Equation 9 are also shown in Table 5, along with the maximum near bed velocity based on Equation 5. Bed shear stress based on Equation 1 with $V_{b,max}$ for V_r and $C_{fr} = 0.016$ is also shown in Table 5. The time-histories of bed shear stress from the propeller jet are shown in Figures 33 and 34. The peak shear in Table 5 is used in the dimensionless shear distributions except for the value of H_p. H_p at Boston Harbor is much greater than the H_p used in developing the dimensionless shear distributions. The

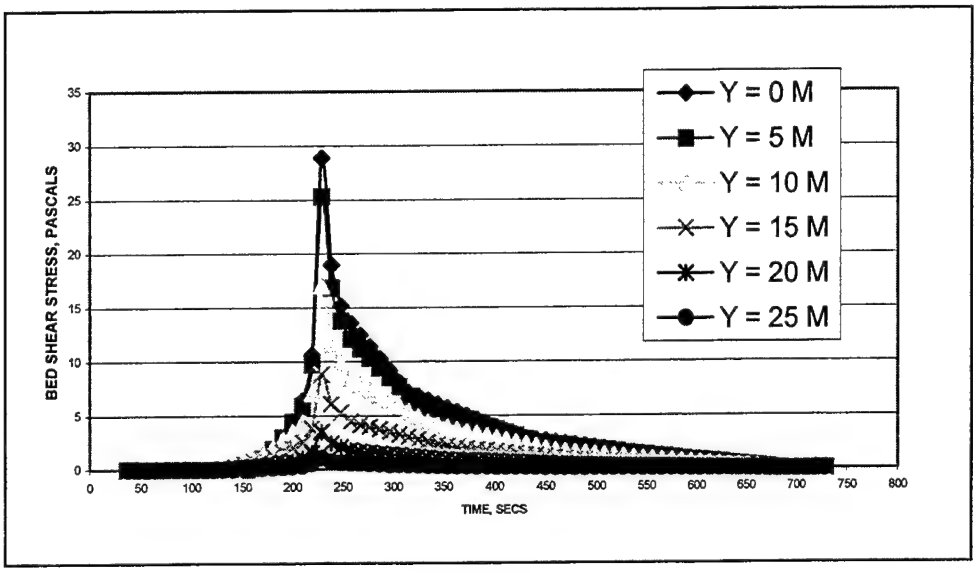

Figure 33. Bed shear stress versus time, *MV Matthew* (water level = +1.7 m (mllw); ship speed = 1.3 m/sec) (after Maynord 2001)

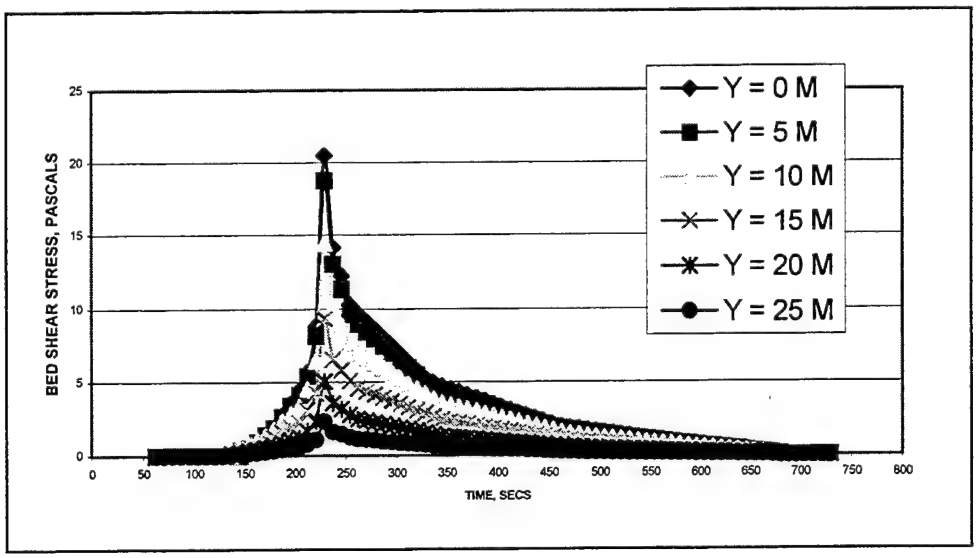

Figure 34. Bed shear stress versus time, *MV Matthew* (water level = +3.4 m (mllw); ship speed = 1.3 m/sec) (after Maynord 2001)

dimensionless parameter containing time in the shear distributions is (time x (vessel speed)/H_p). The ratio of vessel speed to H_p in the development of the shear distributions was about 0.5. The distributions in Figures 33 and 34 are based on limiting H_p in the dimensionless time parameter to values that result in vessel speed/H_p of 0.5.

Timing and location of different shear sources

The distributions for the *MV Matthew* have times shown that reflect their occurrence relative to the other shear sources. Time 0 is passage of the bow of the ship. The bow shear occurs very close to passage of the bow of the ship. The timing of the shear due to return velocity was based on the fall in shear stress corresponding to passage of the stern of the ship. The timing of the propeller shear is based on the peak shear occuring at a distance of 5 x H_p behind the propeller which corresponds to a 12-deg downward angle of the jet coming off the rudder. The return velocity shear acts over the entire cross section. The bow shear acts across the beam of the ship only. The propeller shear varies with lateral distance from the vessel as shown in the distributions. Shear from all sources for a +1.7 m (mllw) water level is shown in Figure 35.

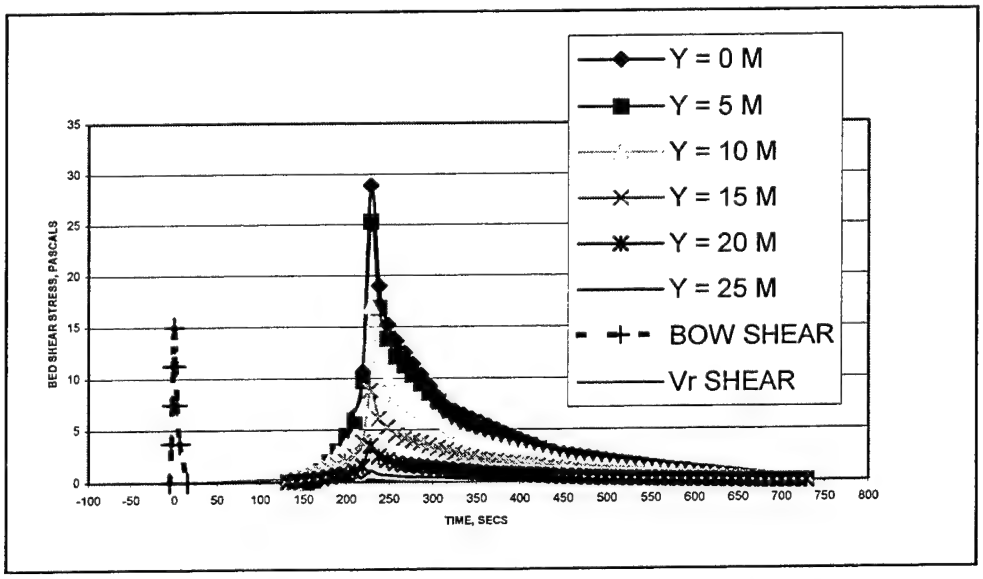

Figure 35. All shear sources versus time, *MV Matthew* (water level = +1.7 m (mllw); ship speed = 1.3 m/sec for propeller, and ship speed = 1.5 m/sec for return velocity, shear, and bow shear) (after Maynord 2001)

Summary and conclusions

Based on bed shear stress calculations presented herein, the ship having the most potential for resuspension of the cap on the Boston Harbor CAD cells is the *MV Matthew*. The tug *MV Matthew Tibbetts* produces small shear stress compared to the *MV Matthew*. The 30-rpm propeller speed reported by the pilots results in a ship speed of about 1.5 m/sec. This ship speed and propeller speed were used to calculate the bed shear from the bow, return currents, and the propeller jet. While shear computations were conducted for tide levels of +1.7 m (mllw) and + 3.4 m (mllw), the small change in bed shear suggests that sediment entrainment calculations be conducted for the +1.7 m (mllw) only.

Erosion Rates of Boston Harbor Sediments[1]

The erosion rates of two reconstituted sediments from Boston Harbor were determined by Roberts et al. (2000) as a function of density and shear stress by means of the High Shear Stress Sediment Erosion Flume at Sandia National Laboratories. One sediment was derived from the CAD cell called the Open Cell (uncapped Cell M8/M11), and one was derived from an area near the CAD cell called the Mid Channel (in the middle of the channel just outside of Cell M8/M11). For all reconstituted cores, the bulk densities were determined as a function of depth and consolidation time. Sediment cores were eroded to determine erosion rates as a function of density and shear stress. In addition, an in situ core from each site was analyzed for bulk density, particle size, mineralogy, and organic content as a function of depth.

Experimental procedure

High Shear Stress Sediment Erosion Flume. The High Shear Stress Sediment Erosion Flume (Figure 36) is essentially a straight flume that has a test section with an open bottom through which a rectangular cross-section coring tube containing sediment can be inserted. The main components of the flume are the coring tube, the test section, an inlet section for uniform fully-developed turbulent flow, a flow exit section, a water storage tank, and a pump to force water through the system. The coring tube, test section, inlet section, and exit section are made of clear acrylic or polycarbonate so that the sediment-water interactions can be observed. The coring tube has a rectangular cross section 10 cm by 15 cm, and can be up to 1 m in length.

Water is pumped through the system from a 120-gal storage tank through a 5-cm diameter pipe and then through a flow converter into the rectangular duct. This duct is 5 cm in height, 10 cm in width, and 200 cm in length. It connects to the test section which has the same cross-sectional area and is 15 cm long. The flow converter changes the shape of the cross section from circular to the rectangular duct. The flow is regulated by a 3-way valve so that part of the flow goes into the duct while the remainder returns to the tank. Also, there is a small valve in the duct immediately downstream from the test section which is opened at higher flow rates to keep the pressure in the duct and over the test section at atmospheric conditions.

At the start of each test, the coring tube is filled with reconstructed sediments. The coring tube and the sediment it contains are then inserted into the bottom of the test section. An operator moves the sediment upward using a piston that is inside the coring tube connected to a mechanical jack and driven by a variable-speed controller. By this means, the sediments can be raised and made level with the bottom of the test section. The speed of the jack movement can be controlled at a variable rate in measurable increments as small as 0.25 mm.

[1] This section is extracted essentially verbatim from Roberts et al. (2000).

Water is forced through the duct and the test section over the surface of the sediments. The shear produced by this flow causes the sediments to erode. As the sediments in the core erode, they are continually moved upwards by the operator so that the sediment-water interface remains level with the bottom of the test and inlet sections. The erosion rate is recorded as the upward movement of the sediments in the coring tube over time.

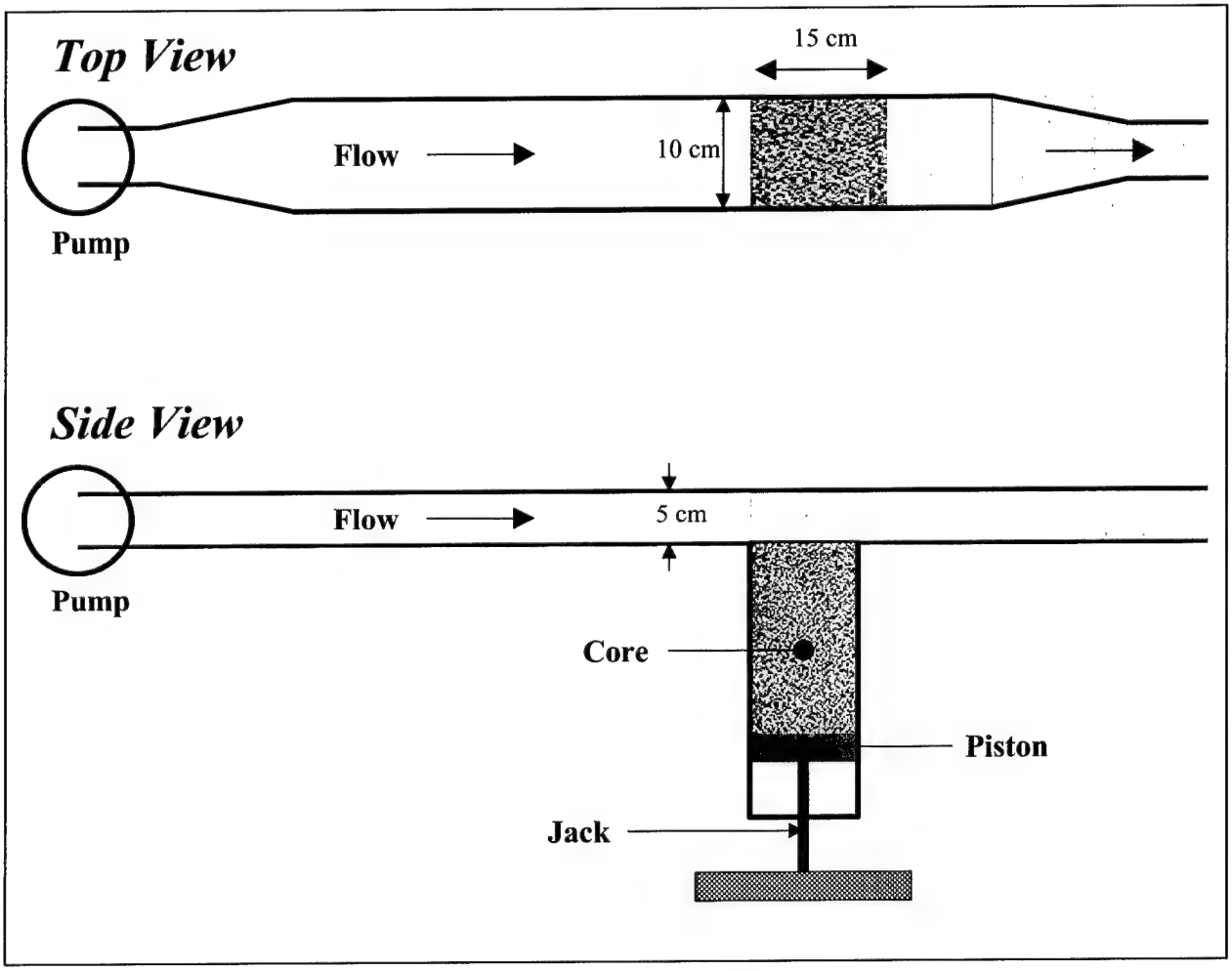

Figure 36. High Shear Stress Sediment Erosion Flume (after Roberts et al. 2000)

Core preparation. Reconstituted sediments were prepared in the laboratory to gain insight on how sediment consolidation parameters (bulk density or water content of the sediment) affect erosion rates. Sediment cores were prepared in the following manner to obtain different bulk densities for the sediments taken from the Open Cell and Mid Channel sites for the erosion tests. Approximately 30 gal of wet sediments were placed in 35-gal cylindrical tanks and mixed until the sediment-water mixture was homogeneous. The sediment mixtures were then poured into 30-cm coring tubes. These cores were allowed to consolidate for 2, 5, 10, 30, 60, 90, and 120 days.

Measurement of sediment erosion rates. The following procedure was used to measure the erosion rates of the sediments as a function of shear stress and depth. The sediment cores were prepared and then moved upward into the test section until the sediment surface was even with the bottom of the test section. A measurement was made of the depth to the bottom of the sediment in the core. The flume was then run at a specific flow rate corresponding to a particular shear stress. Erosion rates were obtained by measuring the remaining core length at different time intervals, taking the difference between each successive measurement, and dividing by the time interval.

The following procedure was generally used to measure erosion rates at several different shear stresses using only one core. Starting at a low shear stress, the flume was run sequentially at higher shear stresses, with each succeeding shear stress being twice the previous one. Generally about three shear stresses were run sequentially. Each shear stress was run until at least 1 to 3 mm, but no more than 2 cm, were eroded. Also, each shear stress was run for a minimum of 20 sec and a maximum of 10 min. This defines the minimum and maximum erosion rates measured by the High Shear Stress Sediment Erosion Flume to be 1.67×10^{-4} and 0.1 cm/sec, respectively. The time interval was recorded for each run with a stop watch. The flow was then increased to the next shear stress, and so on until the highest shear stress was run. This cycle was repeated until all of the sediment had eroded from the core. If after three cycles a particular shear stress showed a rate of erosion less than 10^{-4} cm/sec, it was dropped from the cycle. If after many cycles the erosion rates decreased significantly, a higher shear stress was included in the cycle.

Measurement critical shear stress for erosion. A critical shear stress can be quantitatively defined as the shear stress at which a very small but accurately measurable rate of erosion occurs. In the present study, this rate of erosion was chosen to be 10^{-4} cm/sec. This represents 1 mm of erosion in approximately 15 min.

Measurement of sediment bulk properties. For the analysis of the sediment bulk properties, duplicate cores were made that were prepared the same as the rectangular cores. The core sleeves of these analysis cores were made from 7.6-cm inner diameter thin acrylic tubes of the same length as the rectangular cores.

The sediment analysis cores were frozen, sliced into 2.5-cm sections, and then weighed (wet weight) to determine the bulk density of the sediments at a particular depth and consolidation time. They were then dried in the oven at approximately 75°C for 2 days and weighed again (dry weight). An explicit expression can be determined for the bulk density of the sediment, ρ, as a function of the water content, W, and the densities of the sediment particles and water as

$$\rho = \frac{\rho_s \rho_w}{\rho_w + (\rho_s - \rho_w) W} \tag{10}$$

For the purpose of these calculations, it has been assumed that $\rho_s = 2.6$ g/cm^3 and $\rho_w = 1.0$ g/cm^3.

Particle sizes and particle-size distributions were determined by use of a Malvern Mastersizer S particle sizing package for particle diameters between 0.05 and 900 μm. All sediment samples had particle sizes less than 900 μm. Approximately 5 to 10 g of sediment was placed in a beaker containing about 500 ml of water and mixed by means of a magnetic stir bar/plate combination. Approximately 1 ml of this solution was then inserted into the sizers sampling system and further disaggregated as it was recirculated through the sampling system by means of a centrifugal pump. The sample was allowed to disaggregate for 5 min on the stir plate and an additional 5 min in the recirculating pump sampling system before analysis by the sizer. To ensure complete dissagregation and sample uniformity, the sediment samples were analyzed multiple times and repeated in triplicate. From these measurements, the distribution of grain sizes and mean grain sizes as a function of depth were obtained.

The dry sediment was crushed into powder and then weighed. Approximately 5 ml of 10 percent hydrochloric acid were added to every 1 g of dry sediment. The sample was again dried in the oven at 75 °C, and analyzed in a CO_2 coulometer to determine the total organic carbon content of the sediment.

The mineralogies of the sediments were determined by means of X-ray powder diffraction using an X-ray diffractometer. Samples were crushed to a size of about 10 μm before being measured by X-ray diffraction.

Results of laboratory consolidation and erosion tests

Tests were conducted to determine erosion properties for two sediments retrieved from Boston Harbor with respect to bulk properties, erosion rates, and critical shear stresses. The two sites are identified as Open Cell and Mid Channel. Each site was individually mixed into a homogeneous composite prior to testing.

Bulk properties. Particle size, bulk density, organic content, and mineralogy of each of the two composite sediment mixtures were measured. The size distributions for each composite are shown in Figure 37. The mean particle size was 99.8 and 35.7 μm for the Open Cell and Mid Channel sediments, respectively. The organic content for the composite mixture was 3.02 percent for Open Cell, and 2.23 percent for Mid Channel. The mineralogy of each composite and a summary of all sediment properties is shown in Table 6. Particle size, organic content, and mineralogy were constant with depth for each composite core. Bulk density was the only parameter that was a variable in each core.

Bulk density was determined as a function of depth for 30-cm core lengths. Consolidation times were between 2 and 120 days for each core. Densities were determined by measuring the water content of each core in 2.5-cm increments. Sediment bulk densities are shown in Figure 38 for Open Cell and Figure 39 for Mid Channel. For all cores, the bulk density generally increases with depth and consolidation time. The bulk density for the Open Cell sediments ranged between

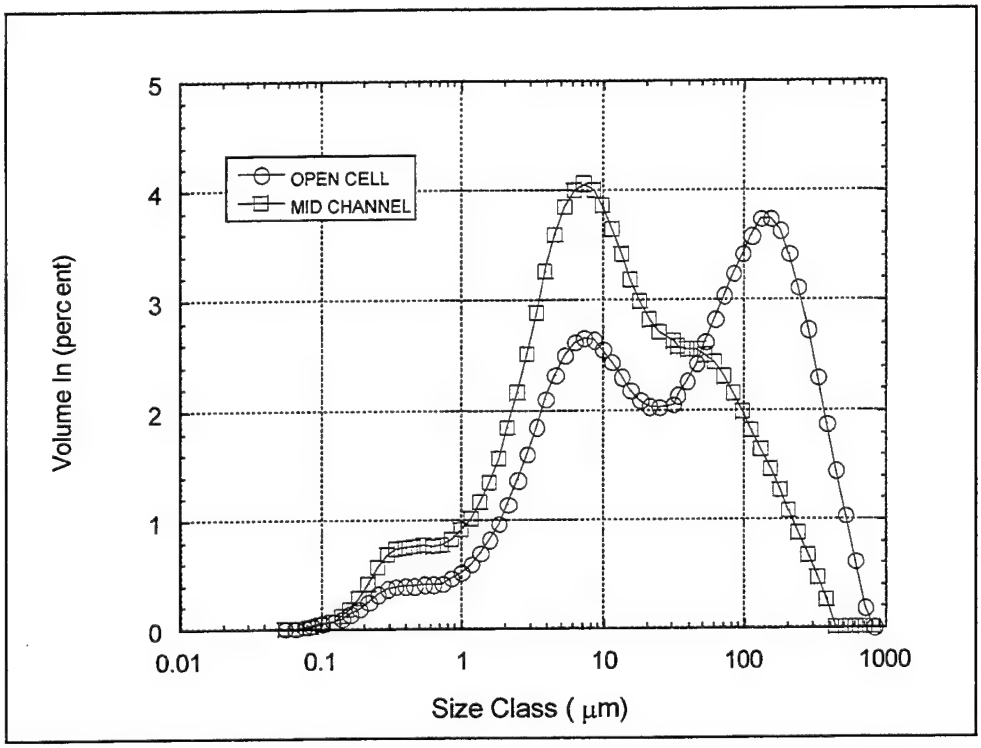

Figure 37. Particle size distribution for open cell and midchannel composites (after Roberts et al. 2000)

Table 6
Summary of All Sediment Bulk Properties

Sediment Name	Bulk Density Range (g/cm^3)	Mean Particle Size (μm)	Mean Organic Content (percent by mass)	Mineralogy (Minerals listed in descending amount)
Open Cell	1.45-1.58	99.8	3.02	1. Quartz, 2. Muscovite, 3. Albite, 4. Chlorite, 5. Microcline
Mid Channel	1.38-1.5	35.7	2.23	Same as above
Control 1	1.37-1.41	55.1	2.80	Same as above
T31	1.35-1.68	83.7	2.84	Same as above
T33	1.50-1.85	-	-	-

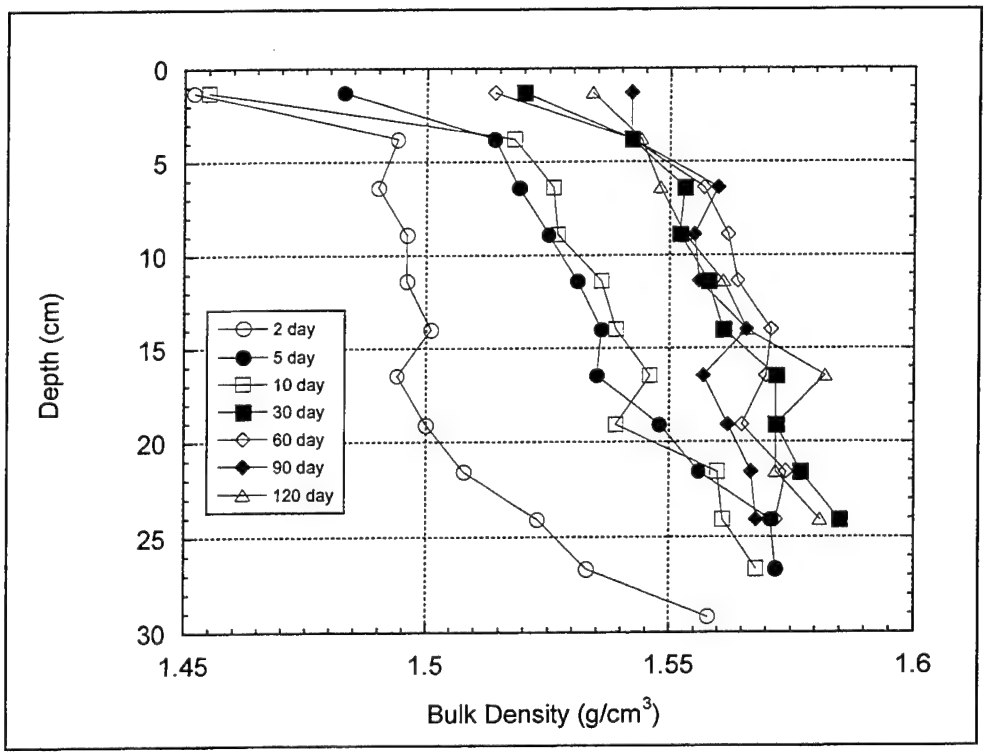

Figure 38. Bulk density as a function of depth and consolidation time for open cell composite (after Roberts et al. 2000)

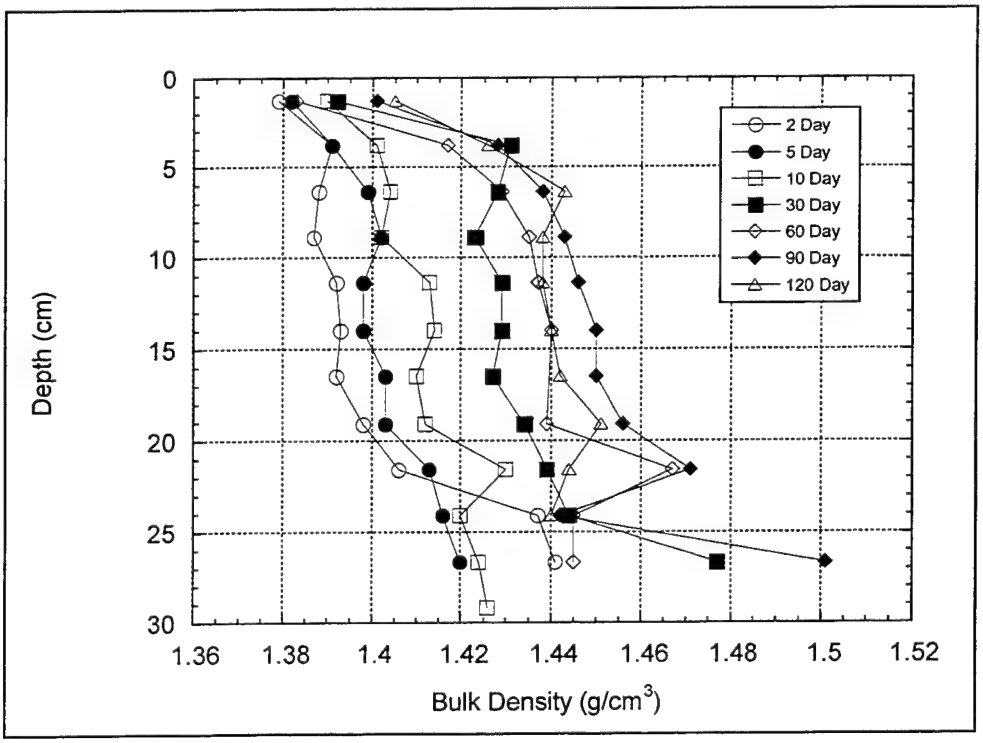

Figure 39. Bulk density as a function of depth and consolidation for midchannel composite (after Roberts et al. 2000)

1.45 g/cm^3 and 1.58 g/cm^3 for up to a 120-day consolidation time. The Mid Channel sediments had a bulk density range of 1.38 to 1.51 g/cm^3. The Mid Channel sediments were less dense and smaller (i.e., lesser mean particle size) than the Open Cell sediments. In general, sediments with smaller mean particle sizes will be less dense than those with a larger mean particle size. However, this is not always the case. Other important considerations are mineralogy and organic content.

Erosion rates. Erosion rates as a function of shear stress and depth were obtained for cores at consolidation times between 2 and 120 days. Erosion rates were measured for shear stresses of 0.5, 1.0, 2.0, and 4.0 N/m^2. The erosion rates for the lower shear stress of 0.5 N/m^2 could only be reasonably measured for the upper portion of the cores and for short consolidation times. That is because erosion either does not occur or is so slow that it would take hours to days to erode a measurable amount of sediment. Likewise, the 4.0 N/m^2 shear could not be tested at all depths because it eroded low bulk density areas too fast for the operator to accurately measure erosion rates.

All of the data for erosion rates as a function of bulk density for shear stresses of 0.5, 1.0, 2.0, and 4.0 N/m^2 are shown for each core in Figures 40 and 41 for site composites Open Cell and Mid Channel, respectively. A large decrease in erosion rate as the bulk density increases can be seen at all shear stresses. This has also been seen in previous experiments by Jepsen, Roberts, and Lick (1997a, b), Jepsen et al. (1998), and Roberts et al. (1998) for other natural and pure quartz sediments in similar laboratory tests. In general, the data can be approximated by an equation of the form

$$E = A\tau^n \rho^m \tag{11}$$

where E is the erosion rate (cm/sec), τ is the shear stress (N/m^2), ρ is the bulk density (g/cm^3), and n, m, and A are constants. The constants are shown in Table 7 for each composite. For each shear stress, the erosion rate as a function of bulk density is shown as a straight line that demonstrates that the preceding equation represents the data quite well and also that the erosion rate is a unique function of shear stress and bulk density. This relationship (with different constants) has been shown to successfully describe seven other natural and many synthetic sediments (Jepsen, Roberts, and Lick 1997a, b; Jepsen et al. 1998; Roberts et al. 1998).

Table 7
Constants for Equation 11 for the Two Composite Sediments

Sediment	*n*	*M*	*A*
Open Cell	3.25	-75	3.35×10^{10}
Mid Channel	3.55	-103	1.32×10^{12}

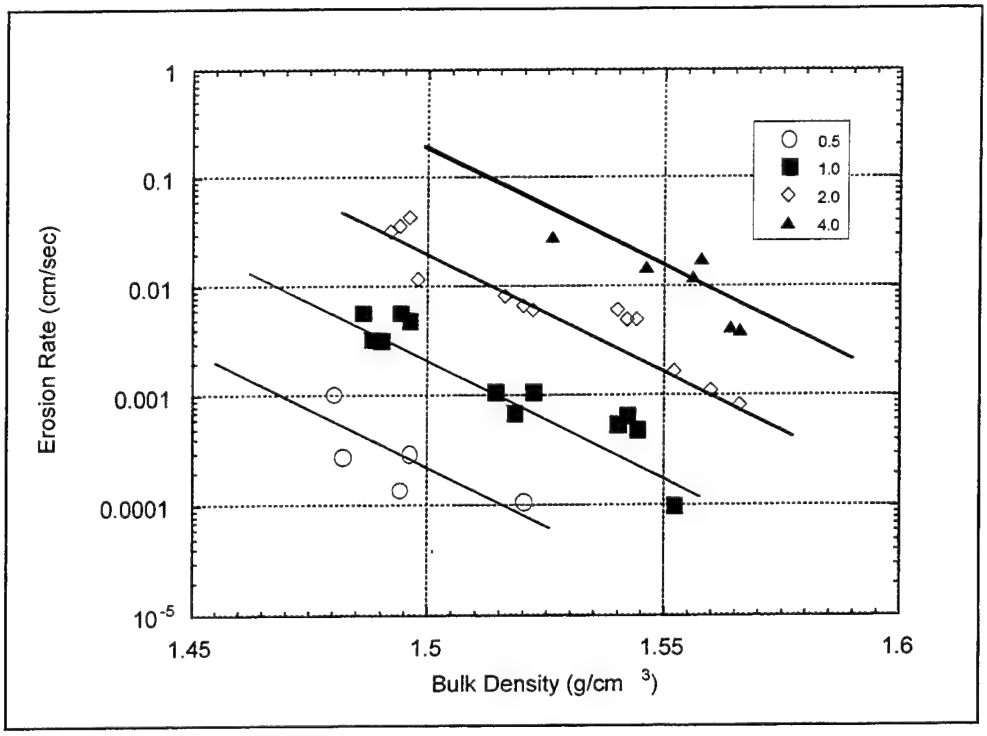

Figure 40. Erosion rate versus bulk density and shear stress for open cell composite (shear stresses = 0.5, 1.0, 2.0, and 4.0 N/m^2) (after Roberts et al. 2000)

Critical shear stress. The critical shear stress can also be determined as a function of bulk density. From Equation 11, the shear stress, τ, can be defined as the critical shear stress, τ_{cr}, by setting the erosion rate, E, to 10^{-4} cm/sec. Solving for τ_{cr} as a function of bulk density gives

$$\tau_{cr} = \left(\frac{E}{A}\right)^{\frac{1}{n}} \rho^{\frac{-m}{n}} \qquad 12)$$

By substituting 10^{-4} cm/sec for the erosion rate and the constants n, m, and A for each sediment into the preceding equation, a general relation for the critical shear stress can be obtained. Substituting the constants listed in Table 7 for each sediment shows that the critical shear stress increases rapidly with small increases of bulk density.

Since tests were done for most of the shear stresses at erosion rates down to 10^{-4} cm/sec, Equation 12 is well supported by experimental data. However, Equation 12 can also approximate the data for erosion rates less than the defined 10^{-4} cm/sec erosion rate for the critical shear stress. Although erosion rates less than 10^{-4} cm/sec may be difficult to measure accurately, the curves plotted in Figures 40 and 41 that are described by Equation 11 could be extrapolated to lower erosion rates. This would allow the critical shear stress to be defined for an erosion rate of 10^{-5} cm/sec as well. For example, Figures 42 and 43 show the

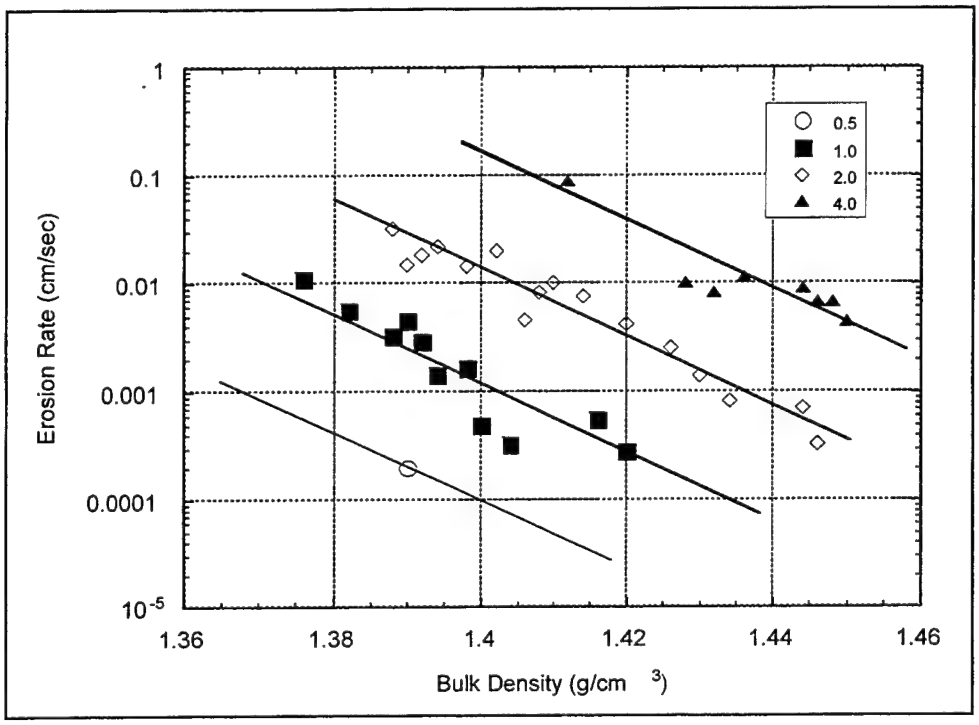

Figure 41. Erosion rates vesus bulk density and shear stress for midchannel composite (shear stresses = 0.5, 1.0, 2.0, and 4.0 N/m^2) (after Roberts et al. 2000)

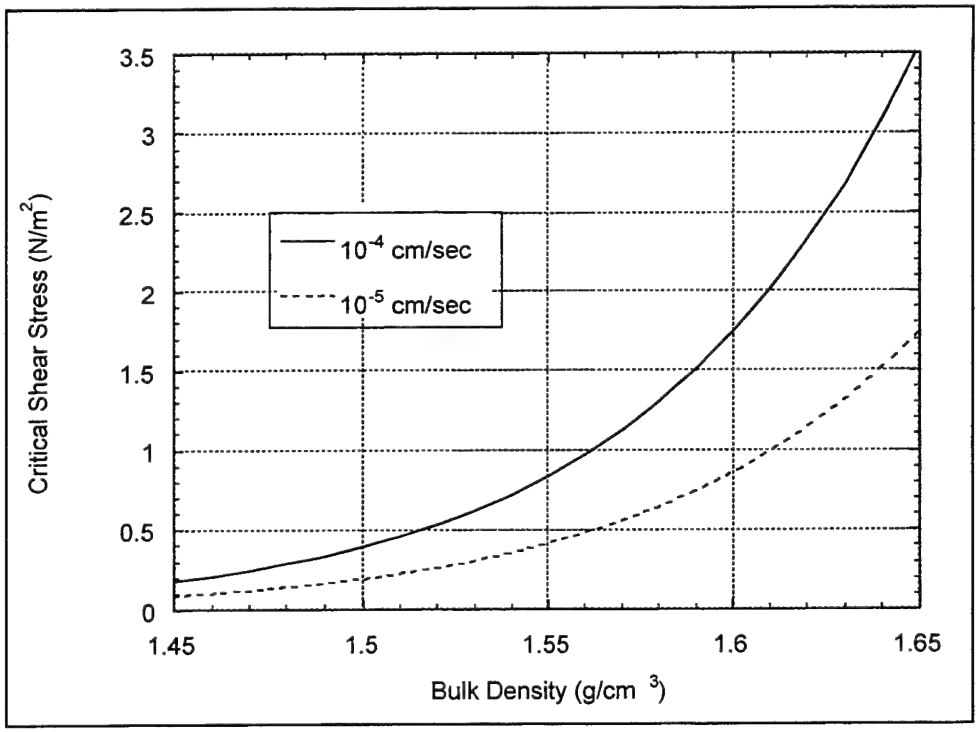

Figure 42. Critical shear stresses as a function of bulk density for open cell composite (after Roberts et al. 2000)

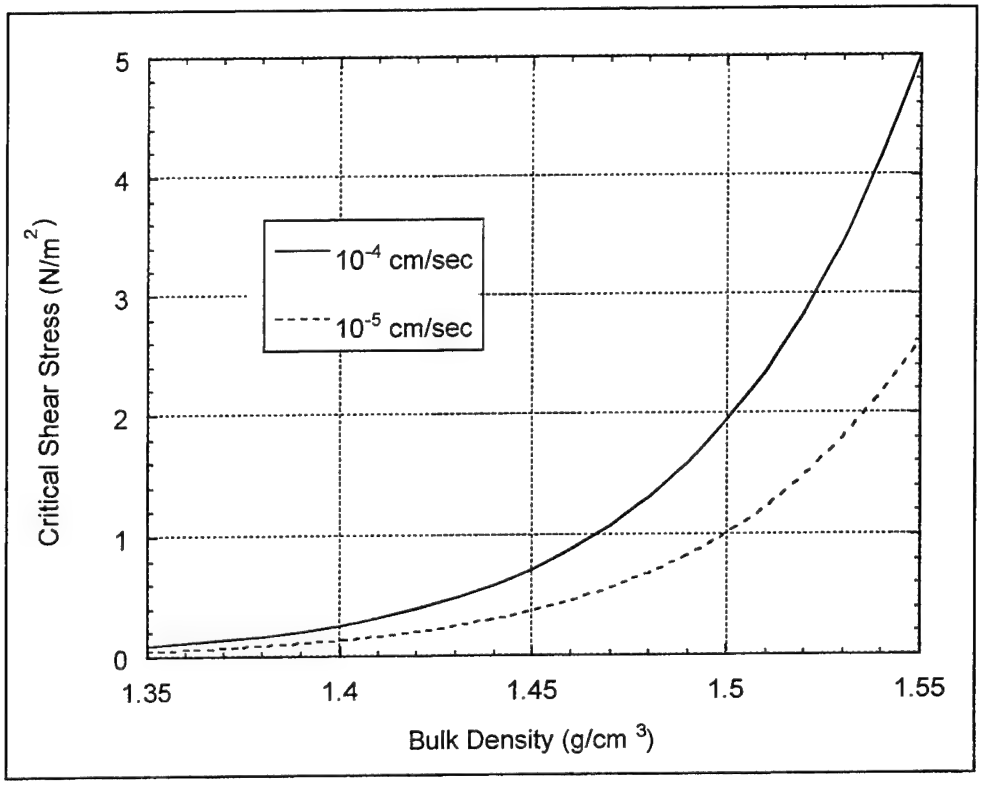

Figure 43. Critical shear stresses as a function of bulk density for midchannel composite (after Roberts et al. 2000)

critical shear stresses (defined for erosion rates of 10^{-4} and 10^{-5} cm/sec) as a function of bulk density as determined from Equation 12 for the Open Cell and Mid Channel composites respectively.

Results of laboratory studies of in situ cores

Tests were conducted to determine sediment bulk properties for three in situ sediment analysis cores retrieved from the Boston Harbor. The three sites are identified as Control 1 (retrieved near the Mid Channel site), and T31 and T33 (retrieved near the Open Cell site). The in situ cores were not analyzed for erosion rate because they were divided into sections onsite prior to shipping with the intention of only doing bulk analysis. That was because a whole in situ core could not be shipped without significant agitation and detriment to the bulk properties. Therefore, erosion rate properties of in situ cores must be done onsite.

Particle size, bulk density, organic content, and mineralogy of the in situ site Control 1 and T31 were measured. For the T33 site, bulk density was the only bulk property measured. The bulk properties of each sediment core were measured with depth, and recorded in 7.6-cm increments from the surface (0 cm) to a depth of 45.7 cm.

Bulk properties for in situ site Control 1. The bulk density (Figure 44) increased from 1.37 g/cm^3 to 1.4 g/cm^3 for the first 11 cm in depth. Then the bulk

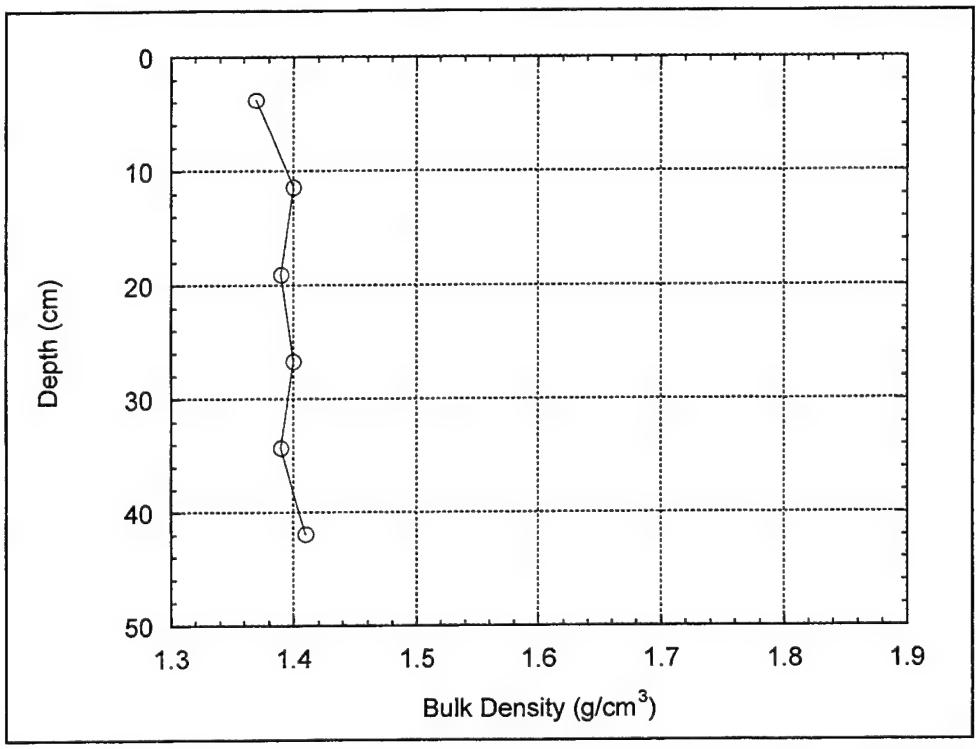

Figure 44. Bulk density as a function of depth, in situ core Control 1 (after Roberts et al. 2000)

density remained constant between 1.39 g/cm^3 and 1.41 g/cm^3 for the remainder of the core. The mean particle size (Figure 45) was 105 μm at the surface; it then decreased and remained relatively constant between 11 cm and 35 cm ranging from 43 μm to 51 μm in size. At the bottom the mean particle size decreased further to 33 μm in size. The organic content (Figure 46) was 4.3 percent at the surface; it then decreased and remained relatively constant for the rest of the core ranging from 2.2 percent to 2.7 percent. The mineralogy was qualitatively constant with depth, and is shown in Table 6, along with a summary of all sediment properties.

Bulk properties for in situ site T31. The bulk density (Figure 47) generally increased with depth throughout the core ranging from 1.35 g/cm^3 to 1.68 g/cm^3 with local decreases in bulk density near 20-cm and 42-cm depths. The particle size (Figure 48) was largest at the surface near a size of 103 μm; it then decreased almost linearly to a depth of 20 cm reaching a value of 65 μm. The mean sized then increased and stayed relatively constant throughout the remainder of the core ranging between 80 μm and 89 μm in size. The organic content (Figure 49) at the surface was approximately 3.2 percent; it then decreased and remained relatively constant between about 12 cm and 35 cm ranging from 2.1 percent to 2.8 percent. The organic content increased at the bottom to its highest value of about 4 percent. The mineralogy was constant with depth and is shown in Table 6, along with a summary of all sediment properties. The mineralogy for the Control 1 and T31 sites were nearly identical, the major difference was that there was more quartz at the T31 site.

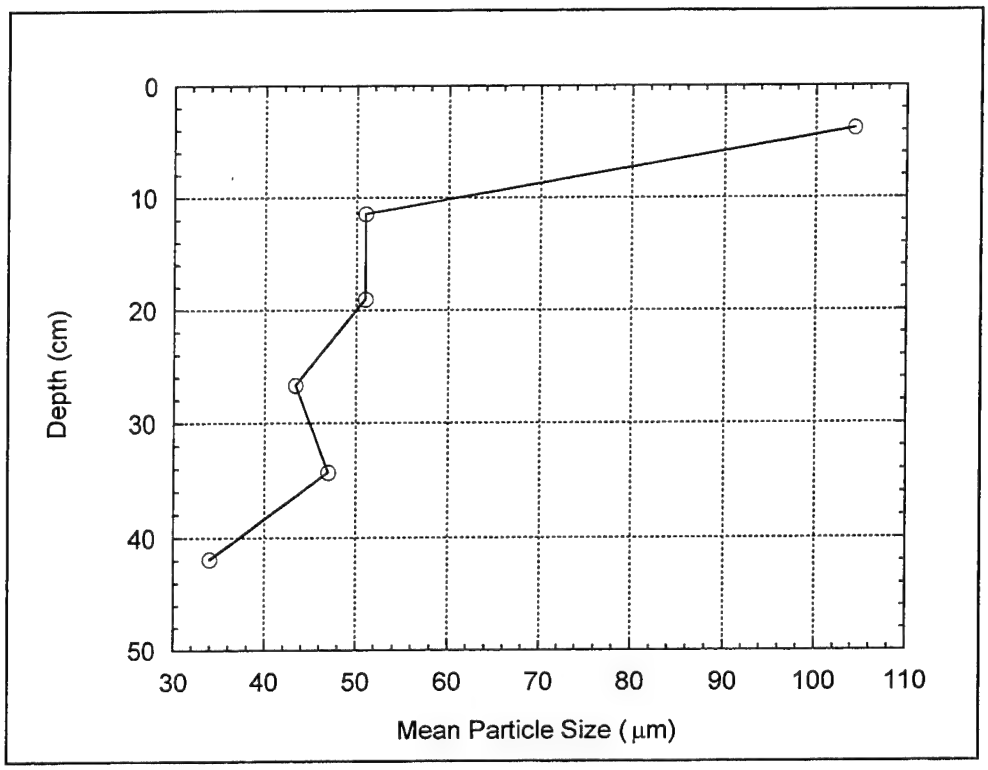

Figure 45. Mean particle size as a function of depth, in situ core Control 1 (after Roberts et al. 2000)

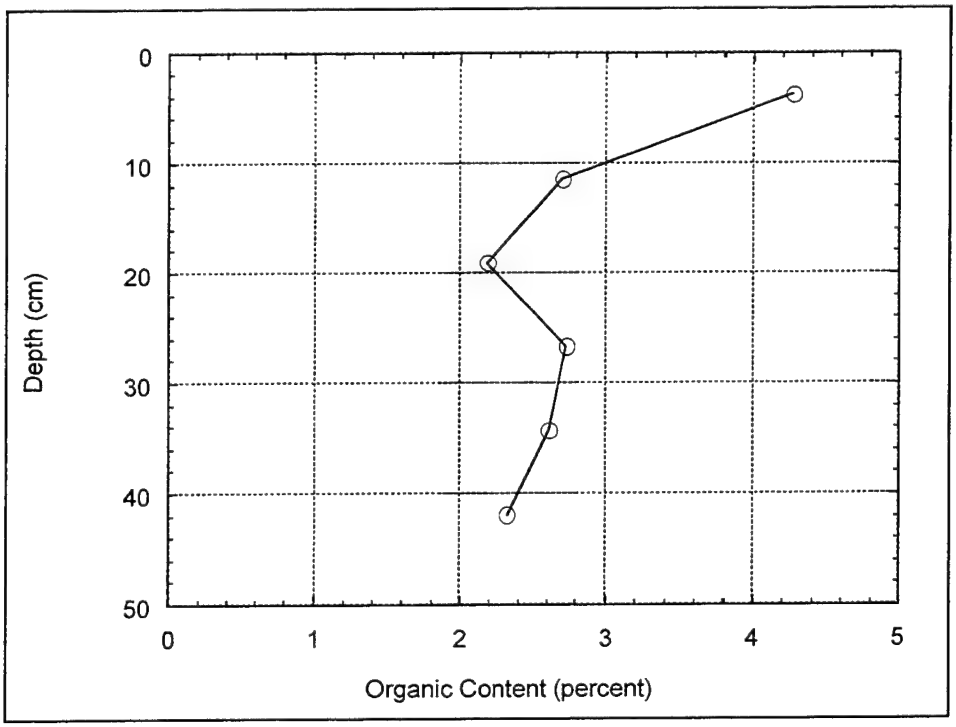

Figure 46. Organic content as a function of depth, in situ core Control 1 (after Roberts et al. 2000)

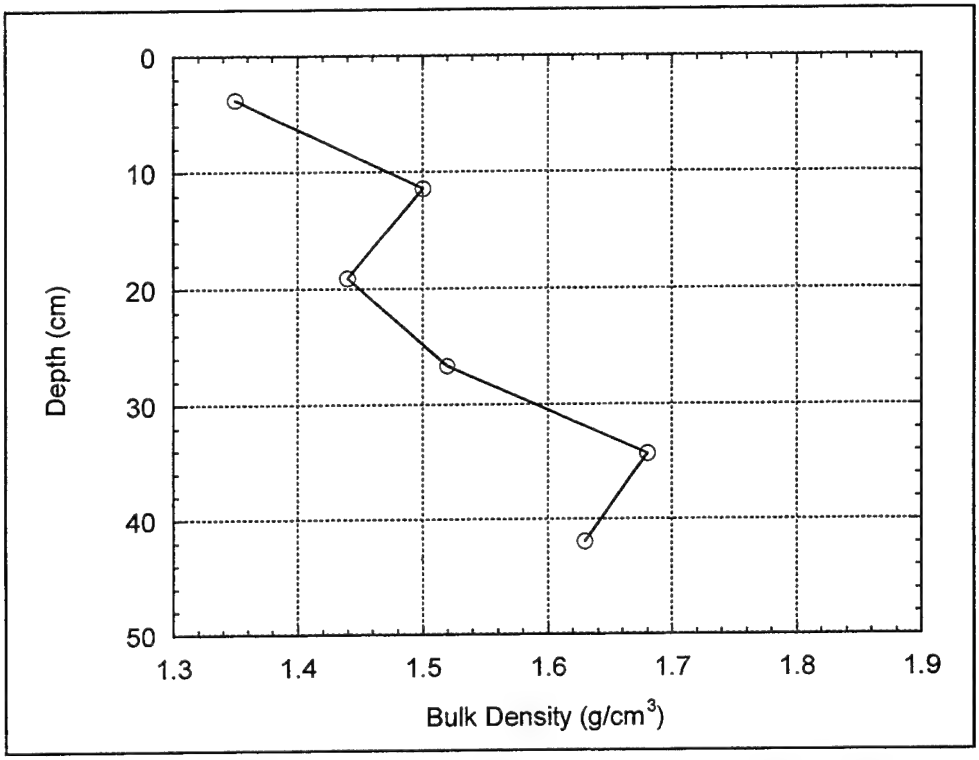

Figure 47. Bulk density as a function of depth, in situ core T31 (after Roberts et al. 2000)

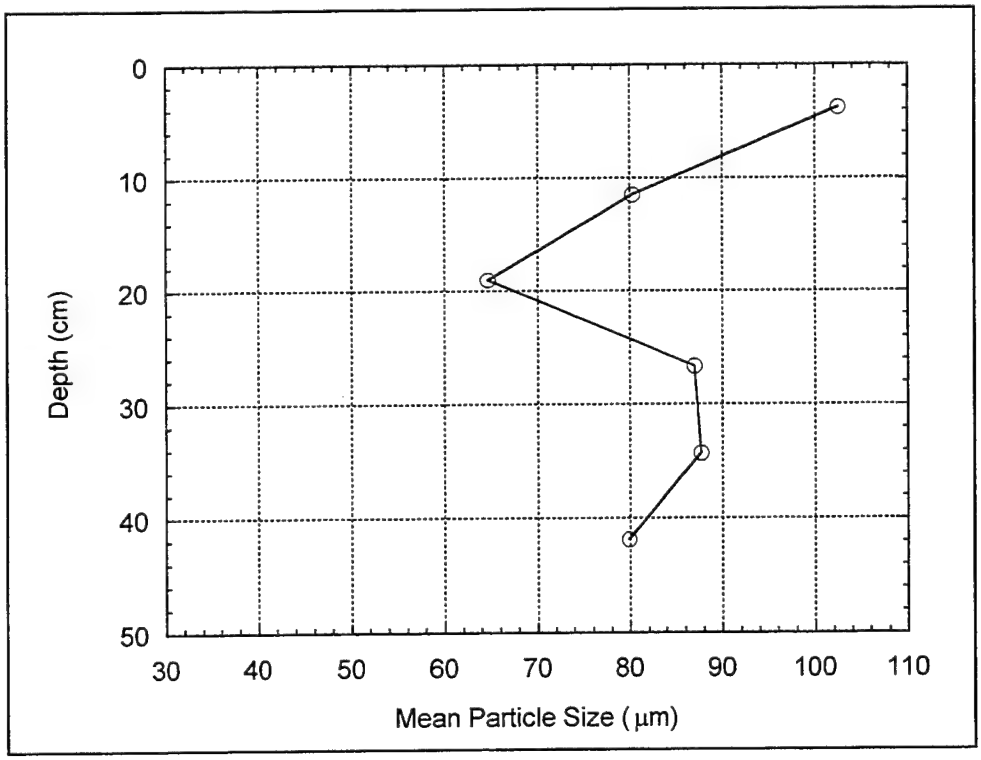

Figure 48. Mean particle size as a function of depth, in situ core T31 (after Roberts et al. 2000)

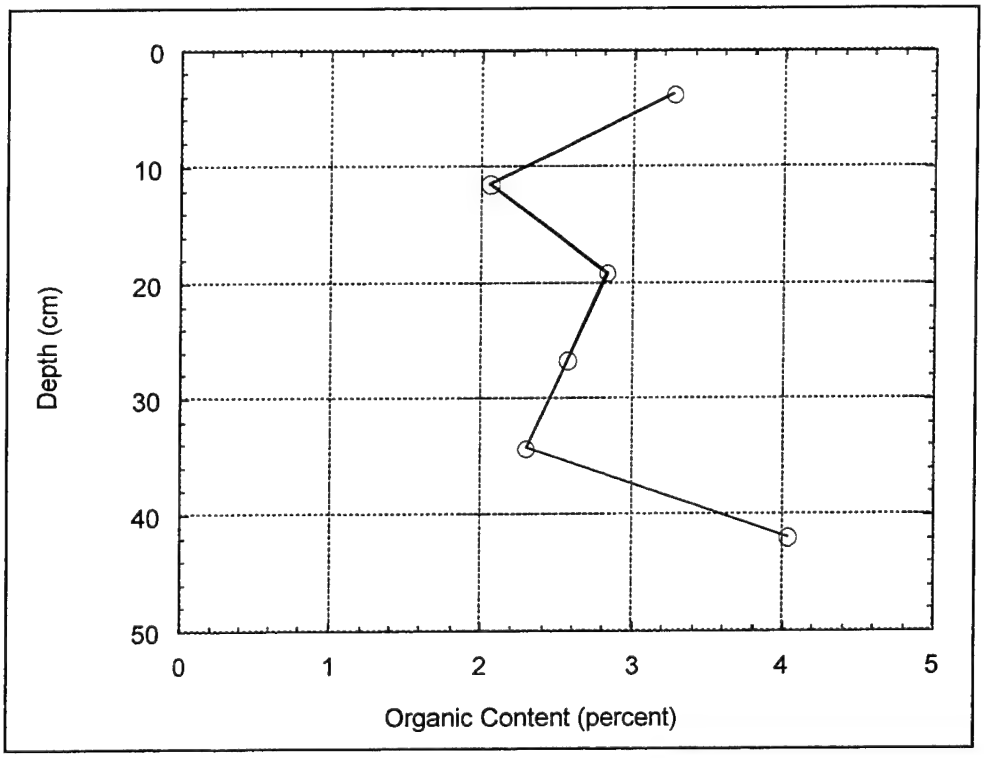

Figure 49. Organic content as a function of depth, in situ core T31 (after Roberts et al. 2000)

Bulk properties for in situ site T33. The bulk density (Figure 50) was smallest at the surface (1.5 g/cm^3); it then increased significantly at a depth of 12 cm. The bulk density remained constant for the rest of the core (ranging from 1.71 g/cm^3 to 1.77 g/cm^3) except for a local increase in the density at a depth of 27 cm to a value of 1.85 g/cm^3.

Discussion of Results

The following compares the bulk properties of the composite sediments and their related in situ cores. Also discussed and compared is the erosion behavior of the two composite sediments.

Bulk properties of in situ and composite sediments. The composite sediment identified as Mid Channel and the in situ core retrieved near the Mid Channel site identified as Control 1 showed general similarities in their bulk properties. First, although the particle size of the surface layer of Control 1 sediment was relatively coarse, the remainder of the core had similar size distributions and mean particle size as that determined for the Mid Channel composite (Table 6, and Figures 37 and 45). Second, except for an increase in organic content at the top and bottom of the Control 1 core, the organic content was similar to that determined for the Mid Channel composite (Table 6, and Figure 46). Finally, the two sediments existed in the same density range and had nearly identical mineralogical properties. Therefore, the studies performed on the

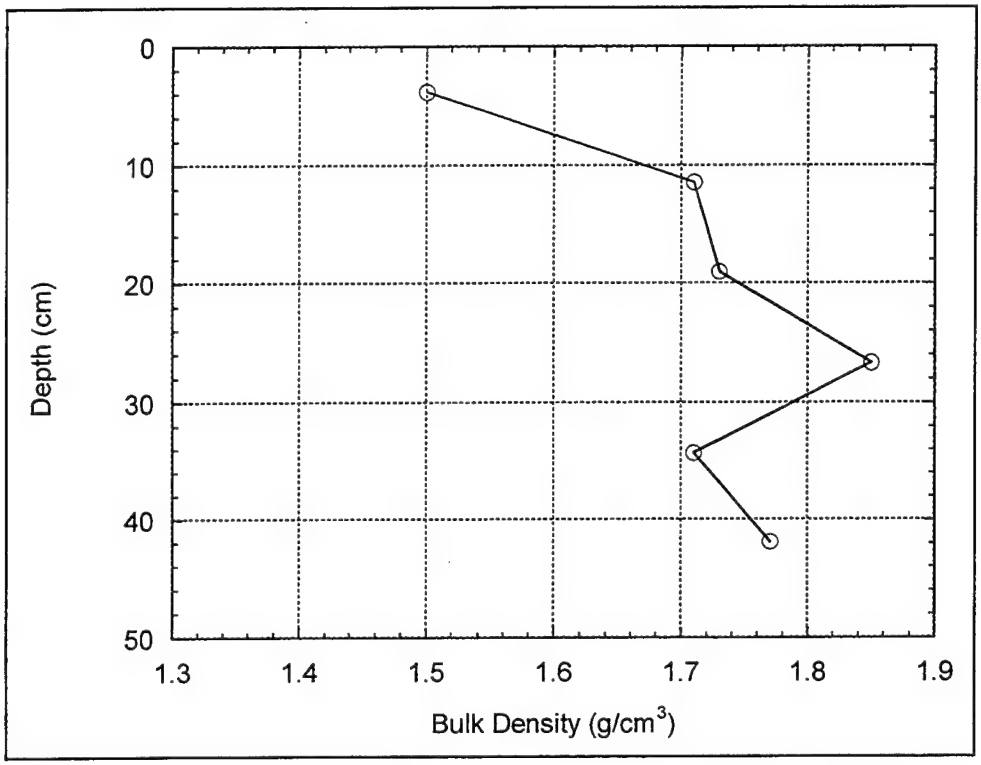

Figure 50. Bulk density as a function of depth, in situ core T33 (after Roberts et al. 2000)

composite sediments are relevant to field conditions and using the consolidation time versus density plot for the Mid Channel composite (Figure 39), it is possible to estimate how long ago the field sediments were deposited. However, the laboratory consolidation studies were conducted for a maximum of 120 days as shown in Figure 39. Hence, the information contained in Figure 39 is best suited to give estimations of in situ sediment consolidation history for residence times less than 120 days.

In situ core T33 retrieved near the Open Cell composites sediments (further away than T31) did not share similar bulk densities with the Open Cell and was therefore not further investigated. In situ core T31 retrieved near the Open Cell shared similar bulk properties with the Open Cell. A unique characteristic of the Open Cell sediment was its distinct bimodal particle size distribution, also present in the T31 sediment but less pronounced. The fine-grained portion of the sediment is very similar to that found in the Mid Channel (Figure 37). Also, the size distribution shows clearly that 100-200 μm sand has been mixed in with the sediment in the Open Cell. The majority of the T31 sediment had a particle size comparable to the Open Cell composite especially at the surface where the composite sample was taken, with an exception at a depth of 20 cm where there was a significant decrease in the particle size. The organic content, mineralogy, and the bulk density ranges for both sediments are similar and overlap. Therefore, the studies performed on the composite sediments are relevant to field conditions and using the consolidation time versus density plot for the Open Cell composite

(Figure 38), one could estimate the residence time of recently deposited sediments (i.e., less than 120 days).

Consolidation and erosion properties for the composite sediments. For the Mid Channel composite the sediment consolidation was relatively slow with time, although after 60 days the consolidation seemed to slow even significantly more. For the Open Cell composite, consolidation was quicker and slowed considerably by 30 days. The reason for the faster consolidation of the Open Cell sediments was probably due to the larger mean particle size which increases the ability for the pore water to be expelled.

The mineralogy for the Open Cell and Mid Channel are qualitatively similar, although by using quantitative techniques it was seen that the Open Cell had approximately 1.5 times more quartz than the Mid Channel. This is most likely due to the large sand content in the Open Cell.

The dependence of erosion on bulk density was greater for the Mid Channel composite sediments, and is quantitatively seen as the steeper slope or greater negative m value seen in Table 7. The m value in Equation 11 can be viewed as a measure of the cohesiveness of the sediments, where noncohesive sediments are attributed with an m value of zero and increasingly negative values are attributed to more cohesive sediments. Therefore the Mid Channel sediments can be viewed as more cohesive than the Open Cell sediments. Since the organic content and qualitative mineralogy are similar, the increase in cohesivity is most likely a result of the smaller mean particle size of the Mid Channel sediment. Again, from review of the particle size distributions (Figure 37), the decrease in mean particle size is a result of the decrease in the quartz mineral constituent above 100 μm.

Summary and concluding remarks

By means of the experiments described here, the effects of sediment bulk density on erosion rates were measured for two composite sediments from two locations in Boston Harbor. From these experiments, the following was determined; (a) the bulk density of the sediments generally increases with depth and time, (b) for each sediment and shear stress, the erosion rate is a unique function of bulk density and decreases as the bulk density increases, and (c) for each sediment, the erosion rate can be approximated as $E = A\tau^n\rho^m$ where A, n, and m are sediment specific, experimentally determined constants.

Additionally, an in situ core from each site was analyzed for bulk density, particle size, mineralogy, and organic content as a function of depth. The bulk properties of these cores proved to be similar to those found for the their respective site composite sediments. Therefore, the studies performed on the composite sediments are relevant to field conditions and may be used to predict present and future erosion properties of those sediments in Boston Harbor.

Modeling of Erosion Due to Propeller Wash[1]

Expected shear stress conditions induced by ship passages have been developed by Maynord (2001). Erosion potential due to ship passages have subsequently been determined by Gailani (2001). Sediments in the Boston Harbor CAD cells are cohesive. Erosion of cohesive sediments is related to sediment bulk properties, including grain size distribution, bulk density, mineralogy, pore water chemistry, and organic content. Although it is known qualitatively how many of these parameters may affect erosion, quantitative methods of relating cohesive sediment erosion to these bulk properties are not available. Therefore, algorithms used to predict erosion rates require site-specific data. Cohesive sediment erosion rates can vary over orders of magnitude based on small variations in bulk properties (Lavelle, Mofjeld, and Baker 1984). Sediment samples were collected from the Boston Harbor CAD cells and reconstituted by Roberts, Jepsen, and Gailani (2001) to develop relationships between erosion rate and sediment bulk density and shear stress. The relationship to bulk density is significant for cohesive sediments because the bulk density generally increases with depth, resulting in significant decrease in erosion rate with depth. To predict erosion from ship passage, the time-histories of shear stress described by Maynord (2001) were incorporated into a model by Gailani (2001) that includes the site-specific experimentally determined erosion algorithms. This includes erosion due to propellers at 5-m increments perpendicular to the center line of the ship going out to 30-35 m. The model simulates a 700-sec period that includes peak shear stress, and continues until near-zero propeller-induced shear stress is reached.

It is well known that ship passage will cause suspension of fine material on the channel bottom. Quantitative estimates have been performed using field data, and models. Many photographs offer qualitative evidence of the large amounts of sediment suspended by propeller wash. However, due to the nature of propeller wash and the erosion/deposition characteristics of cohesive sediment, these models are not universally applicable for soft sediment. The algorithms developed for these estimates combine time and spatial history of bottom shear stress, and vertical variation of erosion rate, for cohesive sediments. It is well documented that cohesive sediment bed erosion reduces with depth due to increased bulk density (e.g., increased strength of cohesive bonds and number of bonds between particles) (Jepsen, Roberts, and Lick 1997a, Roberts et al. 1998, Gailani et al. 2001), and it is important to account for this process when estimating erosion depth. Estimating erosion depth based on erosion rates for surficial sediments may significantly overpredict depth of erosion. Because propeller wash can induce deep erosion depths, this reduced erosion rate must be accounted for when estimating total entrainment.

[1] This section is extracted essentially verbatim from Gailani, J. Z. (2001). "Modeling of erosion due to propeller wash," unpublished document, U.S. Army Engineer Research and Development Center, Vicksburg, MS.

Propeller-induced erosion modeling

Gailani (2001) describes the results of propeller-induced erosion modeling performed by combining the erosion algorithms developed by Roberts et al. (2000) (Equations 10 through 12) and the propeller-induced bottom shear stress estimates developed by Maynord (2001). These algorithms do not include complex turbulent hydrodynamics, but are a screening level tool that combines time-history of bottom shear stress and vertical variation of erosion rate to estimate the total erosion. This model does, however, include deposition processes, but the methods used to estimate these complex deposition processes are not entirely understood. Cohesive sediment concentration profile, floc formation, and settling speed of cohesive sediments during a propeller-induced event have not been quantified. Therefore, the assumptions described subsequently had to be made by Gailani (2001) to simulate these processes. The high shear stress and massive amounts of erosion that will occur in a few seconds under a propeller indicate that deposition processes will be highly significant factors in reducing erosion during the latter part of the event.

Bottom shear stress. Shear stress experienced at the bed were predicted from the model described by Maynord (2001). The time-histories of bottom shear stress underneath the propeller and at 5-m increments moving away from the propeller perpendicular to the *MV Matthew* ship direction are provided in Figures 33 and 34. The first ship scenario (Figure 33) assumes a ship velocity of 1.3 m/sec and a water level elevation of +1.7 m (mllw). The second ship scenario (Figure 34) simulates a ship speed of 1.5 m/sec and a water level elevation of +3.4 m (mllw). Erosion due to both ship scenarios is simulated.

Erosion algorithms. It is well documented that cohesive sediment bed erosion reduces with depth due to increased bulk density. Because propeller wash can induce deep erosion depths, this reduced erosion rate must be accounted for when estimating total entrainment. The experiments and algorithms described previously were incorporated into a model by Gailani (2001) to estimate time-history of propeller-induced erosion. Specifically, Equation 12 is used to predict critical shear stress for initiation of suspension, and Equation 11 is used to estimate the erosion rate if propeller-induced shear stress is greater than the critical shear stress. Both erosion rate and critical shear stress depend on bulk density. Therefore, a layered sediment bed submodel was incorporated into this model to reflect increasing bulk density. Each layer was assigned a thickness, depth below the sediment-water interface, and bulk density. The layered bed model is based on the bulk density profile for sediments that were consolidated for 30-120 days (Figures 38 and 39). Tables 8 and 9 show the layered sediment bed model used for the Mid Channel (in the middle of the channel just outside of Cell M8/M11) and Open Cell (uncapped Cell M8/M11) simulations, respectively. Maximum rate of erosion was set at 0.5 cm/sec. That is equivalent to failure of the bed.

Table 8
Layered Sediment Bed for Midchannel Sediments

Sediment Layer	Depth below sediment/water interface, cm	Bulk density, g/cm^3	Critical shear stress, Pa
1	0-2	1.405	0.55
2	2-5	1.426	0.85
3	5-12.5	1.438	1.09
4	12.5-15	1.440	1.13
5	15-20	1.445	1.25
6	>20	1.450	1.38

Table 9
Layered Sediment Bed for Open Cell Sediments

Sediment Layer	Depth below sediment/water interface (cm)	Bulk density (g/cm^3)	Critical shear stress (Pa)
1	0-2	1.535	0.67
2	2-5	1.54	0.73
3	5-10	1.555	0.91
4	10-15	1.565	1.06
5	15-22.5	1.575	1.22
6	>22.5	1.585	1.42

Concentration profiles and deposition algorithms. When sediment is suspended, it creates a concentration profile. Depending on the sediment and hydrodynamic conditions, it may be fairly well mixed in the water column or almost all sediment may remain near-bottom. Sand particles and aggregates generally remain near-bottom and individual fine particles move higher into the water column. Concentration profiles for sand have been well documented under predominately horizontal flow conditions like tidal currents, river flow, and even near-bottom wave orbital velocities (Fredsoe and Deigaard 1992; van Rijn 1984, 1993). Most experiments have indicated that the majority of sand remains in the first 0.5 m of the water column even under energetic storm wave-breaking and redeposit within a few seconds (Miller et al. 2001)[1]. However, fewer data are available under propeller conditions where there are significant high-speed vertical velocities. The situation for the cohesive material is even less understood. The material often erodes as aggregates that have much greater settling speed than individual particles and do not suspend high into the water column. Often, these

[1] Miller, H., Gailani, J., Hamilton, D., Hands, E., King, E., Resio, D., Smith, E., Smith, J., Smith, S., and Dean, R. (2001). "Nearshore sediment transport during the April 1997 northeaster," unpublished document, U.S. Army Engineer Research and Development Center, Vicksburg, MS.

aggregates move as bed load (Roberts, Jepsen, and Gailani 2001). In addition, settling speed of the individual particles and flocs that form from individual particles is highly dependent on multiple factors including mineralogy, temperature, water chemistry, and other factors. No settling or concentration data or experiments were performed on Boston Harbor sediments. Therefore, assumptions were required for modeling purposes.

Two simulations were performed for each sediment type (Mid Channel and Open Cell). Each simulation assumed that convection and diffusion from the point being studied are minimal compared to the upward movement of the sediment. That is a reasonable assumption because of the short time frame of the erosion event. The first simulation assumed that no settling occurred during the suspension event, and near-bottom concentration did not affect suspension (e.g., there is no maximum near-bottom concentration). That was a most conservative case of pure-erosion and results in significantly greater maximum depth of erosion than for cases where deposition is assumed to occur. The second simulation included deposition, requiring assumptions about concentration profile and maximum near-bottom concentration. That simulation included settling of two different sediment types. The first was sand, with an assumed settling speed of 0.5 cm/sec, and the second was fine material (silt and clay size, including aggregates and flocs) with an assumed settling speed of 0.05 cm/sec. The Mid Channel sediments were simulated with 20 percent sand in the bed, and the Open Cell sediments were simulated with 31 percent sand in the bed. These estimates were derived from the grain size distributions shown in Figure 37.

Erosion was estimated first, followed by vertically averaged concentration. Next, the active layer concentration was estimated according to van Rijn (1993). Near-bottom concentration was compared to active layer concentration. Because there was an assumed vertical profile to the concentration, the near-bottom concentration must be estimated based on the vertically averaged value. For these simulations, the sand was assumed to be 100 times greater near-bottom than the vertically averaged value. The fine-sediment concentration profile was assumed to be a function of the near-bottom shear stress. Higher shear stress indicates that the fine sediment was well mixed in the water column. Low shear stress indicates that the sediment remains near-bottom. Erosion was reset to zero if the near-bottom concentration was greater than the prescribed active layer concentration (e.g., the water column was holding maximum amount of sediment possible at that shear stress). After that, deposition was calculated based on the near-bottom concentration.

Erosion predictions

For each ship passage shown in Figures 33 and 34 by Maynord (2001), erosion patterns were simulated assuming both (a) no-deposition scenarios and (b) deposition scenarios. Each simulation lasted for 700 sec with a 0.1-sec time-step. This time-step was used because of the rapidly changing conditions during a propeller-induced erosion event.

No-deposition scenarios. For the no-deposition scenarios, only depth of erosion under the propeller (maximum depth of erosion) is stated here because it can be assumed that locations away from the propeller will receive significant bed load from under the propeller. The maximum depth of erosion assuming no deposition for Scenario 1 (ship speed = 1.3 m/sec, water level elevation = + 1.7 m (mllw)) for the Mid Channel sediments was 86 cm. The same Scenario 1 with Open Cell sediments resulted in 45-cm maximum depth of erosion. The maximum depth of erosion assuming no deposition for Scenario 2 (ship speed = 1.5 m/sec, water level elevation = +3.4 m (mllw)) for the Mid Channel sediments was 34 cm. The same Scenario 2 with Open Cell sediments resulted in 25 cm maximum depth of erosion. Comparison of Scenario 1 and Scenario 2 results demonstrates the effects of distance from the propeller to the bottom on shear stress and erosion. Additionally, comparison of the Mid Channel and Open Cell results indicates that the Mid Channel sediments are more erosive.

Deposition scenarios. For the deposition scenarios, the erosion was estimated at each location perpendicular to the ship travel direction for which shear stress had been estimated. The 700-sec simulation time permitted redeposition of a significant fraction of the material. The time-history of shear stress and change in sediment bed elevation for the Scenario 1 simulation of the Mid Channel sediments is shown in Figure 51. Peak change in bathymetry occurred slightly before maximum shear stress. The near-bed concentration reached the maximum value before maximum shear stress and deposition began to dominate over erosion despite the high stresses. Maximum depth of erosion was approximately 15 cm. After redeposition, the 15-cm erosion had been reduced to approximately 11 cm. Redeposition will continue, filling in the deficit more, but at some point convection and diffusion due to the ambient current will dominate over propeller effects and the sediment concentration will become more diffuse. The model did not simulate that process. The cross-direction distribution of maximum change in elevation, and change in elevation after 700 sec, for the Mid Channel sediments is shown in Figure 52 for scenario 1. As would be expected, erosion away from the propeller is less, and it is near zero at 25 m from the propeller. The time-history for scenario 1 Open Cell sediments is shown in Figure 53. Maximum erosion was 12 cm, reduced to 8 cm after 700 sec. The cross-direction distribution is shown in Figure 54. Erosion was near-zero approximately 20 m from the propeller.

The time-history of shear stress and bed elevation change under the propeller for scenario 2 Mid Channel sediments is shown in Figure 55. Less erosion occurred in this scenario 2 as compared to scenario 1 because of the higher water elevation and lower bottom shear stress. Maximum change in elevation (maximum depth of erosion) was approximately 11 cm, and this was reduced to 8 cm at 700 sec due to deposition. The cross-direction distribution of maximum change in elevation and change in elevation after 700 sec is shown in Figure 56 for scenario 2. The distribution of bed elevation change perpendicular to ship movement direction was less steep in scenario 2 as compared to scenario 1. The reason for this can be seen in the shear stress distributions described by Maynord (2001). Therefore, scenario 1 caused deeper erosion than scenario 2, but the width of the area experiencing erosion is greater for scenario 2. Erosion is near

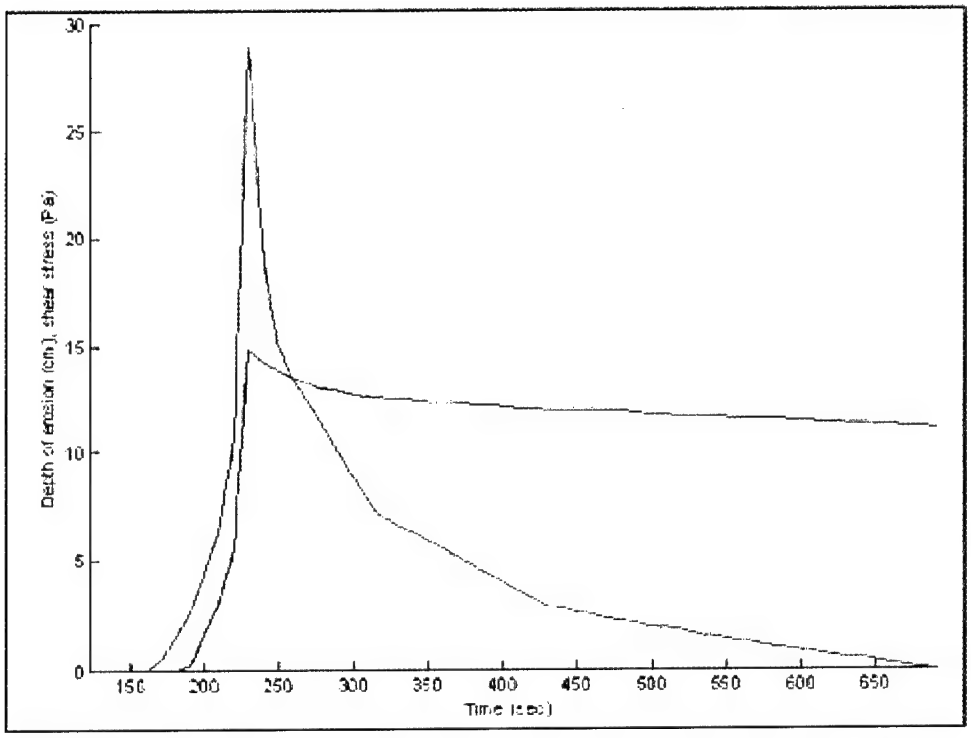

Figure 51. Scenario 1 (ship speed = 1.3 m/sec, water level elevation = 1.7 ft (mllw)) shear stress (red line) and depth of erosion (blue line) time-history under propeller for midchannel sediments (after Gailani 2001)

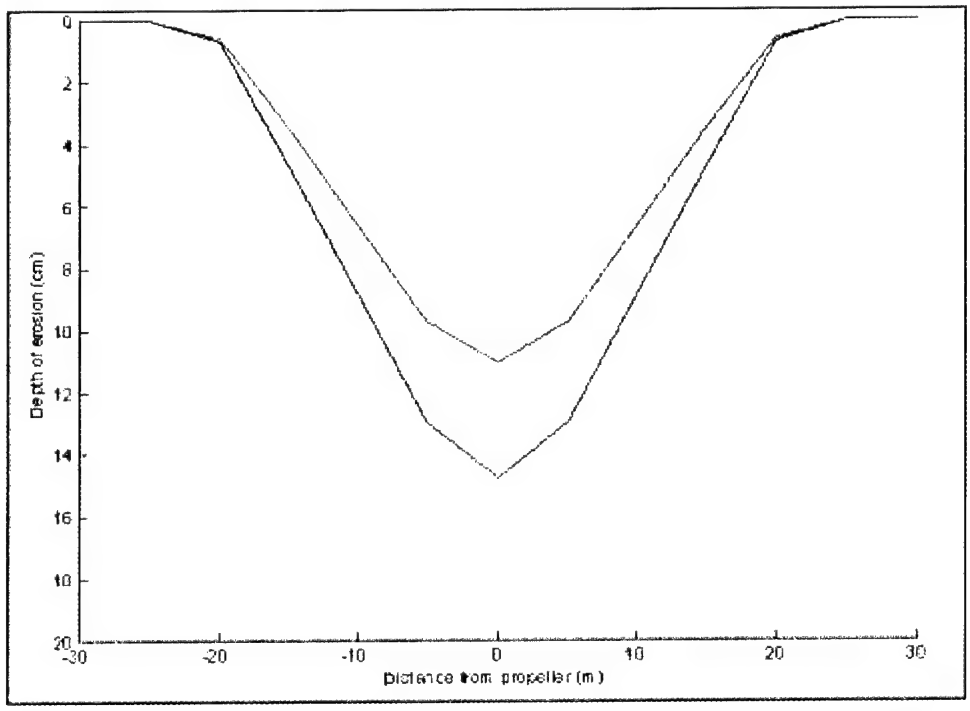

Figure 52. Scenario 1 (ship speed = 1.3 m/sec, water level elevation = 1.7 ft (mllw)) maximum depth of erosion (blue line) and change in depth after 700 sec (red line) perpendicular to the direction of ship movement, for midchannel sediments (after Gailani 2001)

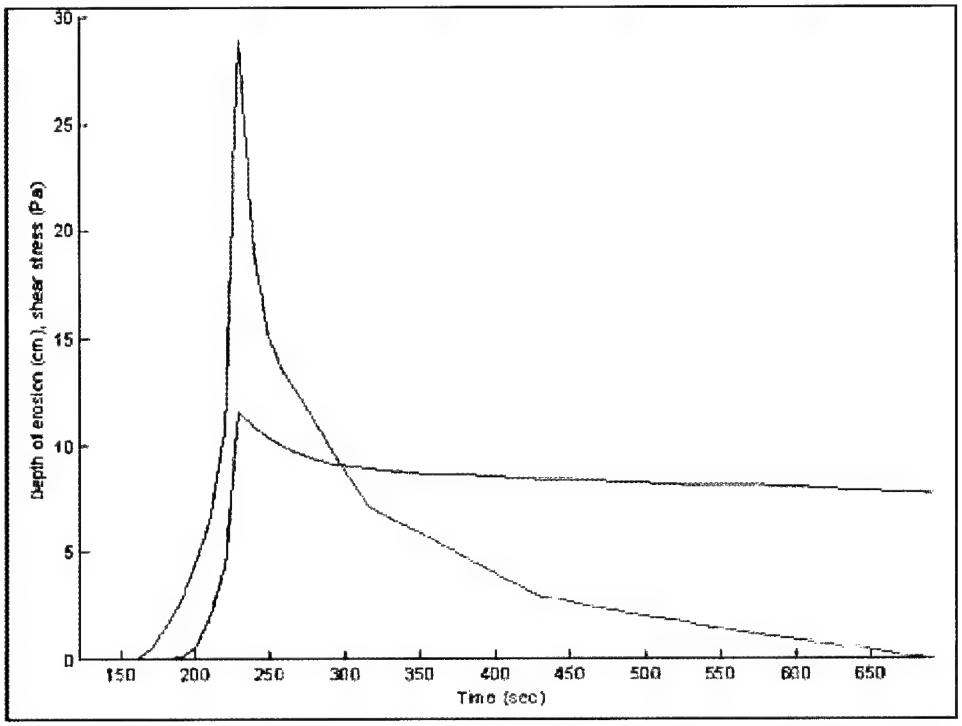

Figure 53. Scenario 1 (ship speed = 1.3 m/sec, water level elevation = 1.7 ft (mllw)) shear stress (red line) and depth of erosion (blue line) time-history under propeller for open cell sediments (after Gailani 2001)

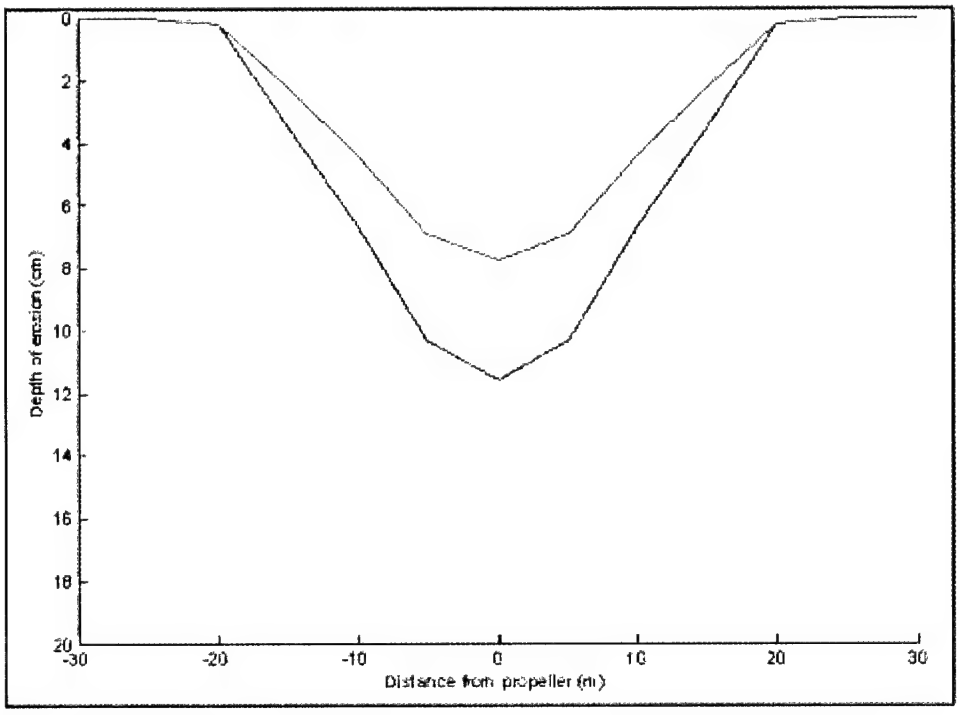

Figure 54. Scenario 1 (ship speed = 1.3 m/sec, water level elevation = 1.7 ft (mllw)) maximum depth of erosion (blue line) and change in depth after 700 sec (red line) perpendicular to the direction of ship movement, for open cell sediments (after Gailani 2001)

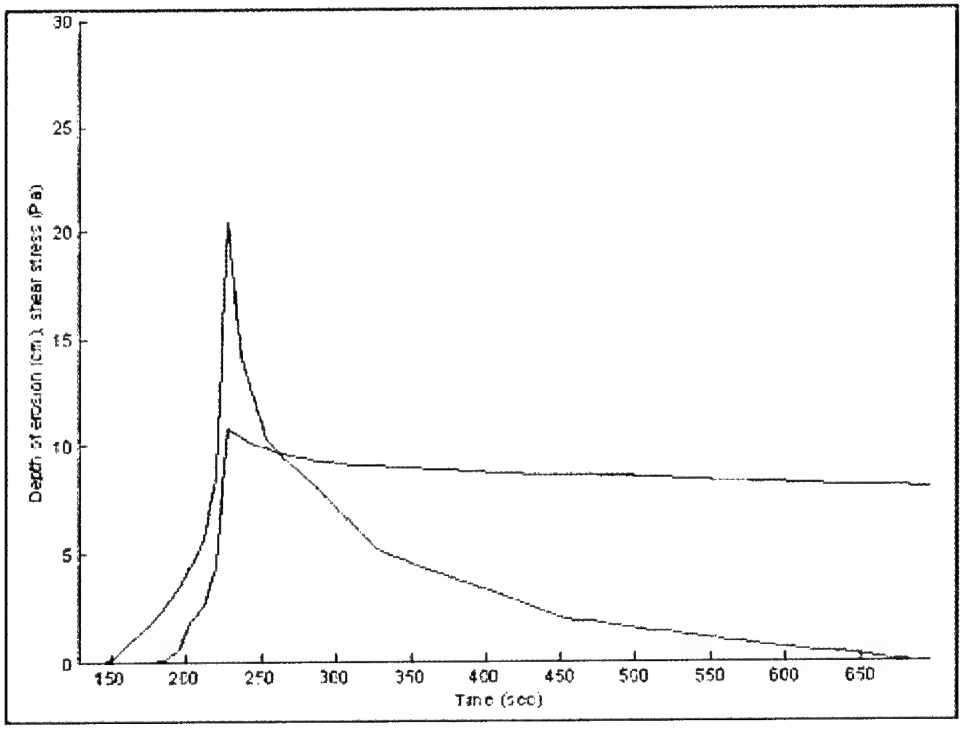

Figure 55. Scenario 2 (ship speed = 1.5 m/sec, water level elevation = 3.4 ft (mllw)) shear stress (red line) and depth of erosion (blue line) time-history under propeller for midchannel sediments (after Gailani 2001)

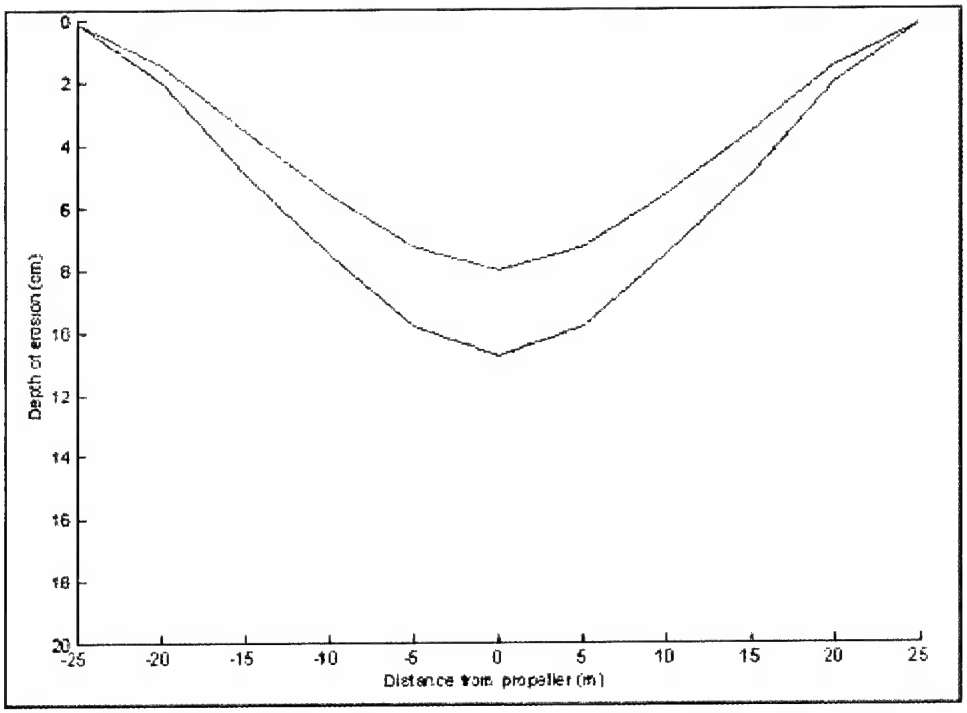

Figure 56. Scenario 2 (ship speed = 1.5 m/sec, water level elevation = 3.4 ft (mllw)) maximum depth of erosion (blue line) and change in depth after 700 sec (red line) perpendicular to the direction of ship movement, for midchannel sediments (after Gailani 2001)

zero approximately 25 m away from the propeller. The time-history of shear stress and bed elevation change under the propeller for scenario 2 Open Cell sediments is shown in Figure 57. Maximum depth of erosion was approximately 8 cm, reduced to 5.5 cm after 700 sec due to deposition. The cross-direction distribution of maximum change in elevation and change in elevation after 700 sec is shown in Figure 58. Erosion is near zero approximately 25 m away from the propeller.

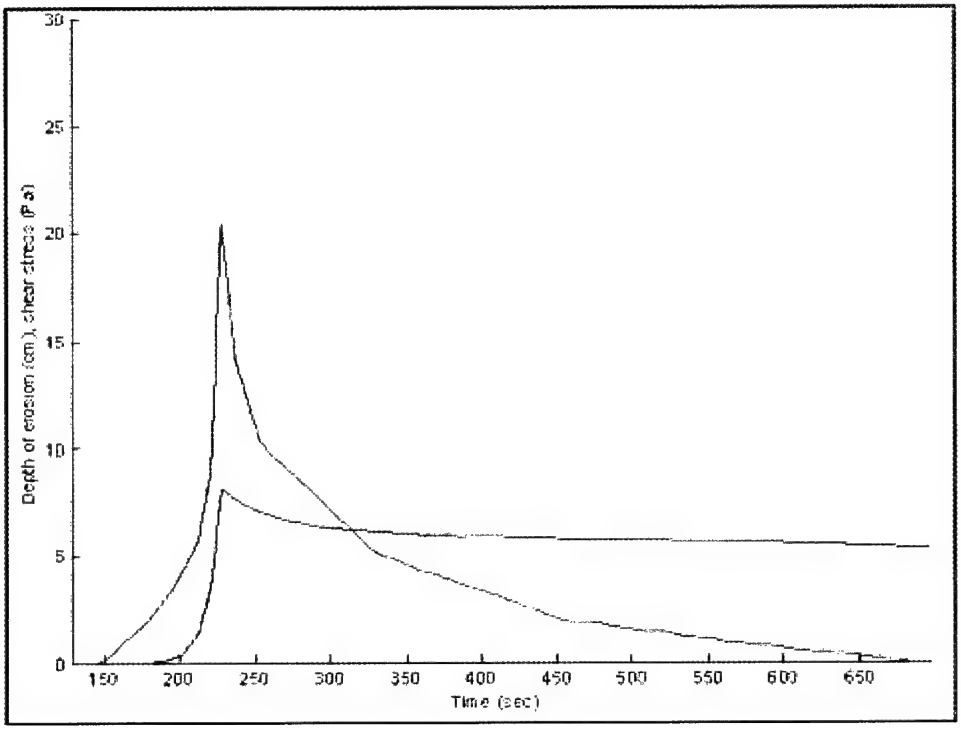

Figure 57. Scenario 2 (ship speed = 1.5 m/sec, water level elevation = 3.4 ft (mllw)) shear stress (red line) and depth of erosion (blue line) time-history under propeller for open cell sediments (after Gailani 2001)

Conclusions

The final bathymetry will depend on how much of the sediment returns to, or near to, the location from which it was eroded. The change in bathymetry after 700 sec could be reduced further, depending on sediment and hydrodynamic conditions in the channel. Additionally, subsequent ship passage may not erode as much sediment because it will be eroding from a more consolidated layer. The redeposited material will be more susceptible to erosion for some time until it can consolidate, but the underlying bed will be more consolidated and more difficult to erode. Additional data on Boston Harbor sediment concentration profile during propeller events, and Boston Harbor sediment settling, flocculation, and aggregate erosion conditions, would reduce uncertainty in this model.

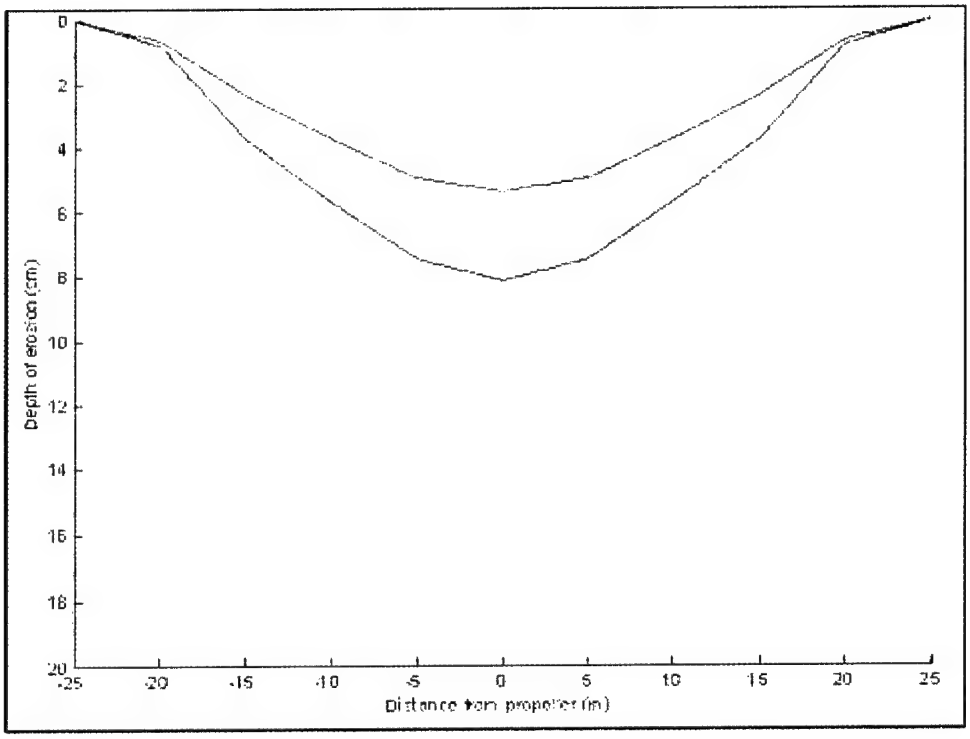

Figure 58. Scenario 2 (ship speed = 1.5 m/sec, water level elevation = 3.4 ft (mllw)) maximum depth of erosion (blue line) and change in depth after 700 sec (red line) perpendicular to the direction of ship movement, for open cell sediments (after Gailani 2001)

5 Summary and Conclusions

Navigation channel maintenance is a primary mission of the U.S. Army Corps of Engineers, sometimes requiring dredging and placement of contaminated dredged material. Sediments in some Corps projects are being found to be contaminated, due primarily to more sensitive testing methods and regulations. Options for placing contaminated sediments are becoming more and more limited. While the use of upland sites is the preferred placement option by many environmentalists, land for such sites is becoming more expensive to obtain or is not available at all. Existing upland sites are reaching capacity in many locations, and are essentially impossible to locate in urban areas where most contaminated material is found. In-channel CAD cells have the potential of providing accessible relatively low cost sites for placement of contaminated sediments.

Boston Harbor Navigation Improvement Project

The Boston Harbor Navigation Improvement Project (BHNIP) involves deepening (maintenance dredging) of the main ship channel and three tributary channels to the Inner Harbor, and associated berthing areas. Lack of an upland disposal site and resource agency denial of permission to place and cap the contaminated sediments at an open water site resulted in the decision to use in-channel CAD cells for placement of contaminated material that would be dredged with an environmentally sensitive clamshell bucket. The main ship channel includes the Inner Confluence and the mouth of the Reserved Channel, while the tributary channels include Mystic River, Chelsea River, and the Reserved Channel.

During phase 1 of the BHNIP, an in-channel CAD cell was constructed for containment of unsuitable dredged material from shipping berths at Conley Container Terminal in South Boston. The fine-grained dredged sediments were disposed into the CAD cell and then capped with sufficient sand to cover the deposit with a 3-ft-thick layer of sand.

Various postcapping monitoring techniques including precision bathymetry, subbottom profiling, and coring were used to evaluate the success of the capping operation. Overall, the survey results indicated that the majority of the CAD cell had been capped with a highly variable thickness of sand, and the southern end of the cell had little or no cap material. Postcapping operations designed to level the

sand cap appear to have resulted in highly uneven sand coverage, and potentially served to enhance mixing of the cap and underlying dredged material. Furthermore, the sediment placed in the cell (both dredged material and capping sand) continued to consolidate after capping.

Recommendations to modify the requirements for dredging and disposal operations were designed around the primary concerns raised by the phase 1 results, including lack of spatial coverage of sand, variable thickness of sand, and potential mixing between the sand and the underlying dredged material. The State of Massachusetts Water Quality Certification (WQC) and the dredging project specifications were modified based on the Phase 1 monitoring results. The method of sand placement was viewed as the main factor resulting in both uneven spatial coverage and variable cap thickness. For phase 2, operations were modified in an attempt to improve placement of the cap material and to increase the ability to diffuse the sand while capping.

As part of the requirements of the WQC during phase 1, the maintenance materials were dredged using an environmental (closed) clamshell bucket. The bucket is designed to limit sediment suspension in the water column, but it has the added effect of introducing large volumes of water into the dredged sediment and subsequently into the CAD cells during dredged material disposal. For phase 2, the recommendation was made to increase the time allowed for consolidation of the fine-grained maintenance sediments prior to capping. By increasing the time allowed for the material to consolidate, the strength and bearing capacity of the material were predicted to increase. However, the phase 1 data provided no clear guidance on the time required for sufficient consolidation prior to capping.

Purpose of MCNP Monitoring

The objective of this monitoring effort by the Monitoring of Completed Navigation Projects (MCNP) program of ERDC,CHL, was to complement the New England District, State of Massachusetts, and dredging contractor monitoring with supplemental monitoring that will help to evaluate the effectiveness of in-channel CAD cells at Boston Harbor. The MCNP monitoring plan was composed of three primary activities:

a. The first activity conducted water quality monitoring of suspended solids near the operation of two environmentally-sensitive clamshell dredges and a normal clamshell, to document the benefits of the special clamshell buckets.

b. The second activity monitored contaminated dredged material consolidation and strength prior to and after placing the sand cap. Laboratory tests measured consolidation, shear strengths, water content, etc., of both the contaminated sediments and the Boston blue clay to refine predictive techniques for mound and cap performance.

c. The third activity calculated cap erosion predictions from both tidal currents and ship propeller wash to characterize the likely amount of cap damage to be expected from either source.

The lessons learned here will assist the New England District and other Corps districts to evaluate the effectiveness of CAD cells as a contaminated dredged material placement option. Additionally, documentation of sediment resuspension by conventional and closed clamshell buckets, and the amount of water added, will assist districts in optimizing between reducing resuspension during dredging versus added water which could make capping more difficult.

Results and Conclusions

Clamshell dredge bucket comparison[1]

Sediment resuspension and loading characteristics were studied under near-similar operating and environmental conditions in Boston Harbor during August 1999 for three clamshell dredge buckets; (a) Great Lakes Dredge and Dock (GLDD) Conventional (open-faced), (b) GLDD Enclosed, and (c) CableArm™. Monitoring was conducted to characterize each bucket's near and far field sediment resuspension characteristics. Bucket loading characteristics were investigated with regard to water-to-solids ratios dredged by the different buckets.

Because a significant fraction of the sediments dredged during the BHNIP phase 1 had elevated levels of some contaminants, the State of Massachusetts Department of Environmental Protection required that either one of two approved enclosed buckets be used to reduce sediment resuspension and potential for water quality impacts. Tests showed no exceedances of the water criteria with either of the approved buckets (GLDD Enclosed bucket or the CableArm navigation bucket). However, the New England District expressed concern that the enclosed buckets were adding additional water to the already soft and weak sediments, possibly causing a further reduction of the bearing capacity of the sediments. This reduction of bearing capacity would, in turn, make the capping operation even more difficult.

Near field results. Based on turbidity measurements, the Conventional bucket produced the highest amount of sediment resuspension spread throughout the water column. Use of the CableArm bucket appeared to reduce sediment resuspension in the water column, as the observed depth-averaged turbidity was 46 percent less than observed for the Conventional bucket. Insufficient TSS data were collected during the CableArm bucket operation to completely confirm this reduction, although the few data collected show an even higher reduction. The Enclosed bucket had the lowest overall turbidity and substantially less in the middle of the water column. Observed depth-averaged turbidity for the Enclosed bucket was 79 percent less than observed for the Conventional bucket. This

[1] This text was taken from Welp et al. (2001).

compared well with observed TSS which showed depth-averaged TSS concentrations for the Enclosed bucket 76 percent less than for the Conventional bucket. Functional seals on the CableArm bucket would have probably further reduced water quality impacts.

Far field results. The Broad Band Acoustic Doppler Current Profiler (BBADCP) provided good qualitative data to indicate relative amounts of sediment resuspension in the plume and delineate its boundaries. BBADCP data results correspond to results from those data collected in the near field. BBADCP coverage provided insight on where to sample with the more quantitative sampling equipment of the BOSS. The data systems provided good insight on the different buckets' sediment resuspension characteristics, but plumes are difficult to track and measure. This difficulty stresses the need to continue developing methods to standardize plume data collection and analysis methodologies for future projects. Also, to account for variations in sediment characteristics, thickness of the dredge cut, etc., multiple days of sampling with each bucket are recommended to provide a more valid statistical basis for comparison.

Geotechnical investigation of CAD Cell M2[1]

Sampling stages and analyses. The sediments placed in CAD Cell M2 were sampled and evaluated for engineering properties during several stages; (a) prior to dredging (in situ survey), (b) during transport (barge sampling), (c) immediately after placement in the CAD cell (T_0 survey), (d) immediately prior to capping (T_1 precap survey), and (e) after capping (postcap survey). The geotechnical investigation was initiated near the end of dredging of the Mystic River; therefore, the in situ survey involved collecting in situ material in the Mystic River channel representative of the dredged sediments. Samples were thus collected in areas of the Mystic River that were not previously dredged as part of the BHNIP. The in situ survey took place simultaneously with the T_0 survey in June of 1999. Grab samples and core samples were taken for analysis during the several different stages. Sample analyses included (a) water content analysis, (b) grain size analysis, (c) Atterberg limit analysis, and (d) shear strength analysis.

Conclusions. The following conclusions were developed from analyses of the grab samples and core samples taken from CAD Cell M2 and the Mystic River.

a. The natural cohesion and strength of the Mystic River sediments were altered by the dredging process, resulting in sediments in the CAD cell that were unstable due to high water content and low shear strength.

b. During the 5-month consolidation time, the change in water content of the surface sediments (as collected in the grab samples) was the single measured geotechnical parameter that clearly provided an indicator of cap-readiness.

[1] This text was taken from SAIC (2000a).

c. Capping-induced consolidation resulted in sediments of strength similar to in situ material, suggesting that precapping might be a useful operational approach for future projects.

d. The results from Core M2-4 and subbottom profiling records suggested that excess pore water was released not only through the cap but also was vented through diapir structures that served to breach the caps in discrete areas.

e. Future projects should include an evaluation of the geological environment under consideration for a CAD project, such as an evaluation of the in situ strength of the material to be capped and the porosity and permeability of the CAD cell sediments. Consideration of innovative capping approaches, including a phased capping approach, should also be considered.

f. Future project sampling plans should be designed to focus on the top meter of material within the CAD cell and at set intervals.

Boston Harbor CAD Cell capping simulation[1]

Geotechnical performance analysis of some of the previously capped cells indicated that the dredged material placed in those cells appeared to have insufficient upper surface bearing capacity to adequately sustain the induced sand cap weight. One cell in particular (Cell M2) was chosen for a more detailed performance analysis prior to, during, and after the cap was placed. Cell M2 observations showed that extending the dredged material sediment consolidation period prior to capping allowed the sediment shear strength to increase sufficiently to adequately resist the superimposed cap weight. Changes in sediment characteristics were observed over about a 5-month span, and it was noted that the sampled spread diameters and initial height differences decreased during that time period. The Cell M2 dredged material sediment was undergoing self-weight consolidation while achieving higher shear strengths and lower water contents during the 5-month period prior to sand capping.

Laboratory simulations were performed using analytical modeling with geotechnical software, physical modeling with a centrifuge, and laboratory testing to obtain material properties. A surrogate dredged material having similar geotechnical properties was chosen to represent the actual contaminated sediment material. Homogeneous soil types of lean clay (CL), fat clay (CH), white kaolinite clay (CL), and silt (MH) were mixed with varying amounts of water to achieve a water content ranging from 31percent to 102 percent. Each soil's remolded undrained shear strength was taken at the corresponding water content using the laboratory miniature vane shear device. The kaolinite soil was chosen as the surrogate dredged material for physical modeling in the centrifuge based on the laboratory test results most closely resembling those from the Cell M2 sediment.

[1] This text was taken from Lee (in preparation).

Analytical modeling of the CAD cell. A two-dimensional finite element program, STUBBS, was available to model the geotechnical parameters assigned to simulate dredged material sediment underlying sand cap layers. The software simulated the complete cap placement process by sequentially placing layered elements until the final CAD cell geometry mesh was created.

The surface geometry of the overlying sand layer was modeled after in situ depth soundings at Cell M2, which indicated that the surface slope of the sand typically varied by a few percent. The mesh elements in the sand layer were thickened to create a small 100-ft- (33-m-) wide mound on the sand surface. The mound reached a maximum height of 0.5 ft (0.15 m) above nominal elevation of the sand surface to create a 1 percent slope. Significant yielding under this slight mound was observed when the assumed strength of the clay sediment was decreased to 17 psf (0.8 kPa). At 5 psf (0.2 kPa) the modeled deformation yielding indicated an essentially complete failure mechanism, although an equilibrium solution was maintained.

At 2.5 psf (0.1 kPa) convergence in the solution could not be obtained. The deformation pattern in all modeled cases indicated that the principal plane of shear developed along the base of the confined aquatic disposal cell rather than within the fill material, suggesting that the size and shape of the cell bottom controlled the critical shear surface. From these modeling results it appeared that an undrained shear strength of about 20 psf (1 kPa) was a reasonable criteria for dredged material strength prior to capping provided the cap thickness can be maintained to the tolerance of the Cell M2.

Physical modeling of the CAD cell capping process. The numerical modeling results provided insight into the lower range of required undrained shear strength in the dredged material and the results appeared to be consistent with Cell M2 field performance. However, the numerical model was based on numerous assumptions, and did not account for possible pore pressure effects related to pore water upwelling as the consolidation process took place. Physical modeling was accomplished using the U.S. Army Centrifuge Facility at ERDC. Physical modeling on the geotechnical centrifuge provided a link between the numerical computations and field observations. The centrifuge intensifies the gravity-induced body forces to allow dimensionally correct scale models that more accurately reflect the physical processes.

The clay-water mixture representing the dredged material fill was placed at a water content which allowed an undrained shear strength of between 20 to 30 psf (a to 1.4 kPa), based on previous laboratory testing results. At this lower strength range, based on the analytical modeling results, the sand cap would be assumed to be minimally stable. To simulate the physical layout of Cell M2, the model was built to scale proportions for which a unit model length equaled 10 length units in the full-scale prototype Cell M2. During centrifuge flight, a specially designed sand dispenser was operated in a fashion imitating the two-dimensional dump scow placement process for the prototype Cell M2 sand cap. After flight, the soil model was analyzed and the layer geometry was noted. As expected, the sand cap remained stable although significant settlement was observed in the sand surface. This settlement likely occurred due to the time-dependent consolidation process in

the kaolinite clay. No significant disturbance in the sand cap was noted due to pore fluid moving upward from the consolidating clay.

Effect of sediment resuspension by *MV Matthew* on water quality[1]

Underway measurements were obtained of temperature, salinity, and turbidity within the water column using the BOSS. Also, concurrent measurements of water column currents and acoustic backscatter intensity were made using a BBADCP mounted on the survey vessel. Data were acquired while the survey vessel followed close behind the 900-ft-long liquid natural gas carrier (*MV Matthew*) as it departed from the Mystic River at the head of Boston Harbor. The track of the LNG carrier passed over uncapped CAD Cell M8/M11 and capped Supercell, then along the navigable channel exiting the Inner Harbor. The 35-ft draft of this vessel was approximately 88 percent of the water depth in the navigable channel.

BOSS survey. The primary objective of this brief monitoring project using BOSS was to determine whether large vessels transiting the Mystic River induce resuspension of unconsolidated dredged material that resided within uncapped CAD cells, by analyzing discrete water samples. Background water property measurements made prior to departure of the *MV Matthew* showed that total suspended solids (TSS) concentrations were low (generally less than 10 mg/L) and spatially homogeneous throughout the Mystic River and Inner Harbor. As the *MV Matthew* departed the Mystic River, four transects made perpendicular to the vessel's wake revealed elevated TSS concentrations (up to 40 mg/L) within a few meters of the bottom beneath the wake. Although these results indicate that bottom sediments are temporarily resuspended during departure of large vessels, the volume of sediments resuspended from capped and uncapped CAD cells is very small (well less than 1 cu m) for each vessel passage. Subsequent monitoring indicated that the resuspended sediments settle to the seafloor within 1 hr of resuspension.

The correlation between in situ transmissometer-based turbidity data and laboratory analyses of TSS concentrations from the discrete water samples was poor for the background sampling events. It is believed that a good correlation exists between the in situ BOSS bean attenuation (BA) values and the TSS concentrations of water samples collected currently with the BA data, but only at higher TSS concentrations (i.e., TSS greater than 10 mg/L). The transmissometer was useful for identifying relative changes in turbidity, such as distinguishing between background water properties and plumes associated with resuspension of bottom sediments. In the absence of discrete water samples from these plumes, and hence, data for calibration of the transmissometer, accurate quantitative estimates of the TSS characteristics within the sediment plumes could not be provided.

BBADCP survey. The BBADCP backscatter data are presented in units of acoustic backscatter above background (ABAB) which is proportional to

[1] This text was taken from SAIC (2000b).

suspended sediment concentration. The background acoustic backscatter level was determined by making BBADCP measurements just prior to the departure of the liquid natural gas carrier *MV Matthew* from its berth in the Mystic River. This background value was then subtracted from all of the ABAB measurements made simultaneously with the BOSS data. The monitoring plan did not include making multiple transects to gather statistics on the variability of the background, so the differences between the monitoring measurements and the background measurements were divided by a standard deviation of 1.5 to give the nondimensional ABAB values. The standard deviation of 1.5 for the background variability is typical of that measured during acoustic monitoring operations with the same ADCP system in Boston Harbor during August 1999.

When viewing the ADCP backscatter results, it is important to remember that air bubbles trapped in the wake of a vessel from propeller cavitation can produce stronger ABAB signals than does suspended sediment. When the ABAB values are associated with suspended sediment, larger values mean higher concentrations of suspended sediment if the grain-size distribution remains constant. For the same concentration of suspended sediment, larger particles produce higher ABAB values than smaller particles. Because of the wake effect on the acoustic measurements, it is difficult to draw conclusions about suspended sediments directly within or under the wake of the liquid natural gas carrier *MV Matthew*.

Sediment resuspension by tidal currents and *MV Matthew*[1]

Concurrent with the study to determine the effect of sediment resuspension by the *MV Matthew* on water quality, monitoring was conducted to determine whether tidal currents and deep-draft vessels could erode the sand cap and expose dredged material in the cells. This monitoring was performed during passage of the deep-draft LNG carrier *MV Matthew* during its departure from the Mystic River approximately 2 hr after high water on the morning of 31 March 2000. The vessel transited through the uncapped CAD Cell M8/M11 and the capped Supercell.

It was determined that the typical currents within the Mystic River are insufficient to induce major erosion of bottom sediments in the navigable channel or within the CAD cells which are 1 to 4 m deeper than the channel. It is possible that currents are intensified during major storm surge events and during periods of intense river discharge, but field observations during these relatively brief event processes are not available.

There is only about 3 m of clearance between the hull of the *MV Matthew* and the seafloor within the navigable channel. Consequently, the vessel causes intensified currents at the seabed during the few minutes the vessel passes over a fixed point in the channel. Near-bottom current speeds can achieve maximum values on the order of 65 cm/sec (averaged over 10 sec) and possibly higher for instantaneous speeds as the propeller(s) of the vessel pass over a fixed location. These speeds are sufficient for erosion of sediments in the navigable channel as

[1] This text was taken from SAIC (2001).

well as within the CAD cells. The near-bottom suspended sediment concentrations within the cells did, however, return to their relatively low background levels within a few minutes of vessel passage, supporting the hypothesis that only a small volume of sediment was actually resuspended along the trackline of the vessel through the cell

Ship-generated velocities and bed shear stress[1]

Two vessels were used in this analysis to determine velocities and bed shear stresses caused by large ships: (a) the liquid natural gas carrier *MV Matthew*, having a 10.7-m draft, 41.2-m beam, and 290-m long ship with an installed power of 36,000 hp; and (b) the tug *MV Matthew Tibbetts*, having a 3.4-m forward draft, 4.3-m aft draft, 7.9-m beam, and 30-m long tug with an installed power of 2,000 hp. This evaluation investigated the displacement effects of the ship and the propeller jets of both the ship and tug. The tests were conducted in the most confined section of channel (i.e., it had the smallest channel area).

Based on bed shear stress calculations, the ship having the most potential for resuspension of the cap on the Boston Harbor CAD cells is the *MV Matthew*. The tug *MV Matthew Tibbetts* produces small shear stress compared to the *MV Matthew*. The 30-rpm propeller speed reported by the pilots results in a ship speed of about 1.5 m/sec. This ship speed and propeller speed were used to calculate the bed shear from the bow, return currents, and the propeller jet. Shear computations were conducted for tide levels of +1.7 m (mllw) and + 3.4 m (mllw). At tide level of +1.7 m (mllw), the peak shear stress was found to be 29 Pa. At tide level of +3.4 m (mllw), the peak shear stress was found to be 21 Pa. Sediment entrainment calculations should be conducted for the +1.7 m (mllw) only.

Erosion rates of Boston Harbor sediments[2]

The erosion rates of two reconstituted sediments from Boston Harbor were determined as a function of density and shear stress by means of the High Shear Stress Sediment Erosion Flume at Sandia National Laboratories. One sediment was derived from the CAD cell called the Open Cell (uncapped Cell M8/M11), and one was derived from an area near the CAD cell called the Mid Channel (in the middle of the channel just outside of Cell M8/M11). For all reconstituted cores, the bulk densities were determined as a function of depth and consolidation time. Sediment cores were eroded to determine erosion rates as a function of density and shear stress. Tests were conducted for most of the shear stresses at erosion rates down to 10^{-4} cm/sec. In addition, an in situ core from each site was analyzed for bulk density, particle size, mineralogy, and organic content as a function of depth.

---

[1] This text was taken from Maynord (2001).
[2] This text was taken from Roberts et al. (2000).

Reconstituted sediments. Bulk density was determined as a function of depth for 30-cm core lengths. Consolidation times were between 2 and 120 days for each core. Densities were determined by measuring the water content of each core in 2.5-cm increments. For all cores, the bulk density generally increases with depth and consolidation time. The bulk density for the Open Cell sediments ranged between 1.45 g/cm^3 and 1.58 g/cm^3 for up to a 120-day consolidation time. The Mid Channel sediments had a bulk density range of 1.38 to 1.51 g/cm^3. The Mid Channel sediments were less dense and smaller (i.e., lesser mean particle size) than the Open Cell sediments. In general, sediments with smaller mean particle sizes will be less dense than those with a larger mean particle size. However, this is not always the case. Other important considerations are mineralogy and organic content.

Erosion rates as a function of shear stress and depth were obtained for cores at consolidation times between 2 and 120 days. Erosion rates were measured for shear stresses of 0.5, 1.0, 2.0, and 4.0 N/m^2. The erosion rates for the lower shear stress of 0.5 N/m^2 could only be reasonably measured for the upper portion of the cores and for short consolidation times. That is because erosion either does not occur or is so slow that it would take hours to days to erode a measurable amount of sediment. Likewise, the 4.0 N/m^2 shear could not be tested at all depths because it eroded low bulk density areas too fast for the operator to accurately measure erosion rates. All of the data for erosion rates as a function of bulk density for shear stresses of 0.5, 1.0, 2.0, and 4.0 N/m^2 are presented in graphical form for both site composites Open Cell and Mid Channel. A large decrease in erosion rate as the bulk density increases was seen at all shear stresses.

In situ cores. Tests were conducted to determine sediment bulk properties for three in situ sediment analysis cores retrieved from the Boston Harbor. The three sites are identified as Control 1 (retrieved near the Mid Channel site), and T31 and T33 (retrieved near the Open Cell site).

The bulk density of Control 1 increased from 1.37 g/ cm^3 to 1.4 g/cm^3 for the first 11 cm in depth. Then the bulk density remained constant between 1.39 g/cm^3 and 1.41 g/cm^3 for the remainder of the core. The mean particle size was 105 μm at the surface; it then decreased and remained relatively constant between 11 cm and 35 cm ranging from 43 μm to 51 μm in size. At the bottom the mean particle size decreased further to 33 μm in size. The organic content was 4.3 percent at the surface; it then decreased and remained relatively constant for the rest of the core ranging from 2.2 percent to 2.7 percent. The mineralogy was qualitatively constant with depth, and is shown in Table 6, along with a summary of all sediment properties.

The bulk density of T31 generally increased with depth throughout the core ranging from 1.35 g/cm^3 to 1.68 g/cm^3 with local decreases in bulk density near 20-cm and 42-cm depths. The particle size was largest at the surface, near a size of 103 μm. It then decreased almost linearly to a depth of 20 cm reaching a value of 65 μm. The mean sized then increased and stayed relatively constant throughout the remainder of the core ranging between 80 μm and 89 μm in size. The organic content at the surface was approximately 3.2 percent; it then

decreased and remained relatively constant between about 12 cm and 35 cm ranging from 2.1 percent to 2.8 percent. The organic content increased at the bottom to its highest value of about 4 percent. The mineralogy was constant with depth. The mineralogy for the Control 1 and T31 sites were nearly identical, the major difference was that there was more quartz at the T31 site.

The bulk density of T33 was smallest at the surface (1.5 g/cm^3); it then increased significantly at a depth of 12 cm. The bulk density remained constant for the rest of the core (ranging from 1.71 g/cm^3 to 1.77 g/cm^3) except for a local increase in the density at a depth of 27 cm to a value of 1.85 g/cm^3.

Modeling of erosion due to propeller wash[1]

Gailani (2001) describes the results of propeller-induced erosion modeling performed by combining the erosion algorithms developed by Roberts et al. (2000) and the propeller-induced bottom shear stress estimates from ship passages developed by Maynord (2001). These algorithms do not include complex turbulent hydrodynamics, but are a screening level tool that combines time-history of bottom shear stress and vertical variation of erosion rate to estimate the total erosion. This model does, however, include deposition processes, but the methods used to estimate these complex deposition processes are not entirely understood. Cohesive sediment concentration profile, floc formation, and settling speed of cohesive sediments during a propeller-induced event have not been quantified. Therefore, assumptions had to be made by Gailani (2001) to simulate these processes. The high shear stress and massive amounts of erosion that will occur in a few seconds under a propeller indicate that deposition processes will be highly significant factors in reducing erosion during the latter part of the event.

For each ship passage shown by Maynord (2001), erosion patterns were simulated assuming both (a) no-deposition scenarios and (b) deposition scenarios. Each simulation lasted for 700 sec with a 0.1-sec time-step. This time step was used because of the rapidly changing conditions during a propeller-induced erosion event.

No-deposition scenarios. For the no-deposition scenarios, only depth of erosion under the propeller (maximum depth of erosion) is given because it can be assumed that locations away from the propeller will receive significant bed load from under the propeller. The maximum depth of erosion assuming no deposition for scenario 1 (ship speed = 1.3 m/sec, water level elevation = + 1.7 m (mllw)) for the Mid Channel sediments was 86 cm. The same scenario 1 with Open Cell sediments resulted in 45-cm maximum depth of erosion. The maximum depth of erosion assuming no deposition for scenario 2 (ship speed = 1.5 m/sec, water level elevation = +3.4 m mllw) for the Mid Channel sediments was 34 cm. The same Scenario 2 with Open Cell sediments resulted in 25-cm maximum depth of erosion. Comparison of scenario 1 and scenario 2 results demonstrates the effects of distance from the propeller to the bottom on shear stress and erosion.

[1] This text was taken from Gailani (2001).

Additionally, comparison of the Mid Channel and Open Cell results indicates that the Mid Channel sediments are more erosive.

Deposition scenarios. For the deposition scenarios, the erosion was estimated at each location perpendicular to the ship travel direction for which shear stress had been estimated. The 700-sec simulation time permitted redeposition of a significant fraction of the material. For scenario 1 simulation of the Mid Channel sediments, peak change in bathymetry occurred slightly before maximum shear stress. The near-bed concentration reached the maximum value before maximum shear stress and deposition began to dominate over erosion despite the high stresses. Maximum depth of erosion was approximately 15 cm. After redeposition, the 15-cm erosion had been reduced to approximately 11 cm. Redeposition will continue, filling in the deficit more, but at some point convection and diffusion due to the ambient current will dominate over propeller effects and the sediment concentration will become more diffuse. The model did not simulate that process. Erosion away from the propeller is less, and it is near zero at 25 m from the propeller. For scenario 1 simulation of the Open Cell sediments, maximum erosion was 12 cm, reduced to 8 cm after 700 sec. Erosion was near-zero approximately 20 m from the propeller.

Less erosion occurred in the scenario 2 Mid Channel as compared to scenario 1 Mid Channel because of the higher water elevation and lower bottom shear stress. Maximum change in elevation (maximum depth of erosion) was approximately 11 cm, and this was reduced to 8 cm at 700 sec due to deposition. Scenario 1 caused deeper erosion than Scenario 2, but the width of the area experiencing erosion is greater for scenario 2. Erosion is near zero approximately 25 m away from the propeller. For Scenario 2 Open Cell, maximum depth of erosion was approximately 8 cm, reduced to 5.5 cm after 700 sec due to deposition. Erosion is near zero approximately 25 m away from the propeller.

References

American Society for Testing Materials. (1999). "Standard practice for sampling freshly mixed concrete," ASTM-C172-99, Conshohoken, PA.

_____ . (2000). "Standard test method for laboratoryminiature vane shear test for saturated fine-grained clayey soil," ASTM-D4648-00, Conshohoken, PA.

Bergh, H. and Magnusson, N. (1987). "Propeller erosion and protection methods used in ferry terminals in the Port of Stockholm," PIANC Bulletin No. 58, Permanent International Association of Navigation Congresses.

Bokuniewicz, H. J. and Liu, F. T. (1981). "Stability of layered dredged sediment deposits at subaqueous sites," *Oceans '81 Conference Record*, Marine Technology Society, 752-754, Washington, DC.

Fredsoe, J. and Deigaard, R. (1992). "Mechanics of coastal sediment transport," *Proceedings, World Scientific*, Singapore.

Fuehrer, M., Romisch, K., and Engelke, G. (1981). "Criteria for dimensioning the bottom and slope protection, and for applying the new methods of protecting navigation canals," *Proceedings, 25th International Navigation Congress*, Permanent International Association of Navigation Congresses, Section 1, Subject 1, 29-50, Edinburgh, Scotland.

Gailani, J. Z., Jin, L., McNeil, J., and Lick, W. (2001). "Effects of bentonite on sediment erosion rates," Technical Note DOER-N9, U.S. Army Engineer Research and Development Center, Vicksburg, MS.

Jepsen, R., Roberts, J., and Lick, W. (1997a). "Effects of bulk density on sediment erosion rates," *Water, Air, and Soil Pollution* 99, 21-31.

Jepsen, R., Roberts, J., and Lick, W. (1997b). "Long Beach Harbor sediment study," Report submitted to U.S. Army Engineer District, Los Angeles, Los Angeles, CA.

Jepsen, R., Roberts, J., Lick, W., Gotthard, D., and Trombino, C. (1998). "New York Harbor sediment study," Report submitted to U.S. Army Engineer District, New York, New York, NY.

Lavelle, J. W., Mofjeld, H. O., and Baker, E. T. (1984). "An in situ erosion rate for a fine-grained marine sediment," *Journal of Geophysical Research* 89(C4), 6,543-6,552.

Lee, L. T., Jr. (in preparation). "Boston Harbor dredged material capping simulation," Coastal and Hydraulics Engineering Technical Note, U.S. Army Engineer Research and Development Center, Vicksburg, MS.

Maynord, S. T. (1996). "Return velocity and drawdown in navigable waterways," Technical Report HL-96-7, U.S. Army Engineer Waterways Experiment Station, Vicksburg, MS.

_____. (1998). "Bottom shear stress from propeller jets," *Ports '98,* American Society of Civil Engineers, Long Beach, CA.

Maynord, S. T. (2000). "Physical forces near commercial tows," Interim Report for the Upper Mississippi River-Illinois Waterway System Navigation Study, ENV Report 19.

McLellan, T. N., Havis, R. N., Hayes, D. F., and Raymond, G. L. (1989). "Field studies of sediment resuspension characteristics of selected dredges," Technical Report HL-89-9, U.S. Army Engineer Waterways Experiment Station, Vicksburg, MS.

Poindexter-Rollings, M. E. (1990). "Methodology for analysis of subaqueous sediment mound," Technical Report D-90-2, U.S. Army Engineer Waterways Experiment Station, Vicksburg, MS.

Roberts, J., Jepsen, R., and Gailani, J. Z. (2001). "Measurements of bedload and suspended load in cohesive and non-cohesive sediments," *Proceedings, ASCE World Water and Environmental Resources Congress*, Orlando, FL.

Roberts, J., Jepsen, R., Gotthard, D., and Lick, W. (1998). "Effects of particle size and bulk density on erosion of quartz particles," *Journal of Hydraulic Engineering* 124(12), 1,261-1,267.

Roberts, J., Jepsen, R., Bryan, C., and Chapin, M. (2000). "Boston Harbor sediment study," Report submitted to U.S. Army Corps of Engineers, New England District, Boston, MA.

Science Applications International Corporation. (1999). "Monitoring results summary from the first three Mystic River CAD cells," SAIC Report No. 466, Report submitted to Great Lakes Dredge and Dock, East Boston, MA.

_____. (2000a). "Geotechnical investigation of CAD cells, Boston Harbor Navigation Improvement Project," SAIC Report No. 503, Report submitted to U.S. Army Engineer Research and Development Center, Vicksburg, MS.

_____. (2000b). "Boston Harbor water quality monitoring – Vessel passage over confined aquatic disposal cells; Monitoring in wake of LNG carrier *MV Matthew* on March 31, 2000," SAIC Report No. 491, Report submitted to U.S. Army Engineer District, New England, Boston, MA.

_____. (2001). "Monitoring sediment resuspension process within a Boston Harbor CAD cell during passage of a deep-draft vessel," SAIC Report No. 492, Report submitted to U.S. Army Engineer Research and Development Center, Vicksburg, MS.

van Rijn, L. C. (1984). "Sediment transport: Part II; Suspended load transport," *ASCE Journal of Hydraulic Engineering*, 110(11), 1,613-1,641.

van Rijn, L. C. (1993). *Principles of sediment transport in rivers, estuaries, and coastal seas.* Aqua Publications, Amsterdam, The Netherlands.

Welp, T., Hayes, D., Tubman, M., McDowell, S., Fredette, T., Clausner, J., and Albro, C. (2001). Coastal and Hydraulics Engineering Technical Note CHETN-IV-35, U.S. Army Engineer Research and Development Center, Vicksburg, MS.

REPORT DOCUMENTATION PAGE

Form Approved
OMB No. 0704-0188

REPORT DATE (DD-MM-YYYY)	2. REPORT TYPE	3. DATES COVERED (From - To)
September 2001	Final report	

4. TITLE AND SUBTITLE

Monitoring of Boston Harbor Confined Aquatic Disposal Cells

5a. CONTRACT NUMBER

5b. GRANT NUMBER

5c. PROGRAM ELEMENT NUMBER

6. AUTHOR(S)

compiled by Lyndell Z. Hales

5d. PROJECT NUMBER

5e. TASK NUMBER

5f. WORK UNIT NUMBER

7. PERFORMING ORGANIZATION NAME(S) AND ADDRESS(ES)

U.S. Army Engineer Research and Development Center
Coastal and Hydraulics Laboratory
3909 Halls Ferry Road
Vicksburg, MS 39180-6199

8. PERFORMING ORGANIZATION REPORT NUMBER

ERDC/CHL TR-01-27

9. SPONSORING / MONITORING AGENCY NAME(S) AND ADDRESS(ES)

U.S. Army Corps of Engineers
Washington, DC 20314-1000

10. SPONSOR/MONITOR'S ACRONYM(S)

11. SPONSOR/MONITOR'S REPORT NUMBER(S)

DISTRIBUTION / AVAILABILITY STATEMENT

Approved for public release; distribution is unlimited.

13. SUPPLEMENTARY NOTES

14. ABSTRACT

The Boston Harbor Navigation Improvement Project (BHNIP) involves deepening of the main ship channel and three tributary channels to the Inner Harbor, and associated berthing areas. Lack of an upland disposal site and resource agency denial of permission to place and cap the contaminated sediments at an open water site resulted in the decision to use in-channel CAD cells for placement of contaminated material that would be dredged with an environmentally sensitive clamshell bucket.

The monitoring plan was composed of three primary activities: (a) water quality monitoring of suspended solids near the operation of two environmentally-sensitive clamshell dredges and a normal clamshell, to document the benefits of the special clamshell buckets, (b) monitoring contaminated dredged material consolidation and strength prior to and after placing the sand cap, and (c) calculating cap erosion predictions from both tidal currents and ship propeller wash to characterize the likely amount of cap damage to be expected from either source.

(Continued)

15. SUBJECT TERMS

See reverse.

16. SECURITY CLASSIFICATION OF:			17. LIMITATION OF ABSTRACT	18. NUMBER OF PAGES	19a. NAME OF RESPONSIBLE PERSON
a. REPORT	b. ABSTRACT	c. THIS PAGE			19b. TELEPHONE NUMBER (include area code)
UNCLASSIFIED	UNCLASSIFIED	UNCLASSIFIED		112	

14. (Concluded).

Sediment resuspension and loading characteristics were studied under near-similar operating and environmental conditions for three clamshell dredge buckets: (a) Great Lakes Dredge and Dock (GLDD) Conventional (open-faced), (b) GLDD Enclosed, and (c) CableArm™. The Enclosed bucket had the lowest overall turbidity and substantially less in the middle of the water column. However, the New England District expressed concern that the enclosed buckets were adding additional water to the already soft and weak sediments, possibly causing a further reduction of the bearing capacity of the sediments.

Grab samples and core samples indicate that: (a) natural cohesion and strength of the sediments were altered by the dredging process, resulting in sediments in the CAD cell that were unstable due to high water content and low shear strength, (b) excess pore water was released not only through the cap but also was vented through diapir structures that served to breach the caps in discrete areas, and (c) future projects should include an evaluation of the in situ strength of the material to be capped and the porosity and permeability of the CAD cell sediments.

Laboratory modeling of the subaqueous sand capping process was conducted to allow a comparison to field performance. Simulations indicated the sand cap was stable when placed on top of clay material having undrained shear strengths greater than 17 psf (0.8 kPa) and water contents below 100 percent.

Underway measurements were obtained of temperature, salinity, turbidity, currents, and acoustic backscatter intensity within the water column. Data were acquired behind the 900-ft-long liquid natural gas (LNG) carrier *MV Matthew*. The track of the LNG carrier passed over uncapped CAD Cell M8/M11 and capped Supercell. The 35-ft draft of this vessel was approximately 88 percent of the water depth in the navigable channel. The volume of sediments resuspended from capped and uncapped CAD cells was very small (well less than 1 cu m) for each vessel passage and settle to the seafloor within 1 hr of resuspension.

The erosion rates of two reconstituted sediments from Boston Harbor were determined as a function of density and shear stress; one from the CAD Cell M8/11, and one from an area near the CAD cell called the Mid Channel. Sediment cores were eroded to determine erosion rates as a function of density and shear stress. The erosion patterns were numerically simulated assuming both (a) no-deposition scenarios and (b) deposition scenarios.

The maximum depth of erosion assuming no deposition for Scenario 1 (ship speed = 1.3 m/s, water level elevation = + 1.7 m (mllw)) for the Mid Channel sediments was 86 cm. The same Scenario 1 with Open Cell sediments resulted in 45 cm maximum depth of erosion. The maximum depth of erosion assuming no deposition for Scenario 2 (ship speed = 1.5 m/s, water level elevation = +3.4 m (mllw)) for the Mid Channel sediments was 34 cm. Comparison of the Mid Channel and Open Cell results indicates that the Mid Channel sediments are more erosive.

For the deposition scenarios, maximum depth of erosion was approximately 15 cm for the Mid Channel sediments for Scenario 1. After redeposition, the 15-cm erosion had been reduced to approximately 11 cm. For Scenario 1 Open Cell, maximum erosion was 12 cm, reduced to 8 cm after 700 sec. Erosion was near-zero approximately 20 m from the propeller. Maximum change in Scenario 2 Mid Channel elevation was approximately 11 cm, and this was reduced to 8 cm due to deposition. For Scenario 2 Open Cell, maximum depth of erosion was approximately 8 cm, reduced to 5.5 cm after deposition. Erosion is near zero approximately 25 m away from the propeller.

15. (Concluded).

Boston Harbor	Confined aquatic disposal	Navigation channel	Suspended sediment
CAD cells	Contaminated sediments	Propeller wash	Tidal currents
Cap erosion	Erosion rate	Sediment resuspension	Turbidity
Clamshell dredge	Monitoring	Ships	Water quality